Fall 1-31-2013

Development of luminescent probes for ultrasensitive detection of biopolymers, their complexes, and living cells

Laura A. Wirpsza
New Jersey Institute of Technology

Copyright Warning & Restrictions

The copyright law of the United States (Title 17, United States Code) governs the making of photocopies or other reproductions of copyrighted material.

Under certain conditions specified in the law, libraries and archives are authorized to furnish a photocopy or other reproduction. One of these specified conditions is that the photocopy or reproduction is not to be "used for any purpose other than private study, scholarship, or research." If a, user makes a request for, or later uses, a photocopy or reproduction for purposes in excess of "fair use" that user may be liable for copyright infringement,

This institution reserves the right to refuse to accept a copying order if, in its judgment, fulfillment of the order would involve violation of copyright law.

Please Note: The author retains the copyright while the New Jersey Institute of Technology reserves the right to distribute this thesis or dissertation

Printing note: If you do not wish to print this page, then select "Pages from: first page # to: last page #" on the print dialog screen

ABSTRACT

DEVELOPMENT OF LUMINESCENT PROBES FOR ULTRASENSITIVE DETECTION OF BIOPOLYMERS, THEIR COMPLEXES, AND LIVING CELLS

by
Laura A. Wirpsza

New luminescent probes with enhanced brightness convenient for bioconjugation were synthesized and tested in major biological applications including the detection of nucleic acids and living cells. The first project used luminescent lanthanide ion probes that take advantage of hyper-sensitive acquisition of their long-lived emission signal in time-resolved mode, which avoids short-lived background fluorescence of the medium. Two model carbostyril fluorophores (cs124-CH_3 and cs124-CF_3) were modified by inclusion of two spacers (diamino and bi-phenyl) for the attachment of amine and thiol reactive cross-linking groups. In this project, time-resolved measurements are presented for spectroscopy and microscopy. The probes were synthesized, then characterized by UV/VIS, NMR, mass spectrometry and then validated in various biological applications. DNA detection using luminescently labeled molecular beacons hybridization probes was performed with sensitivity less then 1 pM, which is about 100 fold higher then that for conventional fluorescent probes. Further 30-fold increase in detection sensitivity was achieved by tethering multiple lanthanide probes to a carrier molecule, avidin. The resulting avidin conjugates were used for imaging of living cells employing time-gated fluorescent microscopy. Six thiol-reactive derivatives of the lanthanide ion probes with bromoacetamido- and maleimido- cross-linking groups were synthesized. It was found that maleimido-compounds displayed exceptional reactivity instantaneously coupling to

thiols at physiological conditions at micromolar thiol concentrations. The second part of the project included the development of light-emitting diagnostic molecules for the detection of human microbial pathogens. The approach employs fluorescently labeled antibiotics, which retain high specificity towards pathogens and render them fluorescent after binding to their cellular targets. These studies present that the obtained derivative 7-aminoDDAO is ~2.8 fold brighter than its predecessor DDAO, with excitation and emission maxima located in the spectral area where body tissues are the most transparent (λ_{em}=680 nm). Using near-infrared emitting dyes, this approach presents non-invasive tomographic detection of the pathogens in the living body, thereby enabling swift and efficient therapies. The desired NIR probes were synthesized and validated in a collaboration study by detection of fungal infections in mice.

DEVELOPMENT OF LUMINESCENT PROBES FOR ULTRASENSITIVE DETECTION OF BIOPOLYMERS, THEIR COMPLEXES, AND LIVING CELLS

by
Laura A. Wirpsza

A Dissertation
Submitted to the Faculty of
New Jersey Institute of Technology
in Partial Fulfillment of the Requirements for the Degree of
Doctor of Philosophy in Chemistry

Department of Chemistry and Environmental Science

January 2013

.

APPROVAL PAGE

DEVELOPMENT OF LUMINESCENT PROBES FOR ULTRASENSITIVE DETECTION OF BIOPOLYMERS, THEIR COMPLEXES, AND LIVING CELLS

Laura A. Wirpsza

Dr. Lev Krasnoperov, Co-Advisor Dissertation — Date
Professor of Chemistry and Environmental Science, NJIT

Dr. Arkady Mustaev, Co-Advisor Dissertation, PHRI — Date
Assistant Professor of Microbiology and Molecular Graphics, UMDNJ

Dr. Edgardo Farinas, Committee Member — Date
Associate Professor of Chemistry and Environmental Science, NJIT

Dr. Haidong Huang, Committee Member — Date
Assistant Professor of Chemistry and Environmental Science, NJIT

Dr. Zafar Iqbal, Committee Member — Date
Research Professor of Chemistry and Environmental Science, NJIT

BIOGRAPHICAL SKETCH

Author: Laura A. Wirpsza

Degree: Doctor of Philosophy

Date: January 2013

Undergraduate and Graduate Education:

- Doctor of Philosophy in Chemistry,
  New Jersey Institute of Technology, Newark, NJ, 2013
- Master of Science in Chemistry,
  New Jersey Institute of Technology, Newark, NJ, 2008
- Bachelor of Science in Biology,
  Susquehanna University, Selinsgrove, PA, 2006

Major: Chemistry

Publications:

Wirpsza, L. Krasnoperov, L. and Mustaev, A. New quinolone-based thiol-reactive lanthanide luminescent probes. 2012. *Accepted at Journal of Photochemistry and Photobiology A: Chemistry.*

Wirpsza, L., Pillai, S., Batish, M., Marras, S., Krasnoperov, L., and Mustaev, A. Highly Bright Avidin-based Affinity Probes Carrying Multiple Lanthanide Chelates. 2012. *Journal of Photochemistry and Photobiology B: Biology.* 116, pp 22-29

Pillai, S., Wirpsza, L., Kozlov, M. Marras, S.A.E., Krasnoperov, L. N., Mustaev, A. New cross-linking quinolone and quinolone based luminescent lanthanide probes for sensitive labeling. 2012. *Proceedings of SPIE.* 8233, pp. 82331C1- 82331C11

Krasnoperov, L., Marras, S. A.E, Kozlov, M., Wirpsza, L. Mustaev, A. Luminescent Probes for Ultra-Sensitive Detection of Biopolymers. 2010. *Bioconjugate Chemistry.* 21 (2), pp. 319-327

Patents:

Mustaev, A., Kozlov, M.,Marras, S., Krasnoperov, L., Wirpsza, L., and Pillai, S. Fluorophore Chelated Lanthanide Luminescent Probes with Improved Quantum Efficiency. WO/2011/088193

I would like to dedicate this dissertation to my family: grandparents, Glen and Velma Pawling, parents, Joyce and Stanley Wirpsza, and my sister, Lillian Wirpsza. Certainly, I would not have been able to complete this degree without your patience, support and love. From all those years of cleaning the apartments, I have gained a vigorous work ethic and passion for my research. And I know for certain there is nothing I cannot accomplish. And that is all because you, all of you. Dad, thank you for sending me to Hun. Mom, thank you, waking me up at 8 am on Saturday mornings to clean. Mom and Dad, please retire now! The house is still in one piece, somehow. Lillian, you are always my inspiration and rock (we have our work cut out for us). Uncle Harold, for the tour at PPPL when I was so young and it has always been an inspiration. To my many many family members, thank you for having the patience to listening to me about life, love and family matters. Lets face it family matters.

My appreciation goes to the Hun School of Princeton for instilling in me honesty, integrity, and curiosity. I am very please to have accomplished my dissertation for my 10^{th} year reunion. I am very eternally grateful to Hun and its community of students, teachers and alumni. The community of the school is truly unique and it is a very special part of who I am. In the future, I am always willing to present my work to future Hun Students and assist in sharing my knowledge from college and graduate school.

To my extended family from Susquehanna University, especially: Magali Laitem, Maria Wing, Jamie Feretic, and Pale Aye. Honestly, I do not know how I have survived without you. I can barely go a day without thinking about all the memories we share and continue to gain. It is amazing that we started all in the same major as SU and have branched off into various fields. I am so happy we have all accomplished/ accomplishing our dreams to earn our PhD and Doctor degrees. I would like to express my gratitude to Leo Laitem and Gabby Laitem for lending me the electric power to see this degree to its completion. They have been extremely kind and always welcoming.

To everyone else, trust me, it is a very *very* long list. No, I have not forgotten you, and I just want to express my thanks for the time you leant me your ear, provided advice, and inspired me. I am sure I would have been up in a sailboat without any wind and against the current towards the jaded rocks behind.

Muchas Gracias. Merci Beaucoup. Большое спасибо. Thank you very much!

"There is more in you of good than you know, child of the kindly West. Some courage and some wisdom, blended in measure. If more of us valued food and cheer and song above hoarded gold, it would be a merrier world."
~The Hobbit, by J.R.R Tolkein

ACKNOWLEDGMENT

My deepest gratitude goes to my research advisors, Dr. Lev Krasnoperov and Dr. Arkady Mustaev, for their patience, wisdom and excellent mentoring abilities. Words cannot begin to express how grateful I am for their advice and motivation. I wish to thank Dr. Edgardo Farinas, Dr. Haidong Huang, and Dr. Zafar Iqbal, for being members of my dissertation committee and providing support and guidance towards the completion of this dissertation. I would also like to express my appreciation and thanks to members of the research group, Dr. Shyamala Pillai and Dr. Mona Batish, who contributed and were vital for the successes of these projects. A special thanks goes to Dr. Salvatorre Marras and Dr. Sanjay Tyagi at PHRI for their insightful drive on many projects. I would like to express my gratitude to the NJIT group members, Manuvesh Sangwan and Beidi He for their assistance in equipment, guidance, and support. Appreciation to the Department of Chemistry and Environmental Science at NJIT and Department of Microbiology and Molecular Graphics at PHRI-UMDNJ for use of their equipment and facilities. Furthermore, I would like to express my thanks and love to my family, especially my parents and younger sister, for their support on this groundbreaking experience.

This work was performed and completed with funding from NIH grants: RO1 GM-307-17-21 and RO1-MH-079197 awarded to Dr. Arkady Mustaev. Fluorophore Chelated Lanthanide Luminescent Probes with Improved Quantum Efficiency is presented and protected under patent application WO/2011/088193. This dissertation has been a great adventure I never knew I was looking for and I am eternally grateful to everyone I have collaborated with and met on this scientific discovery.

TABLE OF CONTENTS

TABLE OF CONTENTS
(Continued)

TABLE OF CONTENTS
(Continued)

TABLE OF CONTENTS
(Continued)

LIST OF TABLES

LIST OF FIGURES

LIST OF FIGURES
(Continued)

LIST OF FIGURES
(Continued)

LIST OF SCHEMES

CHAPTER 1

INTRODUCTION

1.1 Objective

The objective of this dissertation is to present the development and characterization of luminescent probes for the sensitive detection of biopolymers and imaging of living cells. Chapter 1 consists of background information on luminescent probes (specifically lanthanide ion probes and near infrared dyes) and biological validation techniques discussed in future chapters. Chapter 2 provides a thorough explanation of time-resolved spectroscopy and microscopy techniques for the photophysical characterization of the luminescent lanthanide ion probes. Chapter 3 introduces a novel synthesis for carbostyril derivatives with cross-linking groups for amine to present highly sensitive detection in molecular beacons. Chapter 4 describes the use of avidin labeled with multiple probes and shows the sensitive detection of exterior labeled bacteria and mammalian cells. Chapter 5 presents the synthesis and characterization of thiol reactive derivatives and the detection of RNA polymerase, specifically the unique characteristics of maleimide derivatives. The development of the 7-amino derivative of DDAO (7-hydroxy-9H(1,3-dichloro-9,9-dimethyl) acridin-2-one), a near infrared fluorophore, for attachment to antifungal drugs for tissue imaging is covered in Chapter 6. The conclusions and potential future works of these studies are discussed in Chapter 7.

1.2 Background Information

Since the 1800s, fluorophores have played an essential role in the detection of biological material. Especially during the past twenty years, fluorescence has become a dominant methodology in biotechnology, flow cytometry, medical diagnostics, DNA, sequencing, forensics, and genetic analysis. There has been dramatic growth for cellular and molecular imaging to reveal the localization and measurements of intracellular molecules (Lakowicz 2006). Fluorescent probes (aka chromophores, fluorophores or sensors) are highly capable of recognizing and indicating the presence of specific biological target (Chen and Selvin 1999). However, conventional fluorophores (e.g., fluorescein) can be quenched when conjugated to biological material (e.g., proteins) (Loboda, Sokolova et al. 1984). Recent advancements in biological detection (*in vitro* and *in vivo*) require the fluorophores to overcome the short-lived autofluorescence of biological material when bound to specific targets (Hohlbein, Gryte et al. 2010). This dissertation concentrates on the luminescent materials capable of overcoming the autofluorescence of biological matrices due to their unique properties.

Luminescence is the process where a molecular species absorbs light at one wavelength and emits it at a higher wavelength. There are two types of luminescence, fluorescence and phosphorescence. Fluorescence occurs without change in spin, typically S_1-S_0 transitions and "phosphorescence" transitions imply a change in spin, typically T_1-S_0. Figure 1.1 is a schematic of the different ways a molecule can absorb energy from a highly energized light source then emit a wavelength back to the ground state (Lakowicz 2006). The lowest vibrational level of an excited singlet state is relatively stable with a longer lifetime of 1 to 10 ns. Emission from the excited triplet state (T_1),

phosphorescence, occurs on the order of milliseconds to seconds (Hagan and Zuchner 2011). In the case of metal complexes (e.g., lanthanide ion complexes), an antenna (or fluorophore) absorbs high energy then transfers the energy to an emitting entity (e.g., the lanthanide ion). This "antenna effect" results in unique properties that are discussed in depth in future chapters.

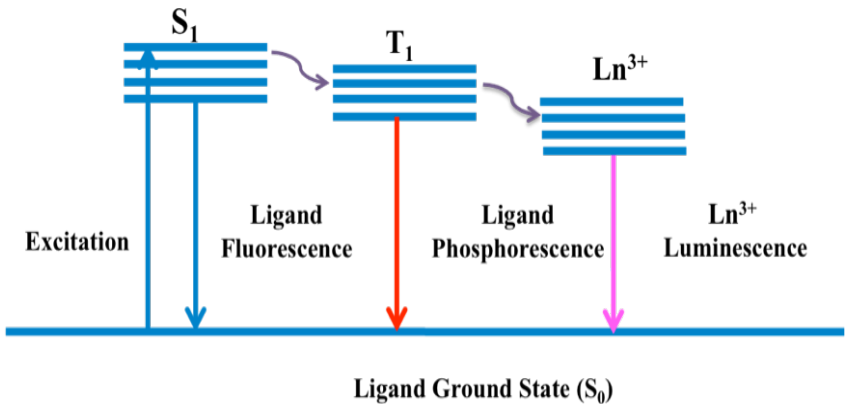

Figure 1.1 Schematic of fluorescence and phosphorescence energy states.

There are many examples of classic organic fluorophores (e.g., quinine, fluorescein, Texas Red, BODIPY-FL, and DAPI), which are used in the detection of biological targets. However, organic molecules are very sensitive to their environment for optimal emission intensity. An ideal nucleic acid dye is devoid of fluorescence in solution with a high binding affinity to nucleic acids, illuminating only after binding to the substrate (Timtcheva, Maximova et al. 2000). Therefore, the label (or fluorophore) may contain a reactive functional group for covalent or strong noncovalent attachment to biomolecule of interest (Patonay, Salon et al. 2004). This work focuses on luminescent labels (specially lanthanide ion complexes and a small near infrared dye) that can overcome problems often associated with short-lived auto-fluorescence in biological samples (e.g., external cell labeling, molecular beacons, and RNA polymerase) (Byassee, Chan et al. 2000).

1.3 Fluorophore Properties

Commonly used organic fluorophores lack the ability to overcome the high autofluorescence generated from various sources in a biological sample (e.g., serum or tissue sample, or membrane) resulting in a weak luminescent background. In addition, some biomaterial is expressed in extremely low copy numbers (Marras 2003). Probes are required to produce a strong signal to overcome the autofluorescence signal and to be detectable at low concentrations (Xiao, Liu et al. 2005). Recently, there has been a demand in the development of noninvasive and simple diagnosis techniques such as *in vivo* imaging and photodynamic therapy (PDT) (Umezawa, Nakamura et al. 2008). Furthermore, the optical widow (spectral range from 650-900 nm) has many advantages: significant reduction of the background signal due to the lowest autoabsorption and autofluorescence of the biomolecules in the near infrared region (NIR), low light scattering and deep penetration of the NIR light and the possibility to use low-cost excitation light sources (Patonay, Salon et al. 2004; Umezawa, Nakamura et al. 2008). For *in vivo* imaging, contributions of oxyhemoglobin, deoxyhemoglovin and water to tissue absorption are lowest in the 650-700 nm, making it optimal for the development of fluorescent indicators (Vo-Dinh 2003).

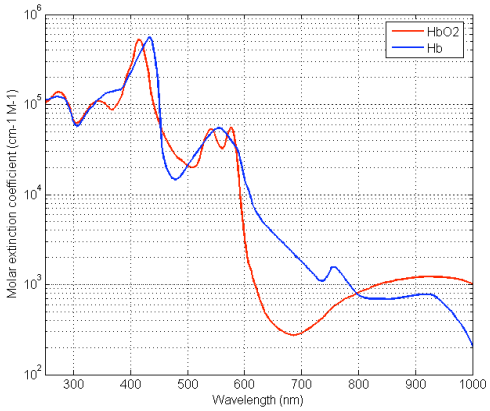

Figure 1.2 Contributions of oxyhemoglobin and deoxyhemoglobin to tissue absorption.

Source: Biomedical Photonics Handbook. (2003) Tuan Vo-Dinh (Editor), CRC Press. New York

Selection of a fluorophore (aka indicators, tags, or materials) depends upon its photo characteristics. Proper usage of the fluorophore *in vitro* and/or *in vivo* applications depends upon their excitation (λ_{ex}) and emission (λ_{em}) wavelengths (Tung 2004). In the literature, fluorophores are presented based on their: 1) excitation and emission wavelengths 2) Stokes Shift, 3) emission lifetime, 4) quantum yield and 5) relative brightness. Stokes Shift is the difference between absorbed energy at a higher wavelength and emission radiation at the lower wavelength. Absorbance is the base log 10 of the initial intensity (I_0) and final intensity (I). Molar absorptivity (molar extinction coefficient, ε) is constant and the absorbance (A) is proportional to concentration (c) of a given substance in a solute and measured at a wavelength across a given distance (l) [Eq. 1.1] (Lakowicz 2006). Typically, when a fluorophore is excited it emits a characteristic spectrum with intensity over a period of time, fluorescence lifetime (τ) (Vo-Dinh 2003; Lakowicz 2006). The fluorescence quantum yield (Φ_f) is the ability of the fluorophore to convert a number of absorbed into emitted photons in a particular environment(Peck, Stryer et al. 1989; Schmidt, Schutz et al. 1995) [Eq. 1.2]. Substances with quantum yield approaching unity (e.g., rhodamines) display the brightest emission. Of all the

parameters, the fluorescence intensity is perhaps the quantity that is most often interrogated in (bio) analytical applications. The combination with the molar absorption coefficient at the excitation wavelength used ($\varepsilon(\lambda_{ex})$) is a measurement of strength of the fluorescence signal to be expected in a particular application. The product of molar absorptivity and quantum yield determines the brightness of a fluorophore [Eq 1.3] (Rurack and Spieles 2011).

$$A=\varepsilon l c \tag{1.1}$$

$$\Phi = \frac{Number\ of\ photons\ emitted}{Number\ of\ photons\ absorbed} \tag{1.2}$$

$$\varepsilon(\lambda_{ex}) \times \Phi_f = \text{brightness} \tag{1.3}$$

1.4 Lanthanide Ion Probes

Lanthanides (Ce – Lu) are unique elements with an electronic configuration of the atoms and ions in a trivalent state Ln^{3+}. However, forbidden parity results in low molar absorption coefficients (typically < 3 $M^{-1}s^{-1}$). Therefore, lanthanide ions are required to be "pumped" by binding the lanthanide ion (through chelation) to an appropriate organic fluorophore (antenna). Chapters 3, 4, and 5 describe the development of luminescent lanthanide probes with a specific class of antenna chromophore, carbostyril (cs124 (7-amino-4-methyl-2 (1H)-quinolinone)) and its derivatives. In this work, only four lanthanide ions will be focused on: Europium (Eu^{3+}), Terbium (Tb^{3+}), Samarium (Sm^{3+}), and Dysprosium (Dy^{3+}) (Krasnoperov, Marras et al. 2010).

Indirect excitation (aka sensitization or antenna affect) is a suitable method for lanthanide ions, since direct excitation of the Ln^{3+} ion rarely yields highly luminescent materials. The antenna affect occurs when the attached organic ligand (chromophore) absorbs light. Energy is then transferred onto one or several excited states of the metal ion resulting in an intense emission signal (Figure 1.3). Since the 1990s, a multitude of organic antenna molecules have been developed (Bunzli and Piguet 2005). Due to their intense emission wavelengths, long emission lifetimes, luminescent lanthanide ion probes are efficient alternatives for radioactivity and standard fluorescent dyes. In addition, these probes can measure energy transfer with static and time-varying distances (Li and Selvin 1995).

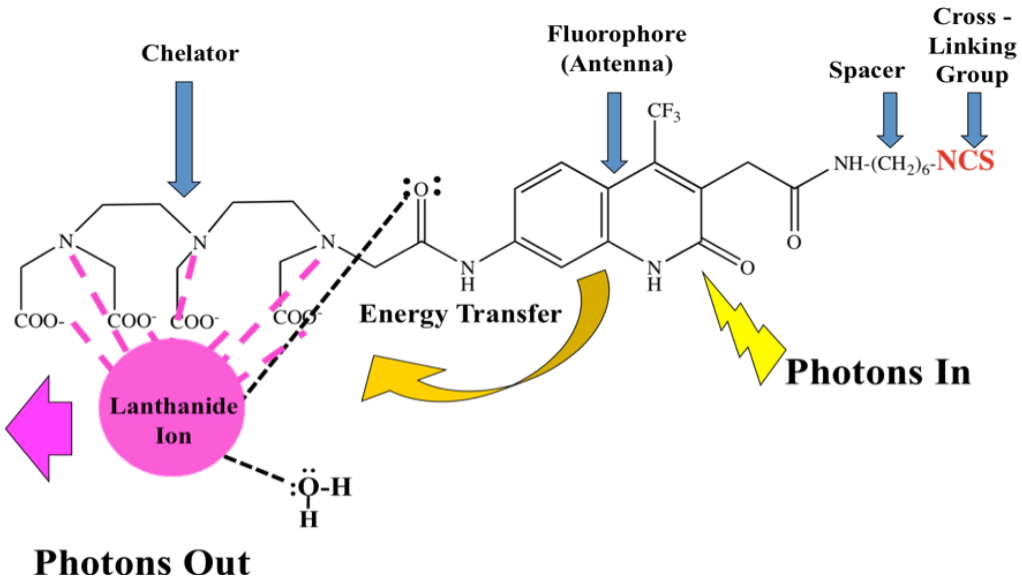

Figure 1.3 Energy transfer scheme of a lanthanide ion probe with antenna, chelator, and cross-linking group.

Presently, two general classes of lanthanide ion probes are being used: incorporate the chromophore into the structure of the chelate or contain a distinct chelate and chromophore. A significant advantage in the latter approach is the development of the

chelate structure and sensitizer separately results in excellent solubility and lanthanide-binding properties. cs124 (7-amino-4-methyl-2 (1H)-quinolinone) and various derivatives (Figure 1.4) have been used as antenna molecules to increase the emission efficiency of lanthanides (Chen and Selvin 2000; Selvin 2002). Recently, cs124 derivatives had been developed to contain three functional units: an antenna, a chelated lanthanide, and a cross-linking group (for attachment to the biomolecule of interest). These probes require a complex synthetic strategy leading to compounds with a size exceeding 1000 Da. These complex probes result in desirable characteristics such as: 1) long-lived excited states (ms range), 2) long wavelength emissions (e.g. 500-750 nm for Ln^{3+}), 3) high solubility in aqueous solutions, 4) high quantum yields and 5) large Stokes shift (Krasnoperov, Marras et al. 2010). Designing efficient antenna probes becomes challenging since the mechanism for the energy transfer remains unknown. In this study, two model cs124 antenna (cs124-CH_3 and cs124-CF_3) were modified with the addition of various spacers (diamino and bi-phenyl) and several various cross-linking groups (Cidalia M.G, Harte et al. 2008; Krasnoperov, Marras et al. 2010).

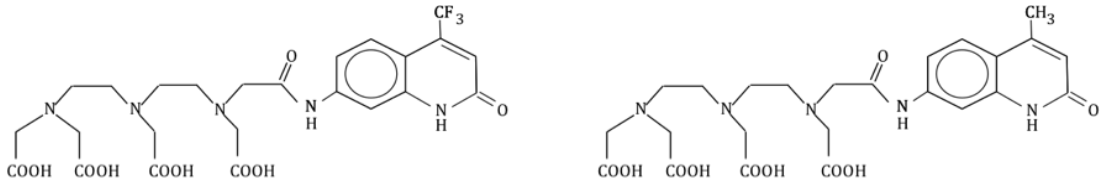

Model Compound 1 Model Compound 2

Figure 1.4 Carbostyril 124 model compounds 1 and 2.

Source: Selvin, P. R. (2002). Principles and biophysical applications of lanthanide-based probes. Annual Review of Biophysics & Biomolecular Structures **31**: 275-302

Two commonly used polyaminocarboxylates class chelates are used for this class of antenna probes; diethylenetriaminepentaacetic acid (DTPA) and tetraaminohexaacetic

acid (TTHA) (Krasnoperov, Marras et al. 2010). DTPA has been the more widely used due to its high binding constant of lanthanides, available dianhydride, solubility, relatively high coordination number of 8, and vibrational spectra. DTPA does not couple away from the excited luminescent state of the lanthanide. However, when water remains bound to the lanthanide there is a quenching of emission (Li and Selvin 1995). In this work, DTPA is the chelate of choice.

Site-specific labeling of oligonucleotides and proteins is commonly used for structural and functional studies of intracellular mechanisms (Jahn, Olsen et al. 2001). Two applicable chemical strategies for selective and efficient covalent attachment of luminophores to biological material can be completed via either lysine amino groups (using isothiocyanates) or cysteine thiols (using acetyl bromide and maleimides). Activated thiol derivatives are ideal due to their stability under anhydrous conditions and can be covalently coupled to proteins at neutral to slightly basic pH (Chen and Selvin 1999; Hagan and Zuchner 2011). Chapters 3, 4, and 5 describe the synthesis and characterization of amine and thiol reactive luminescent probes.

1.5 Near Infrared Dyes

In the 1990s, near infrared region (NIR) dyes originated from conventional organic fluorophores (e.g., cyanine, oxaine, and rhodamines) emitting from 650 to 700 nm (Timtcheva, Maximova et al. 2000; Xiao, Liu et al. 2005; Warther, Bolze et al. 2010). These fluorophores are attractive alternatives to conventional fluorophores because they emit fluorescence in the low absorbance and light scattering region of tissue chromophores (e.g., oxy- and deoxy-hemoglobin, melanin, and fat) (Sevick-Muraca,

Houston et al. 2002) (Figure 1.2). However, these probes have several drawbacks such as short fluorescence lifetimes, are bulky molecules, small Stokes shift, low solubility, and oxidation of photo oxidation. These compounds have been used as laser dyes and are typically rigid with an extended set of conjugated rings or fused aromatic rings. Commonly used NIR dyes include boron-dipyromethene (BDP), Keio Fluors (Umezawa, Nakamura et al. 2008), Alexa Fluor and sulfonated indocyanine dyes (Berlier, Rothe et al. 2003). In this work, Cyanine 5.5 (Cy5.5) is used as the reference organic fluorophore (Figure 1.5A) with λ_{ex}= 675 nm, λ_{em}= 694 nm and quantum yield = 0.23 in water for NIR dyes (Figure 1.5 B) (Berlier, Rothe et al. 2003).

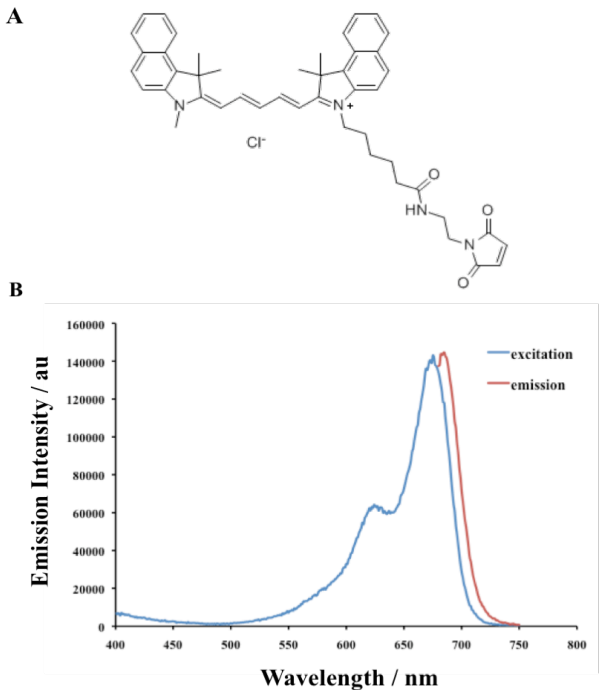

Figure 1.5 (**A**) The structure of a NIR dye Cy 5.5 with (**B**) excitation and emission spectra in H_2O.

One unique NIR fluorophore, DDAO (7-hydroxy-9H (1, 3-dichloro-9, 9-dimethylacridin-2-one), is a small organic molecule that emits in the NIR with a narrow emission spectrum (λ_{ex} = 646 nm, λ_{em} = 659 nm) (Tung, Zeng et al. 2004). DDAO

contains only one polar atom that interacts with water and shows very hydrophilic properties: mixtures in water, forms a normal liquid crystalline phase and micelles. The hydration properties were studied to focus on the uptake of water by single phase using sorption calorimeter (Kocherbitov and Soderman 2006). Only a handful of studies have been completed with this particular NIR dye. DDAO was used in a method with acetylcholinesterase (AChE) to modulate the distance between a gold nanoparticle (Zhang, Hei et al. 2012) and to indicate the presence of β-galactosidase (β-gal) which is a reporter gene in biological research (Gong, Zhang et al. 2009). The synthesis and characterization of a caged 1,3-dichloro-9, 9-dimethyl-9H-acrindin-2 (7)-one (DDAO) was adapted for live cell imaging by limiting toxicity and autofluorescence background (Warther, Bolze et al. 2010). Chapter 6 describes a newly synthesized and characterized DDAO derivatives with optimal emission for in body imaging and was applied by coupling to antifungal drugs for instantaneous detection.

1.6 Biological Validation Techniques

Advances in recombinant DNA technology and analysis of specific genes have been major contributors to genomics. These techniques rely on nucleic acid hybridization probes to detect complementary nucleic acid sequences that has been increasingly used in diagnostic medicine (Bunzli and Piguet 2005). “Light up probes” were developed to take advantage of new chemistries that enhance the hybridization properties of nucleic acid probes by using agents that fluorescence upon binding to nucleic acids. Lights up probes are not fluorescent when free in solution and are useful for monitoring amplification reactions reported in real-time polymerase chain reactions (PCR) and the identification of

specific mRNAs in living cells (Marras 2003). The combination of the time resolved luminescence and genomics has attracted much attention since the first application in 1983 by Siitari et al. Some luminescent lanthanide ion assay systems have been successfully developed such as DELFIA (dissociation enhanced lanthanide fluoroimmunoassasy) by Perkin Elmer, CyberFluor (or FIAgen), enzyme amplified time resolved fluorometric, TRACE (time resolved amplified cryptate emission, and multiple-labeled time resolved fluoroimmunoassay (Hagan and Zuchner 2011).

1.6.1 Molecular Beacons

Nucleic acid hybridization probes have significantly contributed to the advances in recombinant DNA technology by detecting the presence of complementary nucleic acid sequences (Bunzli and Piguet 2005). In the late 1990s, Sanjay Tyagi and Fred Russell Kramer developed hairpin hybridization probes that undergo a conformational change when bound to their complementary oligonucleotides target resulting in a bright emission signal called molecular beacons (Figure 1.6). The loop portion of the beacon sequence is 15 to 30 nucleotides long complementary to the target sequence in the target nucleic acid. The arm sequence is 5 to 7 nucleotides long complementary to each other but not related to the probe or target sequence (Tyagi and Kramer 1996; Marras 2003; Vargas, Raj et al. 2005). The beacon is designed to possess an internally quenched fluorophore whose fluorescence is restored upon hybridization to a specific nucleic acid sequence (Vargas, Raj et al. 2005). The molecular beacons have a unique hairpin structure that enables a higher specificity to recognize their targets than conventional oligonucleotide probes. In addition, these probes can overcome a range of temperatures and mismatched probe-targets do not luminescence at low temperatures. A number of laboratories have

confirmed the use of molecular beacons for the detection of single nucleotide polymorphisms (SNP) (e.g., cystic fibrosis and Tay-Sachs disease gene mutations) (Tyagi, Marras et al. 1996).

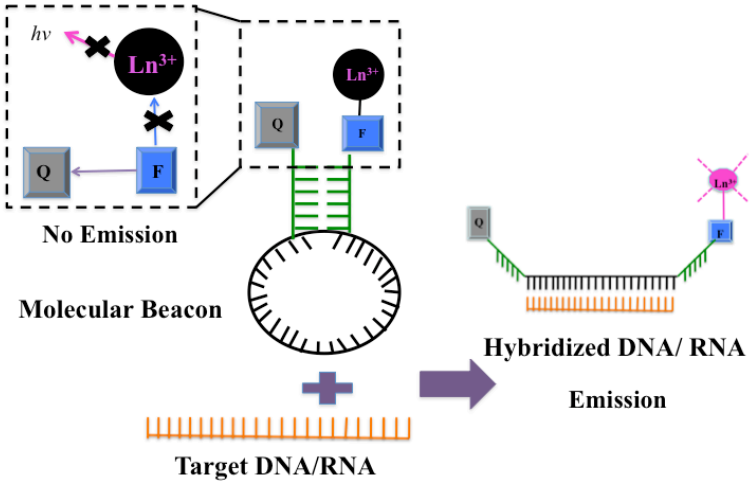

Figure 1.6 Schematic of Molecular Beacon with lanthanide ion probe.

Source: Krasnoperov, L. N., et al. (2010). Luminescent probes for ultrasensitive detection of nucleic acids. Bioconjugate Chemistry **21**: 319-327

Recently, new luminescent lanthanide ion probes (presented in Chapter 3) were developed and used in the context of molecular beacons (Krasnoperov, Marras et al. 2010). Remarkably, the ratio of final fluorescence signal to the background fluorescence of the molecular beacon (which is a fluorescence of molecular beacon solution after subtraction of the background fluorescence of the medium) was >400, which is more than that for typical fluorophore-based molecular beacons. Figure 1.7A shows the time-course for developing of the luminescent signal detected in time-resolved mode in the mixtures containing a newly -based molecular beacon and various concentrations of complementary DNA target. Time-resolved of short-lived background fluorescence, markedly enchancing the sensitivity of detection, which is less than 1 pM. This value is about 50 to 100 times more sensitive than the level achieved with conventional fluorescence-based molecular beacons, and is 10 to 60 times more sensitive than

previously reported for other lanthanide-type nucleic hybridization probes. Other studies (Sueda, Yuan et al. 2000) on the lanthanide-based hybridization probes report a detection limit of 30-50 pM.

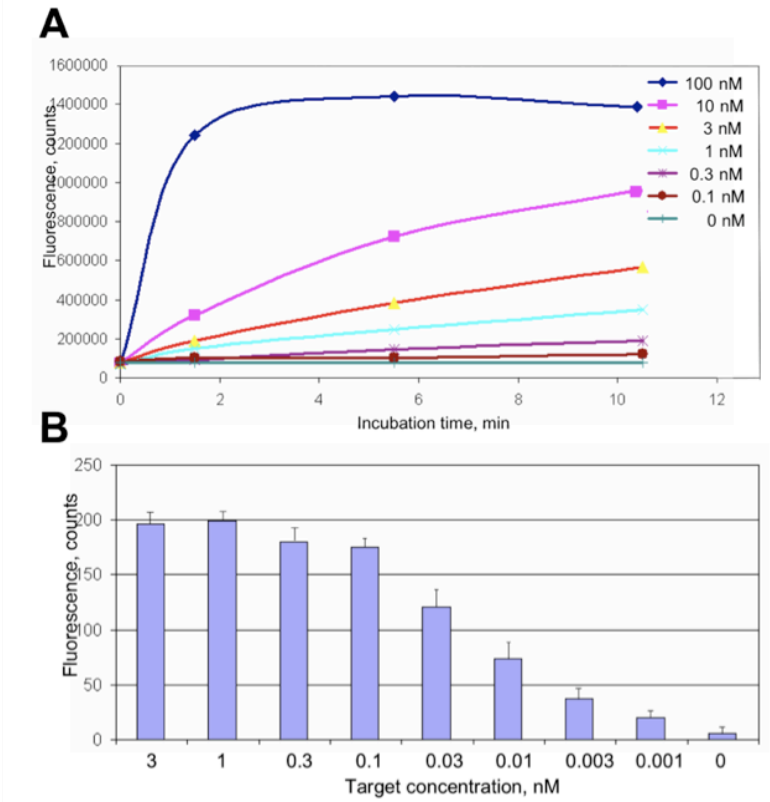

Figure 1.7 Time-resolved detection of complementary DNA oligonucleotide target using Eu^{3+}-probe **1** - based luminescent molecular beacon. A) Molecular beacon (1 nM) was supplemented with the target to the indicated concentration. Luminescent signal was detected at the indicated time. B) End point detection of oligonucleotide target at indicated concentrations in the presence of 10 pM molecular beacon.

Source: Krasnoperov, L. N., et al. (2010). Luminescent probes for ultrasensitive detection of nucleic acids. Bioconjugate Chemistry **21**: 319-327

1.6.2 Cellular Labeling

Since 1942, biological targets (e.g., proteins, DNA, RNA, etc) have been detected using labeled biotinylated derivatives (e.g., fluorophore, horseradish peroxidase, or alkaline phosphate-conjugates) or captured efficiency on avidin/streptavidin-coated solid supports

(e.g., resins, magnetic beads, etc). Avidin is a tetrameric molecule with four binding sites for biotin. Due to non-covalent interactions between avidin/SA with biotin, a highly stable bond forms (K_a on the order of 10^{15} M^{-1}). This bond can resist dissociation in the presence of detergent, high and low pH, protein denaturants (e.g., 8 M guanidine-HCl), and high temperature (Orth, Clark et al. 2003).

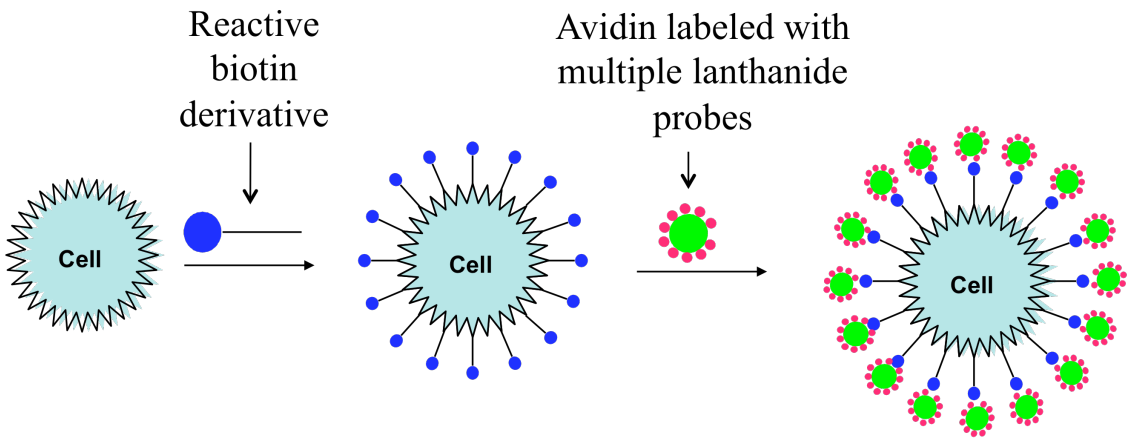

Figure 1.8 Schematic of luminescent labeling of living cells.

It was later found that cells saturated with biotin and lanthanide ion probe bound to avidin enable intense emission detection and to determine the lowest concentration of luminescent probes visible through time resolved measurements. Cells saturated with biotin and lanthanide ion probe bound to avidin enable intense emission detection and determine the lowest concentration of luminescent probes visible through time-resolved measurements (Orth, Clark et al. 2003; Elia 2008). A chemical reagent for protein biotinylation experiments is made up for 1) biotin moiety that interactions with the biotinylated proteins with avidin/SA-based reagents, 2) a space with sufficient length to allow protein capture by immobilized avidin/SA and 3) reactive moiety for the covalent binding of biotin to the proteins (Elia 2008). This experiment was analyzed and performed in Chapter 4 (Figure 1.8).

1.6.3 Near Infrared Optical Imaging

Chapter 6 presents the use of a small NIR dye for in vivo body images. Imaging modalities in the optical regime have the advantages of being sensitive, accessible, relatively low cost and rapid. The development of a number of optical imaging approaches for *in vivo* analysis has been used to accelerate drug-development with real-time *in vivo* assays. These techniques are ideal for imaging small laboratory animals and are much safer to use even in large doses. The compounds are capable of penetrating relatively deep into tissues, does not require a chemical substrate, and is quantifiable. Light may be introduced into tissue repeatedly and not subject to radioactive decay (Vo-Dinh 2003).

The interaction of photons with tissue is based on the absorption of light, scattering of light, and emission of fluorescence that can be used to characterize tissue optical properties. A fundamental observation for optical diagnostic procedures relates to the penetration depth of light in living tissue strongly depends upon the wavelength used. This is due to the number of absorption and scattering events in tissue is a function of wavelength. The absorption of light in tissue originates from oxy- and deoxyhemoglobin and several tissue components (e.g., porphyrins, melanin, NADH and flavins, collagen, elastin, and lipopigments). Fluorescein and indocyanine green (ICG) are fluorescent agents to which enhance fluorescence angiography. Once example is fluorescence-guided identification of tumor margins during surgery as a tool to improve the accuracy and safety of tumor resection (Vo-Dinh 2003).

Furthermore, imaging a larger tissue volume requires light within the NIR spectral range (700 to 900 nm) because the absorption coefficient of tissue is relatively small and

requires depth penetration up to several centimeters. The detection of fluorescent contrast agents is comparable to nuclear imaging methodology, in both modalities the photon sources (fluorescent dye or radionuclide) are distributed through the tissue. Generally, the spectral range of absorption and fluorescence for the dye dictates whether it is detectable on tissue surfaces (UV-vis dyes) or from deeper tissue (NIR dyes) (Vo-Dinh 2003).

CHAPTER 2

PHOTO-PHYSICAL CHARACTERIZATION TECHNIQUES

Fluorescent measurements are classified into two categories: continuous wave and time-gating mode. Steady-state (or continuous wave) measurements are the most commonly performed, with a constant illumination and observation for excitation and emission spectra and intensity. When the sample is first exposed, the steady-state is reached almost instantaneous then the emission spectrum is recorded. On the contrary, time-resolved measurements determine the intensity decays by exposure to a pulse of light, where the pulse width is shorter than the decay time of the sample. In this chapter, two types of time-resolved experimental set ups (e.g., spectroscopy and microscopy) were assembled and described. Both continuous and time-resolved measurements are used in future chapters (Lakowicz 2006).

2.1 Time Resolved Measurements

Temporal and spectral gating measurements are spectroscopy techniques that detect highly sensitivity luminescent probes (Cidalia M.G, Harte et al. 2008; Elia 2008). In order to achieve the maximum luminescence intensity, the luminophore is required to be raised to an excited state (or population inversion) following the excitation pulse. The intense radiance of a laser beam ensures a population inversion is achieved within the excitation interval. Lanthanides ion probes typically require excitation in the late UV region (~340 nm) (Selvin, Rana et al. 1994). By distinguishing between long-lived and short-lived emission, temporal and spectral techniques are capable of detecting lanthanide

emission, even with samples containing a significant short-lived autofluorescence (e.g., biological specimens or tissues) (Elia 2008). Time-resolved spectroscopy can be applied in many areas such as molecular phosphorescence, fingerprint detection, immunoassay, enzyme activity measurements, etc. Luminescence detection of fingerprints provides great sensitivity with treatments such as rhodamine 6G staining and ninhydrin/zinc chloride (Alaoui 2007).

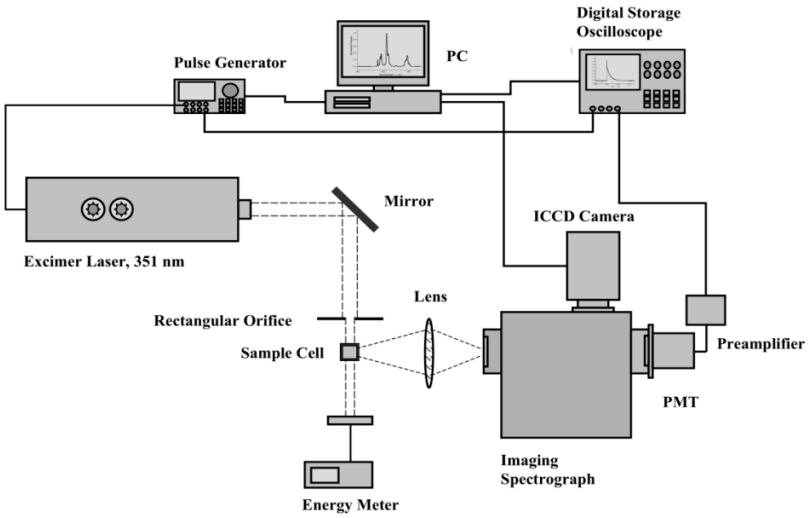

Figure 2.1 Schematic of time resolved spectroscopy for emission spectra and lifetime measurements experimental set up.

Figure 2.1 presents a home built set up of a time-resolved spectroscopy instrument. Excimer lasers are often used in many of today's most advanced industrial, scientific, and medical applications which require ultraviolet and deep-ultraviolet light sources, applications include: microlithographic masking imaging, micromachining, fiber Bragg grating writing, dye laser pumping, pulsed laser deposition, and corneal reshaping (Delmdahl, Spiecker et al. 2003). An imaging device (e.g., Intensified Charged Coupled Device, ICCD camera) is synchronized to a pulse laser that turns on with a delay after the laser pulse and turns off before the next laser pulse. Short-lived background signal decays

before the device is turned on, while the signal from long-lived luminescence is accumulated. Lanthanide ion spectra accumulated in the time-resolved measurements typically indicate a single exponential decay mode. Gated luminescent studies with the photomultiplier tube confirmed this characteristic for the complex probes (Froehilich 1989).

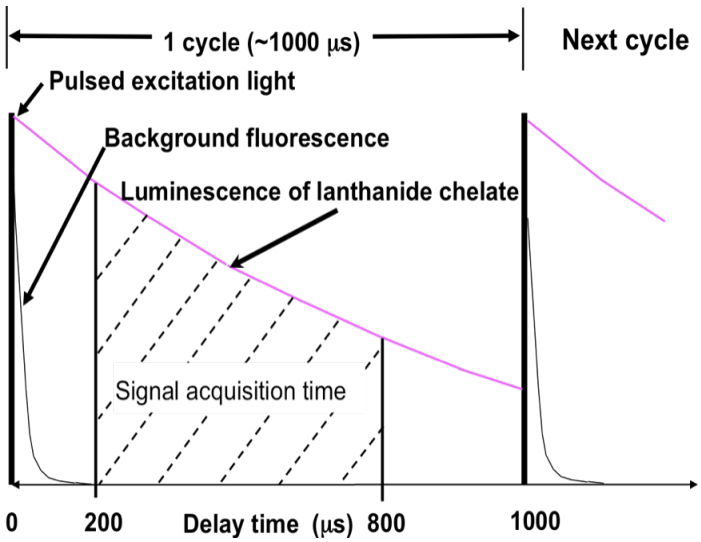

Figure 2.2 Schematic of time-gating mode detection with decays of autofluorescence and luminescence of lanthanide chelate.

Time-gated luminescence techniques operate within the time-domain, directed toward detection of events occurring at longer time scales (e.g. phosphorescence). The detector is gated off while a brief pulse of light is used to excite emission from the sample. The detector is maintained in the off state for a resolving period (gate-delay) while short-lived (< 1 μs) fluorescence fades beyond detection. The detector is then able to capture luminescence in the absence of autofluorescence, increasing the signal to noise ratio (SNR). The substantial increase in the SNR is a critical factor when searching for rare target organisms encountered in autofluorescence environments (Connally and Piper 2008; Connally 2011) (Figure 2.2). Since lanthanide complexes have long lifetimes, that

facilitate time resolve luminescence detection as well as large Stokes shifts (> 150 nm) and multiple, narrow emission bands are easy to isolate spectral signals.

2.2 Total Internal Reflection Fluorescence Microscopy

Cell/substrate contact sites in living cells in culture can be studied with interference reflection microscopy (IRM) or Total Internal Reflection Fluorescence Microscopy (TIRFM). IRM illuminates the cell by visible light through a transparent glass support where the light is partially reflected from different interfaces through the semitransparent sample permitting the visualization of cell/substrate at high contrast but membrane/substrate distances must be interpreted with caution (Giebel, Bechinger et al. 1999; Axelrod 2001). This work used the TIRFM technique.

Early time-resolved luminescence microscopes used mechanical choppers to modulate the continuous wave excitation light sources and effectively shutter charged couple device (CCD) cameras. ICCD cameras offer an effective means of shuttering emission light, as the image intensifier can be gated on/off with nanosecond resolution while simultaneously amplifying the emission signal. The latest ICCD cameras offer a quantum efficiency approximately 50% and small effective pixel sizes (~10 μm) (Gahlaut and Miller 2010). Unlike photomultipliers or avalanche photodiodes, conventional CCDs cannot amplify the number of electrons generated from each photo impact. However, they are capable of integrating charge for several minutes when cooled to minimized thermally induced noise (Connally and Piper 2008).

Overtime TIRFM (Figure 2.3) and multiphoton scanning microscopes were based on shifting the detection pinhole to collect delayed luminescence from a position lagging

the rastering laser beam. The TIRFM utilizes a light beam in the substrate that is obliquely incident upon the substrate liquid interface at an angle greater than the critical angle of refraction (Figure 2.3). At this angle, the light beam is totally reflected by the interface. An electromagnetic field called "evanescent wave" penetrates into the liquid medium and propagates parallel to the substrate surface. The field propagates parallel to the surface with an intensity that decays exponentially at a perpendicular distance from the surface. Therefore, a fluorescent molecule in the evanescent wave can become excited and emit fluorescence; molecules far away will not be excited. For objects adhering to the surface, only fluorescent molecules in closest contact with the substrate will be energized (Axelrod 1981). Typically, the cell membrane is separated from the substrate by 100-150 nm (Giebel, Bechinger et al. 1999; Axelrod 2001).

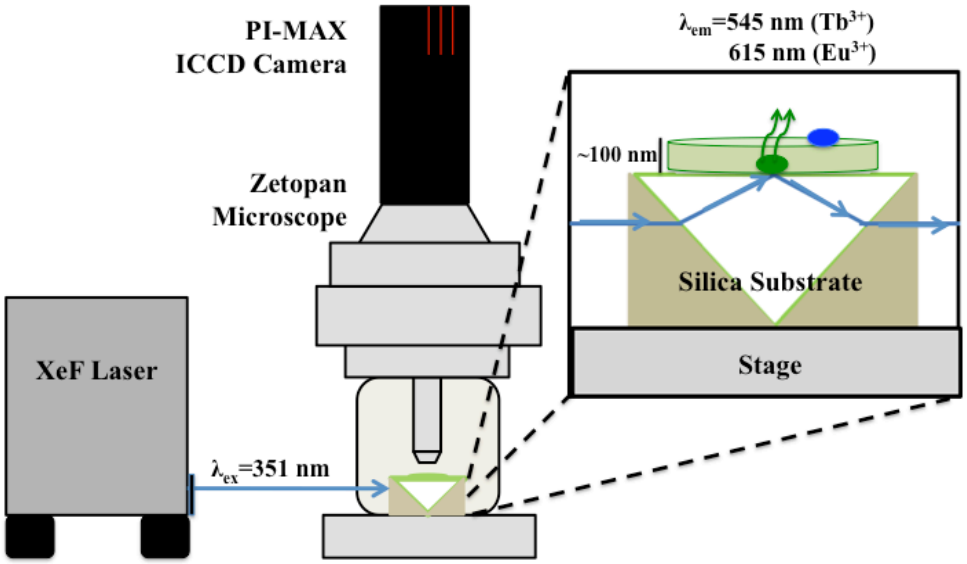

Figure 2.3 Schematic of home built TIRF Microscopy set up with silica substrate.

CHAPTER 3

LUMINESCENT PROBES FOR ULTRA-SENSITIVE DETECTION OF BIOPOLYMERS

Chapters 1 provides an in depth background for luminescent probes and the requirements of biological applications. Chapter 2 includes the time-gated techniques various techniques used in future chapters. In Chapter 3, the synthesis and characterization of long-lived luminescent probes using time-resolved measurements is presented. Novel amine-reactive derivatives of lanthanide-based luminescent labels of enhanced brightness and metal retention were synthesized and used for detection of complementary DNA oligonucleotides in the context of molecular beacons. Time-resolved acquisition of the luminescent signal developed upon hybridization of the probe to the target allowed to avoid short-lived background fluorescence of the media and achieve high sensitivity of detection, which was less than 1 pM. This value is about 50-100 times better than that achieved with conventional fluorescence-based molecular beacons, and 10-60 times better than previously reported for the other lanthanide-based hybridization probes. This allows use of the developed probes in a variety of biological applications that rely on highly sensitive detection (Figure 1.7).

3.1 Introduction

Some lanthanide chelates possess a unique spectral property known as luminescence (Dickson, Pollak et al. 1995; Dickson, Pollak et al. 1995; Heyduk and Heyduk 1997;

Selvin 2002; Johansson, Cook et al. 2004; Parker 2004; Hemmila and Laitala 2005; Bunzli 2006; Petoud, Muller et al. 2007). The principle features of luminescence are long lived excited states (from microseconds to milliseconds range) and sharply spiked emission spectra. Temporal and spectral gating allows unusually sensitive detection of lanthanide emission even in samples containing significant short-lived auto-fluorescence (e.g., biological specimens or tissues). This makes these compounds interesting in a wide variety of technical and biological tasks such as tracing analysis, immunoanalysis, tissue-specific imaging, and ultimately, detection of single molecules in the living cell. Despite the benefits offered by this technique, its spread is impeded by limited choice of instrumentation and extremely high price of the commercial probes. Yet existing probes could be improved to meet the requirements of new challenging applications.

Due to very low absorbance ($\varepsilon < 1\ M^{-1}cm^{-1}$), lanthanide ions are required to be "pumped" which is achieved by tethering the lanthanide ion (through chelation) to an appropriate organic fluorophore (antenna). In such constructs, the energy absorbed by antenna is transferred radiationlessly to the lanthanide, which finally emits the light. The chelating group also shields the lanthanide ion from quenching effect of the media, increasing the quantum yield of the probe. Development of new luminescent probes is challenging, since the energy transfer from antenna to lanthanide is complex and not yet understood in details, being very sensitive to subtle structural variations in antenna fluorophore. Another challenge is the necessity to combine three functional units in the same reporting probe: antenna, lanthanide chelated metal, and cross-linking group (for the attachment to the biomolecule of interest). This requires a complex synthetic strategy and eventually leads to compounds, whose size often exceeds 1000 Da. Two commonly

used classes of lanthanide chelates are diethylenetriaminepentaacetic acid (DTPA) and tetraethylenetetraminohexaacetic acid (TTHA). These chelates attach to the 7-amino quinolones (Selvin and Hearst 1994; Selvin, Rana et al. 1994; Li and Selvin 1997; Chen and Selvin 1999; Chen and Selvin 2000; Ge and Selvin 2003; Ge and Selvin 2004; Ge and Selvin 2008)known as DTPA and/or TTHA-cs124 derivatives. The advantage of these classes is high quantum yield, high solubility in water, and the possibility to introduce chemical modifications in the fluorophore for spectral optimization of energy transfer to lanthanide, or for the attachment of a cross-linking group. A number of methods for the conjugation of these chelates to biomolecules have been suggested. One of them is accomplished through the dianhydride form of DTPA. This is where one anhydride function modifies the amino group of chromophore, while the other reacts with amino group of a biomolecule (Selvin, Rana et al. 1994). Even though this approach is technically simple, it raises concerns about the side reactions (modification of the other nucleophilic groups) due to high reactivity of anhydrides. The second approach takes advantage of the conjugation of one of DTPA anhydride group with the cs124 moiety, followed by reaction of the remaining anhydride function with the diamine. The unmodified amino group of the resulted adduct can then be converted to amine-reactive isothiocyano or thiol-reactive groups (Ge and Selvin 2003). This mode of attachment of the cross-linking group weakens the lanthanide retention in the chelate by eliminating one ligating carboxylate and reduces brightness (Ge and Selvin 2008) (30-1000 %) due to quenching effect of additional coordinated water. These factors can potentially restrict *in vivo* applications where high concentration of metal scavengers is an issue (e.g., intracellular imaging). Analogous derivatives of coumarine fluorophore have been

suggested and used in biophysical studies (Heyduk and Heyduk 1997). However, comparing to the quinolone counterparts they are less bright and do not support Terbium (Tb^{3+}) luminescence. To further perfect the lanthanide probes, two novel approaches for the introduction of cross-linking groups into DTPA and/or TTHA-cs124 chelates by modification of the chromophore moiety were developed. It was demonstrated that the synthesized luminescent probes (Figure 3.1) are more resistant to the EDTA challenge then previously described DTPA-cs124-based probes, and that some of them are highly luminescent. These compounds were validated as luminescent labels in the context of molecular beacon probes widely used for DNA and RNA detection (Tyagi and Kramer 1996). The achieved sensitivity was about 0.5-1 pM, which is the best of ever reported for non-amplified DNA detection systems (Figure 1.7).

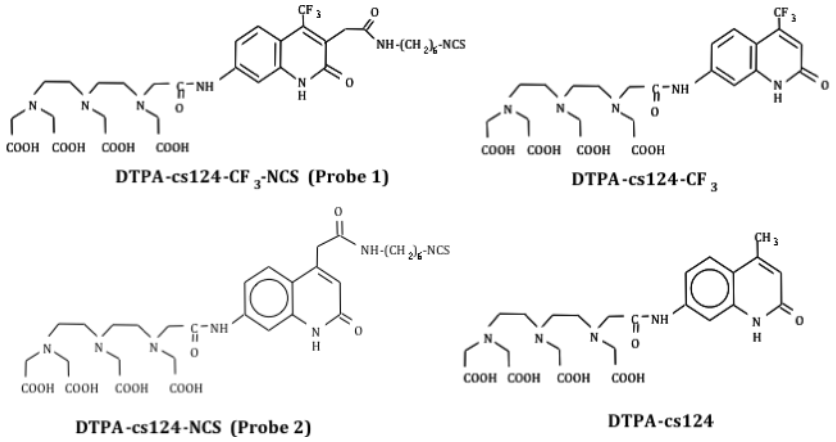

Figure 3.1 The structure of synthesized reactive luminescent probes and reference compounds.

3.2 Experimental Section

3.2.1 Synthesis

The following reagents were purchased from Aldrich: diethylenetriaminepentaacetic acid dianhydride (DTPA); triethylamine; 1,3-phenylenediamine; ethyl 4,4,4-trifluoroacetoacetate; ethylacetoacetate; 1,3-dicyclohexylcarbodiimide (DCC); ethylenedianime; N-trityl-1,4-diaminobutane; N-trityl-1,6-diaminobutane; triphenylmethylchloride; methylbromacetate; anhydrous dimethylformamide and dimethylsulfoxide; 1-butanol; ethylacetate; chloroform; acetonitrile; ethanol; sodium and potassium hydroxide; $TbCl_3$ and $EuCl_3$; silica gel TLC plates on aluminum foil (200 mm layer thick with a fluorescent indicator). Distilled and deionized water (18 MΩ cm^{-1}) was used. All experiments including lanthanide complexes preparation and use thereof were performed either in glassware washed with mixed acid solution and rinsed with metal-free water, or in metal-free plasticware purchased from Biorad. All chemicals were the purest grade available.

3.2.1.1 Probe 1 (Scheme 3.1A).

1. 7-amino-4-trifluoromethyl-3-carbomethoxymethyl-2 (1H) quinolone (II) (cs124CF_3 - CH_2COOCH_3) Trifluoroacetoacetate (2.2ml, 15 mmol) and KOH (0.86 g, 15 mmol) were mixed in 7 ml of dimethylformamide and stirred at 40^0 C until dissolved. To this mixture, 1.5 ml of methylbromoacetate was added and the solution was incubated overnight at room temperature. Then 0.3 g of KOH was added and incubation continued at 60^0 C for 1 h. The mixture was diluted by 20 ml of water and extracted with chloroform. The organic layer was collected, dried over anhydrous sodium sulfate and

evaporated *in vacuo* first at 30^0 C and then at 70^0 C for 30 minutes. The residue (1.9 g, product **I**) was dissolved in 3.5 ml of DMSO and 0.76 g (7 mmol) of 1,3-phenylenediamine was added, followed by incubation at 110^0 C for 6 h. Under these conditions four fluorescent products were detected by TLC in ethyl acetate as developing solvent: R_f = 0.9 (green-blue fluorescence); R_f = 0.45 (blue fluorescence); R_f = 0.3 (blue fluorescence), and R_f = 0.03 (green-blue fluorescence). The mixture was diluted with 30 ml of 0.05 M aqueous NaOH (2 x 15 ml) and extracted with ethyl acetate (2 x 40 ml). The aqueous layer was separated and treated as described below (section **3.2.1.1.2**). The organic layer was extracted with 0.1 M citric acid, and then collected, dried over anhydrous sodium sulfate and evaporated *in vacuo*. The residue was subjected to silica gel chromatography on 40 ml column using hexane/acetone mixture (3:1) as eluent. The fractions corresponding to the products migrating with R_f = 0.45 (product **II**) were collected and evaporated to dryness. The residue was additionally washed with chloroform and dried. *Yield - 130 mg*. UV: λ_{max}=365 nm (ε= 14,300 M^{-1} cm^{-1}), λ_{min}=295 nm (ε= 2,800 M^{-1} cm^{-1}). ^{1}H NMR chemical shifts (d) in DMF are: 3.65 (3H, methyl), 3.94 (q, 2H, 3-methylene, J=3.6), 6.24 (broad, 7 amine), 6.72 (m, 1H, 6H), 6.72 (m, 1H, 8H), 7.48 (1H, 5H), 11.9 (broad, amide).

2. 7-amino-4-trifluoromethyl-3-carboxy-2(1H)quinolone(III) (cs124CF_3-CH_2COOH)

To a 100 mg of product **II** dissolved in 2 ml of dioxane 1 ml of 1 M aqueous NaOH was added. After 4 h incubation at 50^0C, the mixture was diluted to 15 ml by water and extracted with ether. The product was precipitated from aqueous phase by addition of

citric acid to pH 3-3.5, collected by centrifugation, washed a few times by water until neutral reaction, and dried *in vacuo*. *Yield - 70 mg.*

The aqueous phase obtained after ether extraction (see previous section) containing product **III** was acidified by citric acid to pH 3-3.5, the precipitate collected, washed a few times with water, dried and combined with the above. Re-crystallization from ethylacetate afforded pure product **III**. *Total Yield 200 mg*. ^{1}H NMR chemical shifts (d) in DMF are: 3.93 (2H, 4 methylene), 6.19 (2H broad, 7 amine), 6.71 (1H, 6H), 6.71 (1H, 8H), 7.48 (1H, 5H), 11.85 (broad, amide), 12.75 (broad, carboxyl).

3. cs124-CF_3-CH_2C(O)-NH $(CH_2)_6$NH-Tr (IV) One hundred milligrams (~0.3 mmol) of product **III** was dissolved in 8 ml of THF and supplemented with 210 mg (1 mmol) of DCC. In 1 h TLC analysis in ethyl acetate-ethanol (10:1) revealed a single product (R_f = 0.8) with intense blue fluorescence. Four hundred fifty micromoles of N-trityl-1, 6-diaminobutane were added and incubation continued for another 30 min at 20^0 C. TLC in ethyl acetate-ethanol (10:1) developing system revealed the main reaction product (R_f = 0.7). The mixture was diluted with 20 ml of 0.1 M aqueous Na_2CO_3 and extracted by equal volume of chloroform. Then the organic phase was collected and rinsed with 0.2 M citric acid, dried over anhydrous sodium sulfate, and the solvent removed by evaporation under reduced pressure. The product was purified by silica gel chromatography using ethyl acetate-ethanol (10:1) mixture as eluent. *Yield - 160 mg.* ^{1}H NMR chemical shifts (d) in DMF are: 1.45 (m, 8H), 1.65 (m, 2H), 1.78 (m, 2H), 2.03 (q, 2H, J=7.25), 2.41 (t, 1H, J=7.2), 3.08(q, 2H, J=7.2), 3.82 (q, 2H, 4CH_2-, J=4.0), 6.14 (s, 2H, broad, 7 amine),

6.7 (1H, 8H), 6.7 (1H, 6H), 7.18 (t, 3H, p-ArH, J=7.2), 7.30 (t, 6H, m-ArH, J=7.4), 7.48 (d, 6H, o-ArH, J=7.4), 7.48 (1H, 5H), 11.75 (1H, broad, amide).

4. cs124-CF_3-$CH_2C(O)$-$NH(CH_2)_6N=C=S$ (V) One hundred forty milligrams of compound **IV** were dissolved in 2 ml of 90% acetic acid and incubated at 90º C during 15 min. After evaporation *in vacuo* the resulting residue was suspended in water and extracted with ether to remove triphenylcarbinol. The aqueous phase was evaporated to dryness. The resulting residue was dissolved in 2 ml of methanol and 80 mg of thiocarbonyldiimadazole were slowly added to this solution under rigorous agitation. After 10 min incubation at room temperature the mixture was supplemented with 100 µl of trifluoroacetic acid and kept at 50ºC. After 1 h TLC analysis in ethyl acetate-ethanol (12:1) system, revealed near quantitative conversion of the original compound (R_f = 0.05) to isothiocyanate (R_f = 0.4). The product was purified by column chromatography using the same eluent. *Yield - 60 mg.* ^{1}H NMR chemical shifts (d) in DMF are: 1.35 (m, 4H), 1.46 (m, 2H), 1.65 (m, 2H), 3.13 (m, 2H, J=7.25), 3.69 (t, 1H, J=7.2), 3.08(q, 2H, J=7.2), 3.82 (q, 2H, $3CH_2$-, J=3.7), 6.14 (s, 2H, broad, 7 amine), 6.7 (1H, 8H), 6.7 (1H, 6H), 7.48 (m, 1H, 5H), 7.76 (t, 1H, J=5.5) 11.77 (1H, broad, amide).

5. Tb^{3+}, Eu^{3+}, Dy^{3+}, and Sm^{3+} complexes of DTPA-cs124-CF_3-NCS (probe 1) Thirty milligrams (0.1 mmol) of **V** were added to a solution of 80 mg (0.3 mmol) of DTPA dianhydride in 0.8 ml of DMSO. After incubation (45 min at 50°C) the mixture was supplemented with 10 ml of ether, the precipitate was spun down, washed by ether, air dried, dissolved in 1 ml of DMF and mixed with 0.3 ml of water. After incubation for 10

min at 45^0 C the mixture was diluted with 5 ml of water and extracted with 40 ml of butanol. The organic phase was separated and divided into four equal parts. Each portion was mixed with 0.3 ml of 0.1 M solution of a lanthanide trichloride. After vigorous agitation the organic phase was collected and concentrated by co-evaporation with water *in vacuo* at 30ºC. Analytical TLC using acetonitrile-water system (3:1) as developing solvent revealed two main products in case of each Ln^{3+} (R_f=0.25 and 0.5). The products with R_f=0.5 (desired compound) were purified using preparative TLC in the same system. The fluorescent material was eluted by 50% aqueous ethanol, and obtained as a colorless powder after evaporation *in vacuo*. UV: λ_{max}=347 nm (ε=14,800 M^{-1} cm^{-1}), λ_{min}=270 nm (ε=4,700 $M^{-1}cm^{-1}$). MS: Eu^{3+}DTPA-cs124-CF_3-CH_2C (O)-$NH(CH_2)_6N$=C=S (-H^+) 950.1 (found), 950.0 (calc). Ln^{3+} complexes of DTPA-cs124-CF_3 were obtained using the same protocol.

3.2.1.2 Probe 2 (Scheme 3.1B). 1. 7-amino -4- carboethoxymethyl -2 (1H) quinolone (VII) Suspension of 1.36 g (10 mmol) of $ZnCl_2$ in 5 ml of DMSO was supplemented with 1.08 g (10 mmol) of 1,3-phelylenediamine and 2.02 g (10 mmol) of diethyl-1, 3-acetonedicarboxylate. The mixture was kept at 95-100^0C for 24 h. TLC in chloroform/ethanol (10:1) detected one main fluorescent product (R_f = 0.35). The mixture was diluted with 8 ml of ethanol, poured into 150 ml of ice-cold 0.1 M citric acid and left for 3 h at 4^0C. The residue was filtered and successively washed with water (2 x 10 ml), hot acetonitrile (2 x 5 ml) and dried *in vacuo*. *Yield - 1.4 g (60 %).* ^{1}H NMR chemical shifts (d) in DMSO are: 1.17 (t, 3H, -$OCH_2C\mathbf{H}_3$, J=7.2), 3.76 (s, 2H, 3-methylene), 4.06 (q, 2H, -$OC\mathbf{H}_2CH_3$, J=7.2), 5.81 (2H, broad, 7 amino), 6.01 (s, 1H, 3H), 6.37 (d, 1H, 8H,

J=2.4), 6.43 (dd, 1H, 6H, J_1=7.2, J_2=2.4), 7.25 (d, 1H, 5H, J=7.2), 11.28 (1H, broad, amide).

2. 7-amino- 4-carboxamido (6-aminohexyl) methyl-2 (1H) quinolone (VIII) Pre-melted 1,6-diaminohexane (2 g, 17 mmol) was mixed with 0.5 g (2 mmol) of 7-amino-4-carboethoxymethyl-2 (1H) quinolone. After incubation (15 h, 90^0 C) the mixture was poured into 30 ml of water. The precipitate was washed with water (3 x 30 ml), ethyl acetate (3 x 20 ml), then stirred with hot methanol (50 ml), filtered, and filtrate evaporated to dryness *in vacuo*. The product appeared as light-brown crystals. *Yield - 0.5 g.* ^{1}H NMR chemical shifts (d) in DMSO are: 1.2-1.4 (m, 10H), 3.04 (q, 2H, a-CH_2, J=7.2), 3.49 (s, 2H, 4-methylene), 5.75 (2H, broad, 7 amino), 5.98 (s, 1H, 3H), 6.36 (d, 1H, 8H, J=2.4), 6.43 (dd, 1H, 6H, J_1=7.2, J_2=2.4), 7.38 (d, 1H, 5H, J=7.2), 8.07 (t, 1H, amide, J=7.2), 11.3 (1H, broad, amide quinolone).

3. 7-amino-4-carboxamido (6-isothiocyanohexyl) methyl-2 (1H) quinolone (IX) To a solution of 63 mg (0.2 mmol) of product **XIII** in 4 ml of methanol 44 mg (0.22 mmol) of 1,1'-thiocarbonyldiimidazole were added. In 5 min the mixture was supplemented with 10 ml of TFA and incubated for 40 min at 50^0 C. The solvent was removed by evaporation *in vacuo*, the product washed with water and purified by column chromatography on silica gel using chloroform/ethanol mixture (4:1) as eluent. *Yield - 40 mg.* ^{1}H NMR chemical shifts (d) in DMSO are: 1.2 - 1.5 (m, 6H), 1.60 (m, 2H, e-CH_2, J=7.2), 3.04 (m, 2H, a-CH_2, J=7.2), 3.49 (s, 2H, 4-methylene), 3.64 (t, 2H, z-CH_2, J=7.2), 5.75 (s, 2H, broad, 7 amine), 5.98 (s, 1H, 3H), 6.36 (d, 1H, 8H, J=2.4), 6.43 (dd, 1H, 6H,

J_1=7.2, J_2=2.4), 7.38 (d, 1H, 5H, J=7.2), 8.07 (t, 1H, amide, J=7.2), 11.20 (1H, broad, amide quinolone).

4. Tb^{3+}, Eu^{3+}, Dy^{3+}, and Sm^{3+} complexes of DTPA-cs124$_3$ and DTPA-cs124-NCS (probe 2) These products were obtained and purified essentially as described for analogous compounds in section **3.1.1.5**, but incubation time of corresponding isothiocyano compound (**IX**) with DTPA dianhydride was 15 min at 20^0 C. UV: λ_{max} = 341 nm (ε=18,900 M^{-1} cm^{-1}), λ_{min}=308 nm (ε=10,000 M^{-1} cm^{-1}). MS: Tb^{3+} -DTPA-cs124 and DTPA-cs124-NCS (-1) 888.3 (found), 888.0 (calc); Eu^{3+} -DTPA-cs124$_3$ and DTPA-cs124-NCS (-1) 882.3 (found), 882.0 (calc).

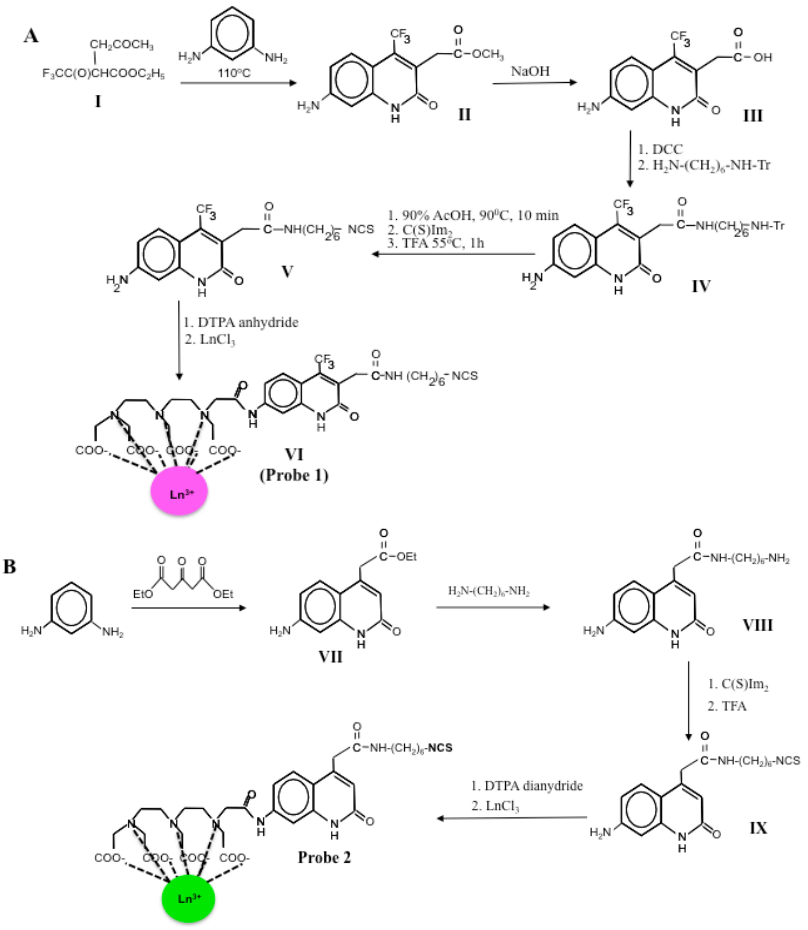

Scheme 3.1 Synthetic scheme of Probes (**A**) **1** and (**B**) **2**.

3.2.2 Physical Methods

Excitation and emission fluorescence spectra in a steady state mode were recorded using QuantaMaster 1 (Photon Technology International) digital fluorometer at ambient temperature. Time-resolved and gated luminescence measurements were performed using a home-built experimental set-up (Figure 2.2). A suprasil fluorescence cell filled with sample solutions was irradiated by pulsed (ca. 15 ns) UV light from an excimer laser (351 nm, XeF). Before passing through the cell the laser beam was formed by a rectangular aperture 0.5 cm x 1.0 cm (width x height). Fluorescence from the cell collected at 90^{o} was focused onto the entrance slit of a grating spectrograph (SpectraPro-300i, Acton Research Corp., diffraction grating 150 groove/mm blazed at 500 nm) using fused silica lens with the focal distance of 2.5 cm. The spectrograph was equipped with a gated intensified CCD Camera (ICCD-MAX, Princeton Instruments) to record the transient spectra. The slit width of 0.5 mm was used in the time-resolved luminescence measurements, which corresponds to the spectral resolution of 5 nm. Time-gated spectra were recorded with the spectral resolution of 0.3 nm (the slit width of 0.01 mm combined with the pixel size of the ICCD camera of 0.026 mm). The ICCD gating, with a delay after the laser pulse, was used to determine the temporal behavior of the transient fluorescence. In the measurements of the luminescence lifetimes, the light was diverted to a photomultiplier tube mounted on the exit slit of the spectrograph. The PMT signal was preamplified and averaged using a digital storage oscilloscope (LeCroy 9310A). High resolution spectra were recorded with a time delay of 1 ms and gate width of 1 ms for probe 1 chelated with Eu^{3+} and Sm^{3+} and probe **2** chelated with Tb^{3+} and Dy^{3+} (Figure 3.3).

3.3 Results

3.3.1 The Synthesis and Properties of Cross - Linkable Lanthanide Chelates

The structure of the synthesized luminescent lanthanide probes is presented in Figure 3.1. These probes are derivatives of previously described cs124-CH_3 and cs124-CF_3 fluorophores (Selvin and Hearst 1994; Selvin, Rana et al. 1994; Li and Selvin 1997; Chen and Selvin 1999; Chen and Selvin 2000; Ge and Selvin 2003; Ge and Selvin 2004; Ge and Selvin 2008). For the synthesis of these compounds the approach was based on condensation of 1,3-phenylenediamine with an ester of acetoacetic acid derivative. Scheme 3.1A presents the synthetic strategy developed by for probe **1**. Alkylation of trifluoroacetoacetate by methylbromacetate in the presence of proton acceptor produced trifluoroacetylmethylethylcuccinate (**I**). Reaction of the later with 1,3-phenylenediamine afforded fluorescent quinolone derivative **II**, which was converted to corresponding carboxyl derivative **III** by saponification. The amino function in this compound was intended to be introduced by treatment with DCC in the presence of 4-nitrophenol and subsequent reaction of nitrophenyl ester with aliphatic diamine. Surprisingly, incubation yielded the product that did not contain 4-nitrophenol. The UV spectrum of this product differed significantly from that of product **III**. In aqueous medium this product converted into **III** with half-time about 30 min at 20^0C. Incubation of this product with aliphatic amines resulted in acylation of the amino groups. Most likely, this reactive intermediate emerged as a result of intramolecular acylation of the amide oxygen of **III** by activated carboxylate. Incubation of this compound with mono tritylated 1,6-diaminohexane yielded desired compound **IV**. After deprotection the resulting aminoalkyl derivative was converted to isothiocyanate **V** by subsequent treatment with thiocarbonyldiimidazole and

trifluoroacetic acid. Under used conditions aromatic amino group of the compound remains intact. Acylation of the compound **V** by DTPA anhydride in anhydrous medium followed by hydrolysis of the second anhydride group afforded compound **VI** (probe **1**) that was separated from the excess of DTPA by partitioning in butanol/water. Further addition of aqueous lanthanide trichloride to butanol extract led to complexation of a lanthanide to the probe. The lanthanide complexes were analyzed and purified by TLC in acetonitrile -water developing system that was proved to be highly efficient (see Figure 3.2).

The developed strategy for the synthesis of probe **2** is shown in Scheme 3.1B. The first step of the synthesis was based on the published protocol (Ge and Selvin 2003) that includes incubation of m-phenylenediamine with diethyl 1,3-acetonedicarboxylate at high temperature to yield the quinolone derivative **VII**. Using mild Lewis acid ($ZnCl_2$) as a catalyst allowed lowering the reaction temperature resulting in dramatic improvement of the yield of the product comparing to the published protocol (from <1 % to ca. 60%). The product with a diamine (was taken in few - fold excess to avoid cross-linked products) at high temperature resulted in formation of aminoalkyl derivative **VIII** with nearly quantitative yield. Cross-linkable DTPA derivative (**X**, probe **2**) was obtained as in the case of probe **1**.

3.3.2 Absorption Spectra

Absorption spectra of the synthesized cs124-CH_3 and cs124-CF_3 derivatives are shown in Figure 3.1. They were nearly identical to published ones for analogous compounds (Selvin and Hearst 1994; Selvin, Rana et al. 1994; Li and Selvin 1997; Chen and Selvin 1999; Chen and Selvin 2000; Xiao and Selvin 2001; Ge and Selvin 2003; Ge and Selvin

2004; Ge and Selvin 2008). Small red shift of 6 nm was observed for probe **1** (comparing to the reference cs124-CF_3) and probe **2** (comparing to cs124-CH_3). The molar extinction coefficients for DTPA-cs124 and DTPA-cs124-CF_3 were determined by direct comparison of the absorption spectra of the original compounds (ε_{max}=18,900 at 341 nm for cs124 and ε_{max}=14,500 at 360 nm for cs124-CF_3) and their acylated derivatives, which was achieved by monitoring of the spectral change of the reaction mixture during the course of reaction (see Scheme 3.1). The presence of isobestic points in both cases was indicative for conversion of the original compounds to a single reaction product. Indeed, chromatographic analysis confirmed the formation of single acylation products in both cases. Thus, ε_{max}=18,200 at 328 nm and ε_{max}=14,800 at 341 nm values were obtained for DTPA-acylated derivatives of cs124 and cs124-CF_3 respectively. Essentially, the same values were obtained for the probes **1** and **2** (Figure 3.1). A significant difference in the absorption spectra of probes **1** and **2** (18 nm) allows selective excitation by common sources (at 351 nm by excimer XeF laser for probe **2**, and at 365 nm by mercury UV lamp for probe **2**). Such selective excitation is important for the applications relying on simultaneous monitoring of two independent processes in the same mixture.

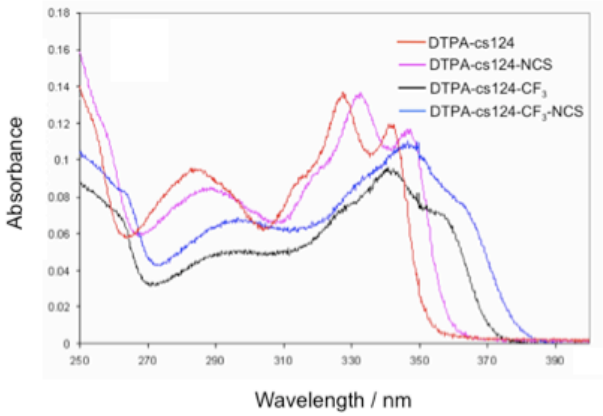

Figure 3.2 UV absorption spectra of synthesized amine reactive luminescent probes and reference compounds.

3.3.3 Emission Spectroscopy of Lanthanide Complexes

Easily observed luminescence of lanthanide complexes is illustrated in Figure 3.3 for probe **2**. All complexes display sharply spiked emission spectra typical for luminescent lanthanide chelates (Figure 3.4). Table 3.1 shows the luminescence intensities of the synthesized reactive lanthanide chelates as well as those for the reference compounds, cs124-CH_3 and cs124-CF_3 described earlier (Selvin, Rana et al. 1994; Chen and Selvin 2000). The process of antenna-mediated lanthanide emission includes the stages of energy transfer from antenna fluorophore to coordinated metal and subsequent emission of photons by excited lanthanide. The first step is the most crucial part of the process because even slight modifications of chromophore-antenna structure can dramatically affect the lanthanide luminescence (Selvin and Hearst 1994). In this work, a synthetic approach was explored to allow the introduction of a cross-linking group in the position 3 (probe **1**) or 4 (probe **2**) of quinolone-based antenna fluorophore. Comparison with reference fluorophores (with non-substituted quinolone position 3, or methyl-substituted position 4) shows the modification affected the brightness of lanthanide chelates in different ways. Thus for cs124-CF_3-based antennae, a significant decrease in brightness was observed for Tb^{3+} (ca 20-fold) and Dy^{3+} (>30-fold) chelates, while the emission of Eu^{3+} and Sm^{3+} chelates was not significantly affected. Similar effect of the substitution was observed before for analogous Tb^{3+}-cs124 chelates (Ge and Selvin 2004). In the case of probe **2**, the substitution of cross-linking group for a methyl in position 4 did not alter significantly the brightness of all lanthanide complexes, moreover, detectable increase in brightness for Eu^{3+} (1.5 fold), Dy^{3+} (1.7 fold), and Sm^{3+} (1.6 fold) complexes was observed. This is consistent with the results (Ge and Selvin 2004) previously obtained for

analogous Tb^{3+} and Eu^{3+} derivatives of cs124 containing a carboxymethyl group at position 4. Surprisingly, detectable luminescence was detected for Tb^{3+}-DTPA-cs124-CF_3 chelates, which were previously reported non-luminescent. The reason is unknown for this discrepancy. As seen in Table 3.1, probe **1** gives the brightest complexes with Eu^{3+} and Sm^{3+}, while probe **2** is optimal for Tb^{3+} and Dy^{3+}. Time resolved measurements revealed single-exponential decay mode for luminescent signal for probe **1** and probe **2** chelates Figure 3.4, which is indicative for homogeneity of the complexes. An example of the emission kinetic curve for probe-**1** is presented in Figure 3.5.

Table 3.1 Emission and Relative Brightness of Lanthanide Chelates at Various Conditions

Compounds	Emission in H_2O, counts	Emission in D_2O, counts	Relative brightness H_2O/D_2O	Relative brightness in H_2O, %	Lifetime in H_2O (ms)	Lifetime In D_2O (ms)	Number of coordinated H_2O molecules
Tb^{3+} complexes (emission at 545 nm)							
DTPA-cs124*	169000	260000	1.53	100	1.5 (1.55*)	2.3 (2.63**)	0.97 (1.1**)
DTPA-cs124-NCS (probe 2)	137000	190000	1.4	81	1.2	1.7	1.03
DTPA-cs124-CF3*	12200	14170	1.16	7.2	0.2	0.2	N/A
DTPA-cs124-CF_3-NCS (probe 1)	833	790	0.95	0.5	N/A	N/A	N/A
Eu^{3+} complexes (emission at 615 nm)							
DTPA-cs124*	5050	22000	4.36	100	0.6(0.62*)	1.6 (2.42**)	1.1 (1.26**)
DTPA-cs124-NCS (probe 2)	7300	25000	3.42	145	0.6	0.2	1.19
DTPA-cs124-CF3*	10350	41000	3.96	205	0.5	1.9	1.54
DTPA-cs124-CF_3-NCS (probe 1)	9450	35000	3.70	187	0.5	1.7	1.7
Dy^{3+} complexes (emission at 482 nm)							
DTPA-cs124 *	2720	10522	3.87	100	0.011	0.033	N/A
DTPA-cs124-NCS (probe 2)	4550	13000	2.86	167	0.009	0.027	N/A
DTPA-cs124-CF3**	555	917	1.75	20	0.0023	0.0045	N/A
DTPA-cs124-CF_3-NCS (probe 1)	N/A	N/A	N/A	N/A	N/A	N/A	N/A
Sm^{3+} complexes (emission at 482 nm)							
DTPA-cs124 *	114	513	4.5	100	0.0082	0.023	N/A
DTPA-cs124-CF3*	192	764	3.98	168	0.0080	0.036	N/A
DTPA-cs124-NCS (probe 2)	180	1010	6.6	158	0.0082	0.034	N/A
DTPA-cs124-CF_3-NCS (probe 1)	230	900	3.91	200	0.0092	0.042	N/A

Source: Ge, P. and P. R. Selvin (2004). Carbostyril Derivatives as Antenna Molecules for Luminescent Chelates. *Bioconjugate Chemistry 15:* 1088-1094.
** model compounds

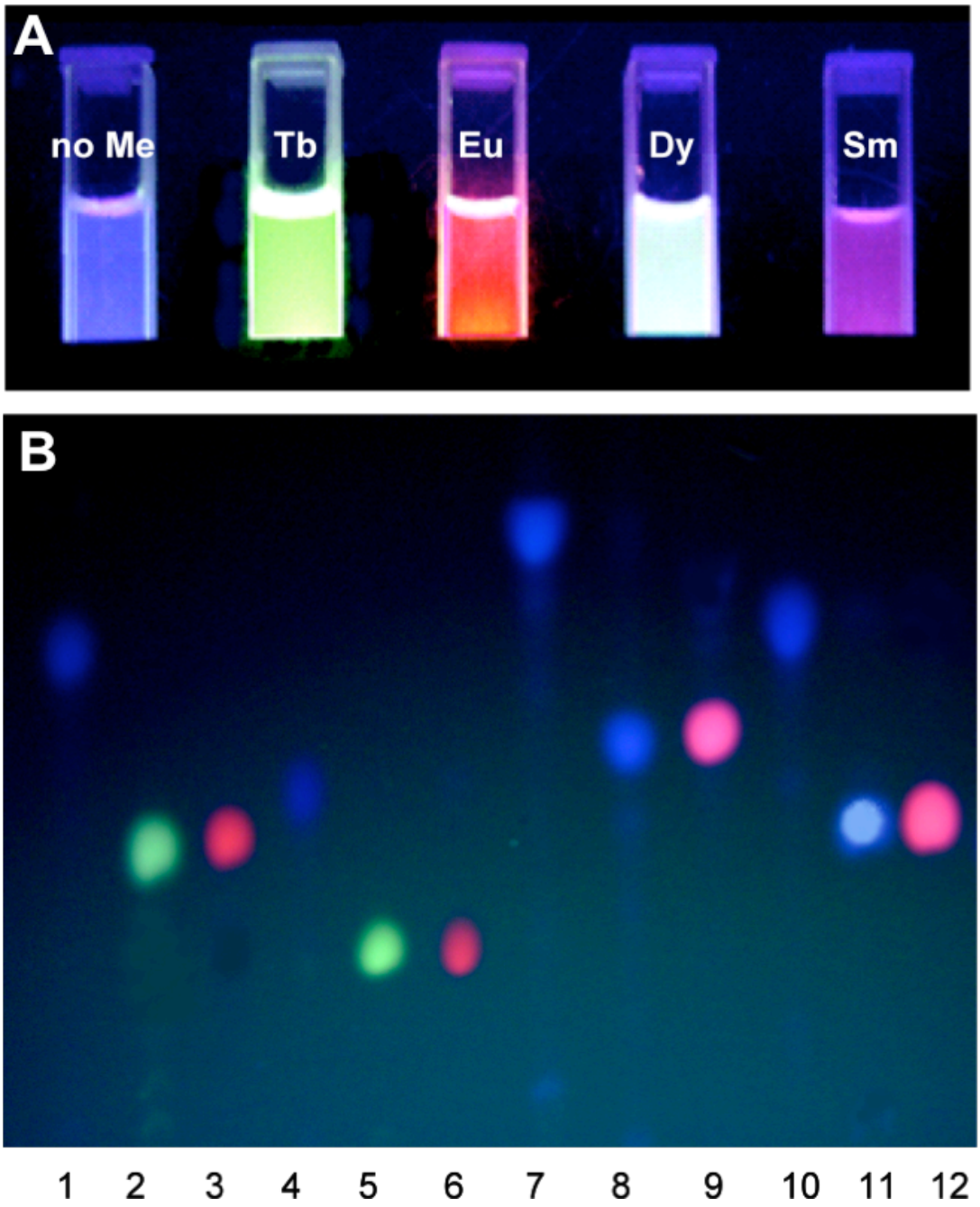

Figure 3.3 Luminescence of synthesized chelates. **A**) Photograph of 50 mM solution of the ligand probe **2** (far left) and its complexes in heavy water with Tb^{3+}, Eu^{3+}, Dy^{3+}, Sm^{3+} (from left to right respectively), excited by standard laboratory transilluminator (308 nm). **B**) Photograph of ligand antenna compounds and their lanthanide complexes after separation by TLC and UV excitation.

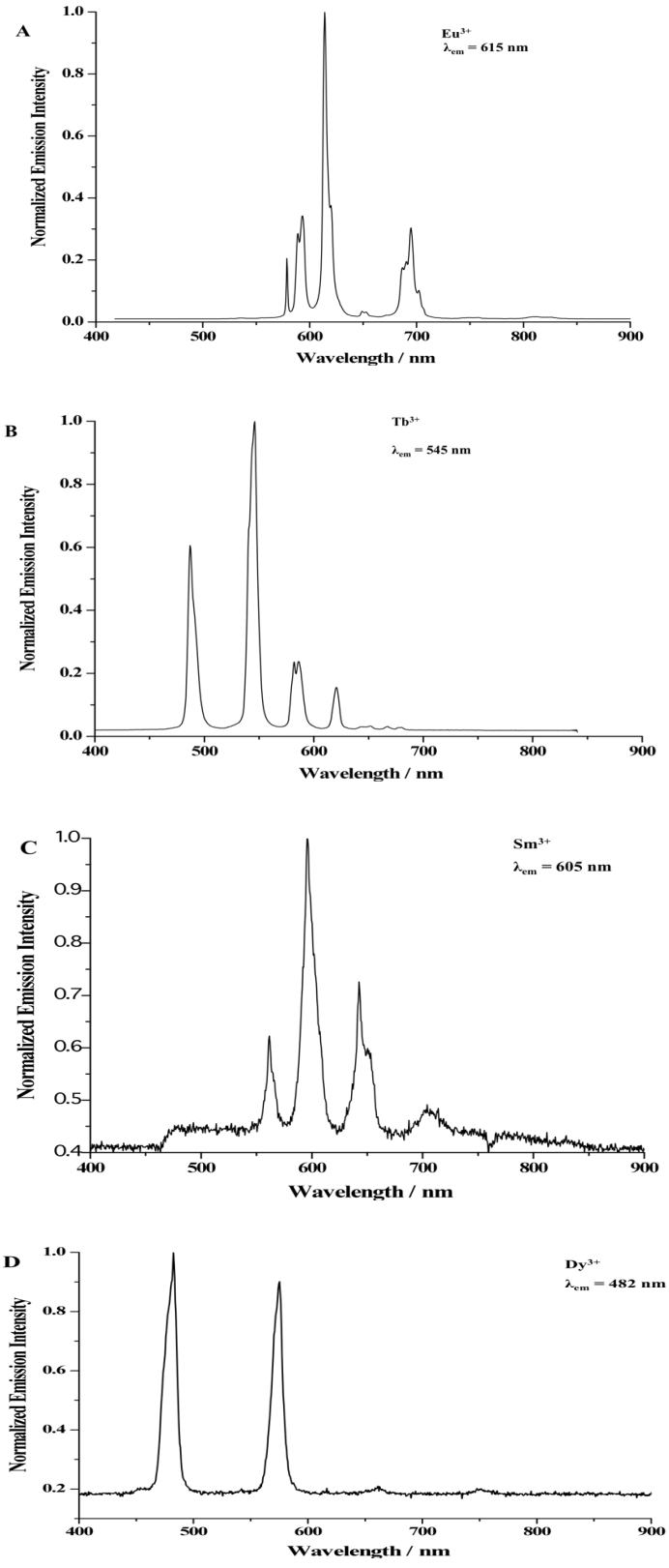

Figure 3.4 Normalized time resolved emission spectra in water for four respective lanthanide ion labeled probes (**A**) Eu^{3+}, (**B**) Tb^{3+}, (**C**) Sm^{3+}, (**D**) Dy^{3+}.

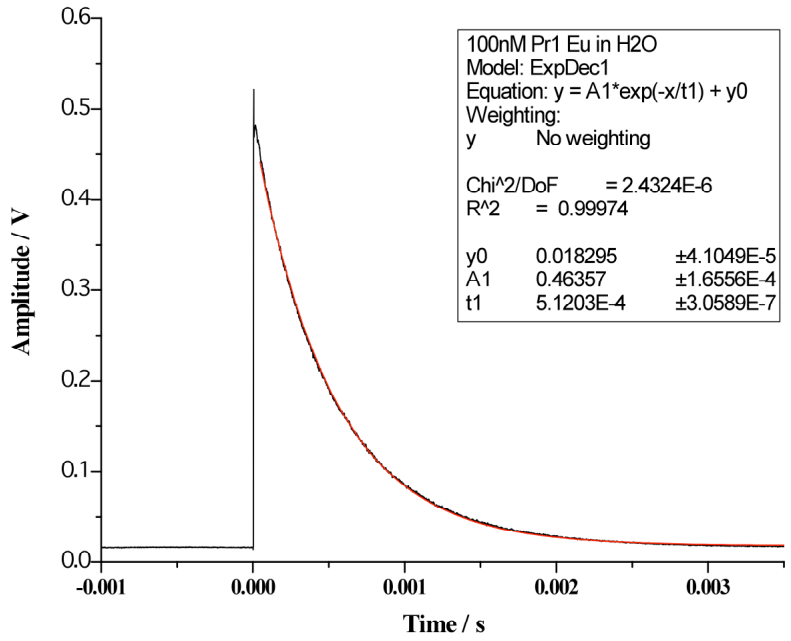

Figure 3.5 Emission kinetic curve for 100 nM Probe **1**-Eu^{3+} in H_2O at λ_{em}=615 nm.

3.3.4 Effect of Heavy Water on the Lanthanide Chelates Emission

Quantum yield of excited lanthanide ion (defined as a probability of the excited state to emit photon) in the antenna-chelate complex strongly depends on the number of coordinated water molecules due to non-radiative dissipation of the energy of the excited state through vibration of O-H bonds (Li and Selvin 1995; Selvin 2002). This process does not occur with heavy water due to different frequency of O-D bond vibration. This effect accounts for enhanced brightness of lanthanide luminescence in heavy water. Indeed, as seen from Table 3.1 for DTPA ligands in D_2O the brightness of the Tb^{3+} chelates was 1.3-1.5 fold higher than in H_2O-based solutions. As expected, the effect was more pronounced for DTPA-Eu^{3+} chelates (~3-3.8 fold) as well as for Dy^{3+} and Sm^{3+} complexes (~ 4-6 fold). The number of coordinated water molecules in Tb^{3+} and Eu^{3+} complexes can be calculated based on luminescence lifetime in water and deuterium oxide-based solutions (Xiao and Selvin 2001). These probes present a close to unity,

which is in agreement to the results reported for similar compounds. The same is expected for Dy^{3+} and Sm^{3+} chelates, since they have analogous coordination chemistry.

3.3.6 Chemical Reactivity of Synthesized Luminescent Probes

Chemical reactivity of the synthesized probes was first evaluated in reactions with aliphatic diamines and cysteine whose reaction products (corresponding thioureas and thiocarbamates) can be easily identified by TLC due to strong retardation effect. Used incubation conditions nearly quantitative conversion of the probes to corresponding reaction products was observed either immediately upon mixing (with 0.1 M cysteine) or after 2-3 h at 56^0 C (with 10 mM diamine), suggesting that isothiocyanate ITC groups in the probes survived purification (Table 3.2). At the same time, non-reactive control chelates (Ln^{3+}-DTPA-cs124, and Ln^{3+}-DTPA-cs124-CF_3) did not change their mobility upon the incubation in the same conditions (Table 3.2).

Table 3.2: R_f Values of Amine Reactive Derivatives with Cysteine

Compound	R_f for original compound	R_f for cysteine reaction product
Probe **1** – Eu^{3+}	0.47	0.29
Probe **2** – Eu^{3+}	0.37	0.26
Probe **2** – Tb^{3+}	0.36	0.23

3.4 Conclusions

Due to lanthanide based probes unique photon emission properties, they are suitable for a wide variety of applications that rely on ultrasensitive detection of biomolecules. Progress in this field depends on the availability of efficient probes. The complexity of energy pathways in luminescent lanthanide chelates, is not fully understood yet leaving room for trials and fails in the field. Even though the first probes of this class were

synthesized more than three decades ago, many of them are being commercialized. The development of new more efficient probes is still in great demand due to emerging challenging applications (design of environment-sensitive probes, single molecule detection, etc.).

New synthetic strategies that obtained highly luminescent probes with high yield improved the existing probes. The synthesized probes are ready-to-use since they contain pre-bound lanthanide, unlike those described in the previous applications, in which the biomolecule of interest was first modified with metal free chelate, followed by addition of a lanthanide (Heyduk and Heyduk 1997; Li and Selvin 1997). The new compounds were validated in the context of molecular beacons-widely known nucleic acid hybridization probes. The testing experiments revealed high sensitivity of detection, unachievable with conventional fluorescence-based molecular beacons. The detection sensitivity was 10-60 times better than previously reported for the other lanthanide-based hybridization probes (Figure 1.7). Also, the brightness of the probes significantly increased in heavy water suggesting the use of this medium to increase the sensitivity of detection.

CHAPTER 4

HIGHLY BRIGHT AVIDIN-BASED AFFINITY PROBES

Chapter 4 presents a study to further increase the sensitivity of lanthanide-based probes by using multiple luminescent labels attached to a carrier molecule, avidin. It was concluded that up to 30 lanthanide chelates could be attached to avidin creating highly bright conjugates. These constructs with Eu^{3+} chelate display a synergistic effect that enhances the brightness of heavily modified samples; while the opposite effect was observed for Tb^{3+} chelates thereby significantly reducing their light emission. This undesirable quenching of Tb^{3+} luminophores was completely suppressed by the introduction of an aromatic spacer between the chelate and the protein attachment site. The estimated detection limit for the conjugates is in the 10^{-14}-10^{-15} M range. This study demonstrated a high sensitivity for the new probes by using them to label living cells of bacterial and mammalian origin.

4.1 Introduction

Long lifetime of lanthanide luminescence allows its highly sensitive detection in time-gated mode (Dickson, Pollak et al. 1995; Dickson, Pollak et al. 1995; Selvin 2002; Parker 2004; Hemmila and Laitala 2005; Werts 2005; Bunzli 2006; Eliseeva and Bunzli 2010; Hagan and Zuchner 2011), making luminescent probes an attractive alternative to radioisotopes. To compensate for the low inherent absorbance of lanthanide ions, the luminescent probes contain an antenna fluorophore, which absorbs the light and transfers

the energy to a tethered Ln^{3+} ion that finally emits the light ((Selvin 2002; Werts 2005; Bunzli 2006) and references therein). One of the ways to significantly increase the detection sensitivity of light-emitting probes is to bundle them onto a carrier molecule, which then can be attached to an object of interest (Rowley, Henriksson et al. 1987; Haralambidis, Angus et al. 1990). With conventional fluorophores this approach is complicated due to self-quenching, which is facilitated by the fluorescence resonance energy transfer (FRET) from an excited to a nearby non-excited dye molecule that efficiently absorbs the energy (Rowley, Henriksson et al. 1987; Haralambidis, Angus et al. 1990). The degree of quenching is highly dependent on the spectral overlap between the excitation (absorption) and emission of a particular fluorophore. The majority of conventional fluorophores have a small (10-30 nm) Stokes shift (the spectral separation between the emission and absorption maxima) causing a significant spectral overlap. High molar extinction of the common fluorescent dyes also contributes to quenching. On the contrary, lanthanide luminescent probes possess an extremely large Stokes shift (150-250 nm), which prevents efficient energy transfer between the excited and non-excited fluorophore molecules. Previously, this approach was explored on streptavidin with Eu^{3+} chelate (Diamandis 1991). Parent protein, avidin possesses 32 lysine residues at which luminescent labels can be attached, which makes it a superior scaffold for multiple label attachment comparing to streptavidin (which has 12 lysine residues). In the present study, avidin conjugates were obtained with a new generation of high-quantum-yield lanthanide chelates of Eu^{3+} and Tb^{3+} containing cs124-CH_3 and cs124-CF_3 antennae-fluorophores synthesized in the current and previous studies (Krasnoperov, Marras et al. 2010). It was found that unlike typical fluorophore BODIPY, the light emission

efficiency of the Eu^{3+} probes was not affected by self-quenching. In fact, the cumulative luminescence of the conjugate as a function of the number of the attached residues displayed a super-linear behavior, suggesting synergistic effect (Diamandis 1991). This effect was due to the enhanced antenna-to-lanthanide energy transfer. When tested the same approach with Tb^{3+}-based luminescent probes, which possess higher quantum yield compared to the cs124-Eu^{3+} chelates. Significant self-quenching was observed when these multiple Tb^{3+} probes were attached to avidin. However, introduction of a biphenyl spacer between the chelate and the cross-linking group completely suppressed the quenching, yielding highly bright conjugates. The obtained luminescent avidin constructs were used for labeling bacterial and mammalian cells giving highly contrast images in time-resolved detection mode. These new probes can find a broad range of applications in the biological and biomedical fields that rely on high detection sensitivity.

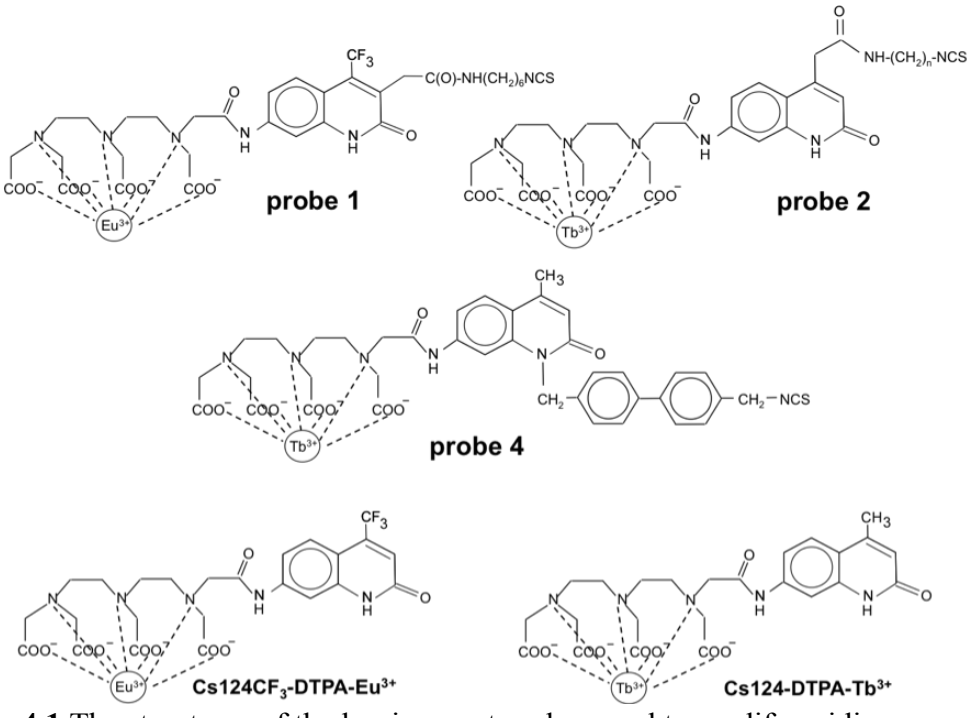

Figure 4.1 The structures of the luminescent probes used to modify avidin.

4.2 Experimental Section

4.2.1 Synthesis

The following reagents were purchased from Sigma Aldrich: Avidin; diethylenetriaminepentaacetic acid dianhydride (DTPA); triethylamine; butylamine; 1,3-phenylenediamine; ethyl 4,4,4-trifluoroacetoacetate; ethylacetoacetate, 1,3-dicyclohexylcarbodiimide (DCC); ethylenedianime; methylbromacetate; anhydrous dimethylformamide and dimethylsulfoxide; 1-butanol; ethylacetate; chloroform; acetonitrile; ethanol; sodium and potassium hydroxide; $TbCl_3$ and $EuCl_3$; silica gel TLC plates on aluminum foil (200 mm layer thick with a fluorescent indicator). Distilled and deionized water (18 MΩ cm^{-1}) was used. All experiments including lanthanide complexes preparation and using thereof were performed either in glassware washed with mixed acid solution and rinsed with metal-free water, or in metal-free plasticware purchased from Biorad. All chemicals were the purest grade available. Probe **2** was synthesized as previously described (Krasnoperov, Marras et al. 2010). Biotinylated oligonucleotide containing BHQ had a structure: 5'NH_2-ACCTGGTGCCTCGTCGCCGCAGCTCAGG dT (BHQ2) TT-3'-biotin. NHS-dPEG_{12}-biotin was purchased from Quanta Biodesign.

4.2.1.1 Probe 4 (Scheme 4.1). **1. Product XI** To a solution of 106 mg (0.6 mmol) of cs124 in 0.8 ml of DMF 72 ml of 10 M NaOH was added followed by rigorous agitation until the water phase disappeared. This solution was mixed with a 300 mg 4, 4'-bis (chloromethyl) biphenyl dissolved in 2 ml of DMF. After 20 min incubation at room temperature the TLC analysis in hexane-acetone (1:1) revealed the formation of a

single reaction product. The mixture was supplemented with 100 mg of lithium azide and heated for 20 min at 50 °C followed by precipitation with 20 ml of water. The residue was collected by centrifugation, washed with water and dissolved in 20 ml of hot acetonitrile. The acetonitrile was removed by evaporation under reduced pressure and the residue was washed a few times with hot hexane and subjected to silica gel chromatography in hexane-acetone (1:1) developing system. *Yield -120 mg*. ^{1}H NMR in DMSO: 7.65 (dd, 4H, o,o'biphenyl H, J_1 = 11.1, J_2 = 8.4), 7.45 (dd overlapped, 1H, 5H), 7.45 (dd,2H, biphenyl m-H, J_1 = 8.25, J_2 = 5.1), 7.25 (d, 2H, biphenyl-m'- H, J – 8.1), 6.49 (d, 1H, 6H), 6.44 (dd, 1H, 3H, J= 1.8), 6.21 (s, 1H, 8H), 5.8 (s, 2H, 7-amino), 5.38(s, 2H, N-CH_2), 4.4 (s, 2H, -CH_2-N_3), 2.36 (d, 3H, 4-methyl, J = 0.9).

2. Product XII Solution of 68 mg of product X**I** in 0.5 ml of DMF was supplemented with 1.5 molar excess of triphenylphosphine, incubated for 1 h at 50°C and 0.13 ml of 25 % aqueous ammonium hydroxide was added. The mixture was incubated for 1 h at 50°C and left for 20 min at -20°C. The precipitate was collected by centrifugation, washed by ether and dried *in vacuo* affording 36 mg of product X**II**.

3. Product XIII The solution of 30 mg of product X**II** in 0.5 ml of DMSO was titrated with thiocarbonyldiimidazole dissolved in 0.1 ml of chloroform. Addition was continued until the subsequent portion of C(S) Im_2 stopped decolorizing. TLC analyzed the reaction mixture in a hexane-acetone (1:1) developing system, revealing nearly complete conversion of the original cs124 derivative. Small excess of C(S)Im_2 was required to complete the reaction. The mixture was supplemented with 5 ml of TFA and left for 1 h

at 45°C and monitored by TLC. The product was precipitated by water (13 ml), collected by centrifugation and washed by water two more times. Most of the remaining residue was dissolved in 10 ml of acetonitrile and the remaining material was removed by centrifugation. Acetonitrile solution was evaporated to dryness *in vacuo* affording 20 mg of product X**III**. ^{1}H NMR in DMSO: 7.66 (m, 4H, o,o'biphenyl H), 7.48 (dd overlapped, 1H, 5H, J=2.1), 7.45 (d, 2H, biphenyl m-H, J = 8.1), 7.3 (d, 2H, biphenyl-m'- H, J – 8.4), 6.7 (s, 1H, 8H), 6.62 (dd, 1H, 6H, J_1=9.0, J_2 = 1.8), 6.55 (d, 1H, 3H, J=1.8), 6.25 (s, 2H, 7 amino), 5.5 (s, 2H, -CH_2-NCS), 4.48 (s, 2H, N-CH_2).

4. Probe 4 Solution of 35 mg (0.1 mmol) of DTPA dianhydride in 0.3 ml of DMSO obtained under heating to 60-80 °C was cooled down to room temperature and added to 20 mg (0.048 mmol) of compound X**III**. The reaction was carried on for 15 min at 20°C. The mixture was supplemented with 4 ml of water, left for 20 min at room temperature and pH was adjusted to 5.0 with LiOH. The product was purified by preparative C-18 HPLC column (20 x 250 mm) using linear gradient (0.5: l) of acetonitrile in water (0–70 %). The elution rate was 2 ml/min. The fractions containing desired product were combined and supplemented with one equivalent of a lanthanide salt. The resulting solutions were concentrated *in vacuo* by co-evaporation with acetonitrile under gentle heating (25-30 °C) to final concentration 20 mM.

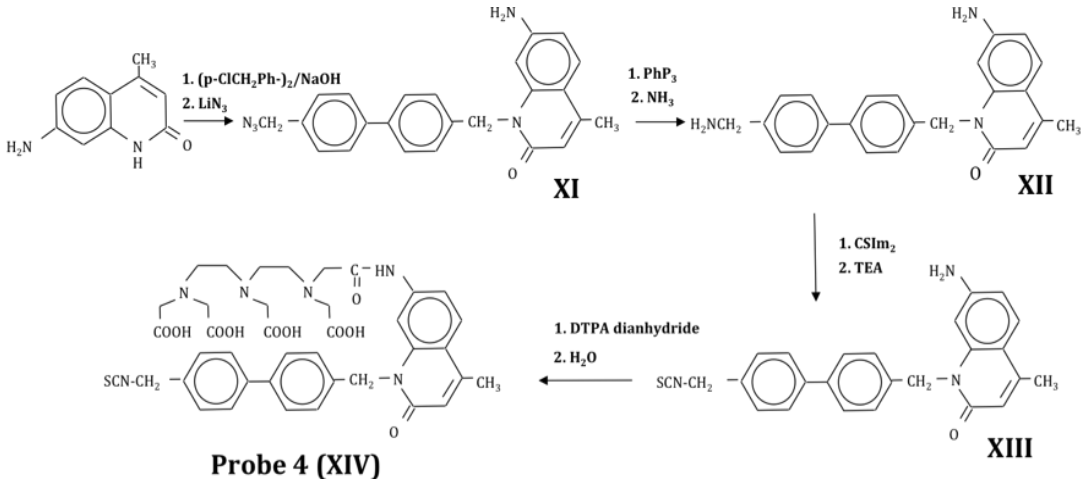

Scheme 4.1 Synthetic scheme for amine reactive probe 4.

4.2.1.2 Modification of Avidin with Light - Emitting Probes. The reaction cocktails (10-16 µl) were prepared by mixing of 7 ml of avidin (20 mg/ml), 1 ml of 1 M sodium borate buffer pH 10.0, and 1-8 ml of a reactive light-emitting probe at concentrations specified in figure legends. After incubation for 4 h at 56 °C the mixtures were diluted to 100 ml by water and subjected to size-exclusion chromatography on Sephadex G-50 "medium" in 10 mM Hepes-HCl buffer pH 8.0 containing 50 mM NaCl. The fractions corresponding to modified avidin were collected by visual detection using UV monitor (365 nm light).

4.2.1.3 Preparation of *E. coli* Cells Labeled with Modified Avidin. LB broth (100 ml) was inoculated with suspension of 10 µl of *E. coli* cells (RL721 strain) and incubated in a 500 mL Erlenmeyer flask overnight at 37°C. The cells were harvested by centrifugation (4,000 rpm, 5 min), washed with PBS and re-suspended in the same buffer containing 50 % glycerol at a final density of 32 mg ml^{-1}. Thirty microliters of this suspension containing ca 1 mg of cells was washed 3 times with 1 ml of 0.1 M sodium

borate buffer, pH 8.5, and each time collected by centrifugation. After the last wash, the cells were suspended in 50 µl of the same buffer and 4 µl of 100 mM DMSO solution of NHS-dPEG$_{12}$-biotin was added. After incubation at room temperature for 30 minutes the cells were washed 4 times with 500 µl of PBS. After the final wash, cells were suspended in 15 µl of PBS buffer and supplemented with 15 µl of 5 µM avidin modified with one of the lanthanide labels [AV-Probe **4**-Tb^{3+} (n=15) and AV-Probe **1**-Eu^{3+} (n=19)]. After 25 minutes of the incubation at room temperature cells were washed by PBS (4 x 500 µl) and suspended in 100 µl of the same buffer.

4.2.1.4 Preparation of Chinese Hamster Ovarian Cells (CHO) Labeled with Modified Avidin. CHO cells were grown in Dulbecco's modified Eagle's medium, supplemented with 10% fetal bovine serum, 200mM L-glutamine and 100 µg/ml Penicillin/streptomycin solution. Once the cells reach 80-90% confluency, they were trypsinized and collected by centrifugation (1000 rpm for 5 min), washed with 0.1 M Na-borate buffer pH 8.5 (3 x 0.5 ml) and spun down at 3,000 rpm for 30 seconds. The cells were suspended in 500 µl of sodium-borate buffer, divided into 5 equivalent volumes 100 µl each, and supplemented with various volumes (0.5 µl, 1 µl, 2 µl, and 4 µl) DMSO solution of 100 mM NHS-dPEG$_{12}$-biotin. 100 µl of the suspension was kept for auto fluorescence reference. The cells in each tube were washed with 150 µl of PBS buffer three times, suspended in 20 µL of PBS and supplemented with 15 µl of 5 µM AV-Probe **1**-Eu^{3+}. After incubation at room temperature for 20 minutes, the cells were washed with 100 µl of PBS buffer and suspended in 50 µl of the same buffer.

4.2.1.5 Preparation of the Cells for Microscopic Detection. One microliter of poly-L-lysine was spread onto a fused silica microscope substrate into an area of 0.3 cm^2 and removed. One microliter of the cell suspension of labeled cells (*E. coli* or CHO cells) containing 10^9-10^{10} cells cm^{-3} in PBS buffer was spread into the same area and left to air dry for 15 minutes.

4.2.2 Physical Methods

Excitation and emission fluorescence spectra in the continuous excitation mode were recorded using QuantaMaster 1 (Photon Technology International) digital fluorometer at ambient temperature. Time-resolved and gated luminescence measurements were performed using the previously described home-built experimental set-up(Krasnoperov, Marras et al. 2010). A Hacker Instruments Zetopan microscope was equipped with an ICCD Camera (PI-MAX, Princeton Instruments). In the experiments, the images were taken in luminescence light using evanescent wave excitation at 351 nm as well as in scattered light using standard top illumination by xenon lamp. In the evanescent excitation, a right angle fused silica prism was illuminated with laser light (351 nm) from a XeF laser (OPTEX, Lambda Physik). The sample was located on the hypotenuse side of the prism positioned horizontally. Images taken in scattered light from a xenon lamp were taken before and after the luminescent images collected in the photon counting mode. Online thresholding mode was used to discriminate photon pulses from the readout noise as well as the "cosmic events". The 1024 x 1024 camera pixels were 8 x 8 binned resulting in 128 x 128 $pixel^2$ images. The microscope used an objective with the magnification of x56 and the numerical aperture of 0.90. Combined with the intermediate "ocular" lens with the magnification of x10 it provided the field of view of

14 x 14 μm^2. In some experiments, an x5 intermediate "ocular" lens was used resulting in the 28 x 28 μm^2 field of view.

4.2.2.1 Microscopic Detection of Living Cells Utilizing Avidin Labeled with Multiple Probes Using Total Internal Reflection Fluorescence Microscopy (TIRFM). The cells labeled with avidin carrying multiple probes (Probe **1**-Eu^{3+} and Probe **4**-Tb^{3+}) were placed on the hypotenuse side of the prism mounted at the microscope base (Figure 2.2). The excitation of probes occurred in the evanescent wave by laser light totally internally reflected from the hypotenuse side inside the prism. The probes with Eu^{3+} have emission lifetime of ca. 0.5 ms, while the probes with Tb^{3+} have emission lifetime of ca. 1.5 ms. Therefore, samples labeled with Eu^{3+} probes a gate width of 1 msec and the gate delay of 50 μsec and for samples labeled with Tb^{3+} probes 2 msec gate width and 100 μsec gate delay were used. Images in luminescence light were acquired in the photon counting mode; typically 1000 pulses were accumulated (at the repetition rate of 2 Hz). The number of probes per cell was calculated based on the total photon count with the subtraction of the background count.

The calibration of the set-up was performed by collection of luminescence light from a thin layer of the probes solution excited directly by the laser beam at the right angle from the bottom of a thin fused silica substrate. This procedure allowed determination of the calibration coefficients, which lump sum the solid angle of light collection of the objective lens, the microscope throughput coefficient, the photocathode quantum efficiency, as well as the photon counting efficiency. The microscope field of view in these experiments was 14 x 14 μm^2 (Figure 4.7). To achieve homogeneity of the

excitation beam, the beam was passed through a 0.32 cm^2 diaphragm. The pulse energy was measured after the diaphragm (0.32 mJ $pulse^{-1}$). This allowed a reliable determination of the laser light fluence. Measured volume of the probes solutions (1.12 mM Probe **1**- Eu^{3+} or 0.107 mM Probe **4**-Tb^{3+}) in glycerol were placed on the top of the substrate and spread upon the surface with a cover slip (the spot area of 3.80 cm^2 and the thickness of the layer of 2.63 μm). The luminescence light intensity was calculated based on the photon fluence, the absorption cross-sections of the probes at 351 nm (2.1 x 10^{-17} cm^2 $molecule^{-1}$ and 3.6 x 10^{-17} cm^2 $molecule^{-1}$ for probes Eu^{3+} and Tb^{3+}respectively), the luminescence quantum yield (0.167 for Eu^{3+} (Xiao and Selvin 2001)), and the total number of probes in the field of view. This was compared with the total number of photons counted in the image. The number of probes illuminated per pixel was computed with the concentration of the molecules illuminated in the visible region at 8 x 8 binning (4.96 x 10^3 for Eu^{3+} and 2.0 x 10^3 Tb^{3+}). The probability of excitation was calculated using the cross-section of the probes at 351 nm (2.14 x 10^{-17} cm^2 $molecule^{-1}$ for Eu^{3+} and 3.59 x 10^{-17} cm^2 $molecule^{-1}$ for Tb^{3+}), the fraction of light passing through the microscope, counting efficiency of the ICCD camera (3% for 615 nm for Eu^{3+} and 7% for 545 nm for Tb^{3+}) and estimated quantum yield of the luminescent probe (0.167 for Eu^{3+} (Xiao and Selvin 2001)). Coefficients for calculations of probes per object were determined in 14x14 μm^2 field of view with concentrated probe samples illuminated from the bottom. 1.12 mM Probe **1**-Eu^{3+} had 4.96 x 10^3 probes $pixel^{-1}$ illuminated from the bottom with averaged experiments of 6.19 counts $pixel^{-1}$ at excitation energy of 1 mJ cm^{-2} through the orifice with 100 pulse accumulations. Coefficients resulted for Probe **1**-Eu^{3+} as 8.0 x 10^4 in 14x14 μm^2 field of view and 2.0x10^4 in the 28x28 μm^2 field of view (Eq.

4.1). 0.107 mM Probe **4**-Tb^{3+} resulted in $2.0x10^3$ probes $pixel^{-1}$ with an averaged 1.59 counts $pixel^{-1}$ with energy through the orifice at 0.512 mJ cm^{-2} and 100 pulse accumulations; coefficients resulted in $6.5x10^4$ at 14x14 μm^2 field of view and $1.63x10^4$ in the 28x28 μm^2 field of view (Eq. 4.2). The number of illuminated probes per object was determined with the respective field of view and probe coefficient (listed above) divided by the energy upon the prism multiplied by the number of pulse accumulations then multiplied by the difference of photon electrons (Δpe) of generated by the object and background.

$$\text{Probes} = \frac{8.0 \times 10^4}{E_A/(mJcm^{-2}) \times N}(\Delta\text{pe Counts}) \tag{4.1}$$

$$\text{Probes} = \frac{6.5 \times 10^4}{E_A/(mJcm^{-2}) \times N}(\Delta\text{pe Counts}) \tag{4.2}$$

The average number of the probes per externally labeled *E. coli* cells was determined to be $2.1x10^5$ and $2.9x10^5$ for Eu^{3+} and Tb^{3+} probes, respectively. Externally labeled CHO cells were prepared in a similar manner. The cells were labeled with avidin conjugates carrying multiple Eu^{3+} chelates of probe **1** with an average $1.6x10^7$ probes per cell.

4.2.2.2 Measurement of Light Emission of Lanthanide Chelates in Continuous Wave Mode. The detection of light emission of a lanthanide chelates and their conjugates with avidin as well as of BODIPY-modified avidin was performed in a measuring cell (150 ml) in a buffer containing 10 mM Hepes pH 8.0. Water-based or deuterium oxide-based solutions were used.

4.3. Results

4.3.1 The Synthesis and Properties of Reactive Luminescent Lanthanide Probe 4

(Pillai, Kozlov et al. 2012) found a convenient modification reaction for the cs124-CF_3 fluorophore, which allows introduction of the cross-linking groups at N1 position. Here the same reaction with parent cs124 compound was completed to obtain probe **4**. Similarly to corresponding trifluoro-derivative, alkylation of cs124 fluorophore by bifunctional biphenyl compound produced alkylation product at N1 with high yield (Scheme 4.1). After the alkylation, the remaining reactive function was converted to an azido group by incubation with lithium azide (compound X**I**). The later was reduced to corresponding amino-compound X**II** by incubation with triphenylphosphine and ammonium hydroxide. This compound was converted to isothiocyano-derivative X**III** by subsequent incubation with thiocarbonyldiimidazole and TFA. Acylation of compound X**III** with DTPA dianhydride produced final product, which was chelated with Tb^{3+} ion by addition of $TbCl_3$ to yield probe **4**.

4.3.2 Modification of Avidin by Reactive Light Emitting Labels

As expected, incubation of various reactive fluorophores with avidin resulted in covalent attachment to the protein as judged by size-exclusion chromatography. The dependence of the number of attached fluorophore residues of probe **1**, **2,** and **4** per avidin molecule on probes concentration is shown in Figure 4.2. Since the probes are amine-reactive it is expected that they will predominantly attach to lysine residues. It can be seen that at a high concentration 24 to 31 out of 32 lysine residues of the protein can be modified by the probes. Attempt to obtain highly modified protein with BODIPY fluorophore was not

successful since the attachment of more than 4 residues caused precipitation of the protein (Pillai, Wirpsza et al. 2012; Wirpsza, Pillai et al. 2012) .

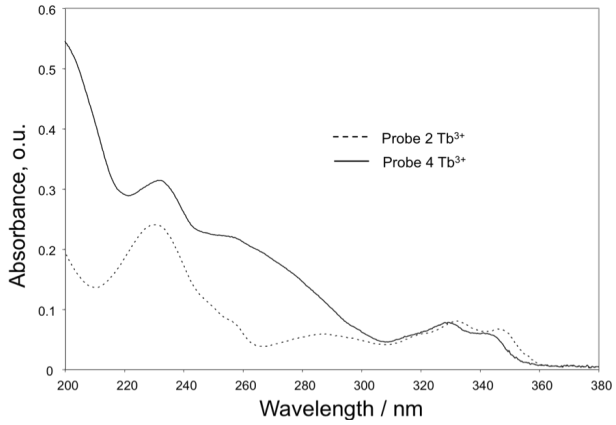

Figure 4.2 UV absorption spectra of probes **2** and **4.**

4.3.3 Light-Absorbing and Light-Emitting Properties of the Lanthanide Probes and Their Conjugates with Avidin

As seen from Figure 4.2, in comparison to probe **2,** probe **4** possesses a significant absorption in the range of 240-300 nm, which is obviously due to the presence of the biphenyl chromophore. Also, modification of the cs124 moiety at N1 causes a small (6 nm) batochromic shift of the absorption in the region of 320-360 nm. Biphenyl modification only slightly affects the brightness of the chelate as compared to the brightness of previously designed probe **2** (Table 4.1 and Figure 4.2), which makes this position a convenient site for the introduction of cross-linking or other functional groups. Strong light absorption of the biphenyl group in the region 240-300 nm does not interfere with the light absorption properties of the antenna and antenna-to-lanthanide energy transfer, as biphenyl- and quinolone moieties are not conjugated. As seen from Figure 4.3A and B, a shift in the light absorption of probe **4** results in the same shift of the fluorescence excitation spectrum. The excitation spectrum of probe **4** displays a significant maximum in the region 240-300 nm where the biphenyl group absorbs the

light. This is indicative for energy transfer from the excited state of the biphenyl group to the cs124 chromophore, favored by close proximity of the moieties. Heavy water caused a significant enhancement of lanthanide emission (Figure. 4.3C and D) due to the elimination of the excitation energy dissipation by coordinated water molecule through O-H bond vibration.

Table 4.1 Fluorescence of Avidin Conjugates in Water and Deuterium Oxide Solutions

Probe	No. residues per avidin	Fluorescence (per 10 nM avidin) in H_2O	Fluorescence (per 10 nM avidin) in D_2O	Specific fluorescence (calculated for 10 nM fluorophore) in H_2O	Specific fluorescence (calculated for 10 nM fluorophore) in D_2O
1	31	67 500	210 000	2 250	7 000
2	24	75 000	100 000	3 100	4 200
4	30	377 000	520 000	12 600	17 300
2 (non-attached)	N/A	N/A	N/A	34 500	42 000
4 (non-attached)	N/A	N/A	N/A	30 700	37 000
1 (non-attached)	N/A	N/A	N/A	2 300	7 500
Reference compounds (Figure 4.1)					
cs124-DTPA-Tb^{3+}	N/A	N/A	N/A	40 000	65 000
cs124CF_3-DTPA-Eu^{3+}	N/A	N/A	N/A	2 500	10 000

Avidin represents highly stable tetrameric structure containing 32 lysine residues to which the reactive probes can be attached (Figure 4.4A). Avidin is able to bind tightly to biotin ligand producing virtually irreversible complex. This property of the protein makes it a convenient carrier for the attachment of various probes. Avidin conjugates thus obtained can be used to label biotinylated molecules of interest. It is seen in Table. 4.1, the attachment of Tb^{3+} luminescent chelates **2** and **4** to the protein at low concentration of the probes caused ca. 3 fold quenching comparing to emission of non-attached probes. For probe **2,** increasing the number of attached probes resulted in further progressive quenching (Figure 4.4B), while for probe **4** the dependence of the cumulative fluorescent signal on the number of the cross-linked probes remained linear. Attachment of Eu^{3+}-based probe **1** also resulted in 3 fold quenching, however when the

number of the conjugated probes increased, a significant non-linear luminescence enhancement was observed. This effect can be explained by enhancement of antenna-to-lanthanide energy transfer, which is supported by decrease of antenna fluorescence and simultaneous increase of lanthanide emission in the complex (Table 4.2). One factor that reduces the brightness of the probe could be quenching due to the contact between the antenna-fluorophore and protein surface. This is supported by the superior properties of the probe **4** possessing a rigid spacer between the antenna fluorophore and the cross-linking group. This spacer could prevent the quenching by restricting the fluorophore contacts with avidin.

As expected, light emission of avidin conjugates increased in heavy water (Table 4.1). Thus 1.3 and 3 fold enhancement was observed for Tb^{3+} and Eu^{3+} chelates correspondingly, which is close to enhancement factors for corresponding non-attached probes (Krasnoperov, Marras et al. 2010).

Table 4.2 Antenna-to-Eu^{3+} Emission Ratio for Probe **1** Attached to Avidin in H_2O at pH 8.0 for 10 nM Avidin

No. of attached residues per avidin	Eu^{3+}emission (counts)	Antenna emission (counts)	Eu^{3+}/Antenna emission ratio
3	3000	3760	0.79
6	7100	5000	1.42
9	8300	24300	0.34
20	42000	21700	2.0
31	67500	26000	2.6
10 nM PrIEu^{3+}	2300	2300	1.0

As examined from Figure 4.4D, attachment of more than one BODIPY fluorophore to avidin dramatically decreased the cumulative fluorescent signal due to expected FRET quenching.

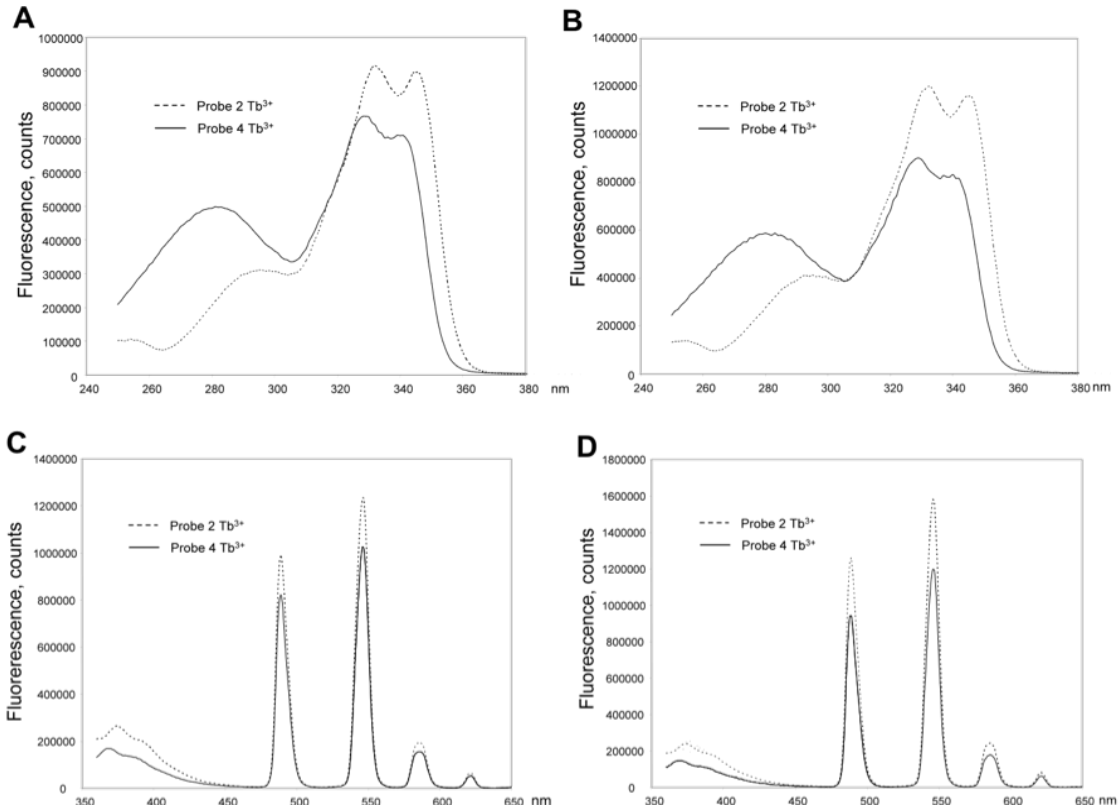

Figure 4.3 Fluorescence spectra for probe **4** and probe **2**. (**A, B**) excitation spectra at emission wavelength 490 nm. (**C**, **D**) emission spectra at excitation wavelenght 329 nm (for probe **4**), and 332 nm (for probe **2**). (**A**, **C**) spectra in water; (**B**, **D**) spectra in deuterium oxide.

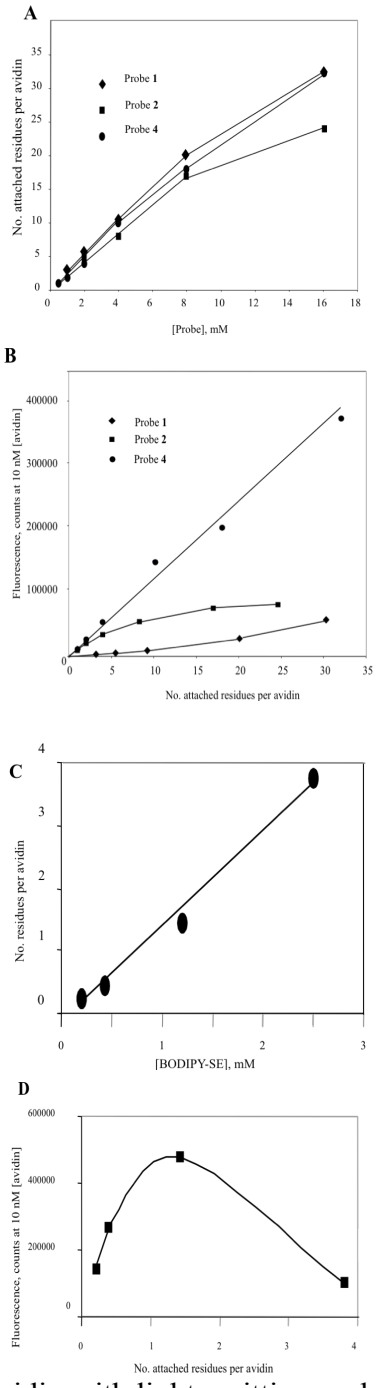

Figure 4.4 Modification of avidin with light emitting probes and fluorescent properties of the modified conjugates. A, C, dependence of the number of the attached probes **1**, **2**, and **4** residues (**A**) and BODIPY residues (**C**) per avidin on the concentration of the reactive probes. B, D, dependence of the fluorescence of the avidin modified with probes **1**, **2**, and **4** (**B**) and BODIPY (**D**) on the number of the attached residues.

Source: Wirpsza, L., S. Pillai, et al. (2012). Highly Bright Avidin-based Affinity Probes Carrying Multiple Lanthanide Chelates. Journal of Photochemistry and Photobiology B: Biology **116**: 22-29

4.3.4 Modified Avidin Conjugates are Capable of Biotin Binding

Extensive modification of avidin could potentially interfere with biotin binding. To test the binding ability of the modified protein, the conjugate with biotinylated oligonucleotide carrying BHQ quencher was titrated. As seen from Figure 4.5, incubation caused a dramatic decrease in brightness suggesting quenching of the modified protein through binding of the biotinylated oligonucleotide. As expected, ca. 4 fold excess of the oligo was required to achieve maximal quenching, which corresponds to saturation of all biotin-binding sites.

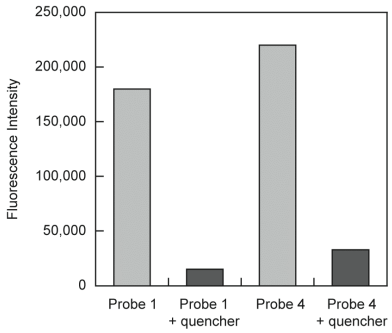

Figure 4.5 Light emission spectra of luminescent avidin conjugates in the absence (striped bars) and in the presence (solid bars) of biotinylated DNA oligo carrying a Black Hole Quencher.

4.3.5 Microscopic Imaging of Living Cells Using Luminescent Avidin Conjugates

To image the cells, first they were treated with acylating biotin derivative, which resulted in covalent attachment of the biotin residues to the cellular surface (Figure 4.6). As expected, subsequent incubation with luminescent-labeled avidin conjugates resulted in the attachment to the cells as judged by visual inspection under UV light. For microscopic imaging of the cells in time-gated mode Total Internal Reflection Fluorescence Microscopy (TIRFM) (Schneckenburger 2005; Wazawa and Ueda 2005). Total internal reflection is an optical phenomenon, which occurs when light propagating

in a dense medium (such as glass) meets an interface with a less dense medium, such as water. If the light meets the interface at a small angle, some of the light passing through the interface is refracted and some is reflected back into the dense medium. At a certain angle all of the light is reflected. This angle is known as the critical angle, and its value depends on the refractive indices of the media (n_1, n_2): $Q_c=\mathrm{Sin}^{-1}(n_1/ n_2)$. However, some of the energy of the beam propagates a short distance (a few hundred nanometers) into the water, generating an evanescent wave. If this energy is not absorbed, it passes back into the glass. However, if a fluorophore molecule is within the evanescent wave it can absorb photons and be excited. This way, it is possible to get fluorescence with a very low background of excitation light. The principle was used in the design of the experimental setup for imaging of small luminescent objects (Figure 2.2). This allowed selective excitation of the surface attached objects. Repetitive laser pulses excited labeled cells and the luminescent signal collected after a short time delay allowing the decay of short-lived background fluorescence. Light emission images were acquired and accumulated using an ICCD camera. Optical and time-gated luminescent images for bacterial and mammalian cells are shown in Figure 4.7. As expected, the images were highly contrasted.

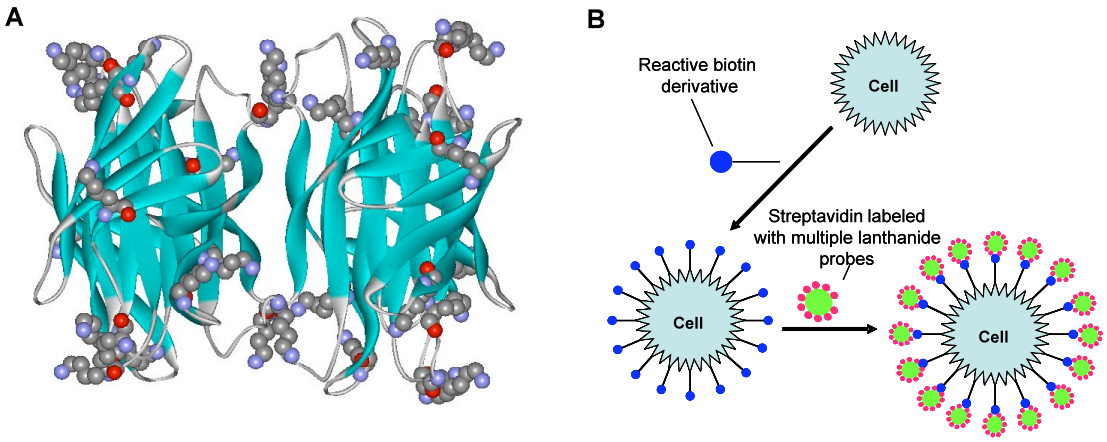

Figure 4.6 The scheme for luminescent labeling of living cells. **(A)** X-ray structure of avidin with lysine residues to which reactive light-emitting probes can be attached. **(B)** The strategy for cell labeling. The cells are treated with reactive biotin derivative, followed by attachment of the luminescent labeled avidin conjugates to biotinylated cells.

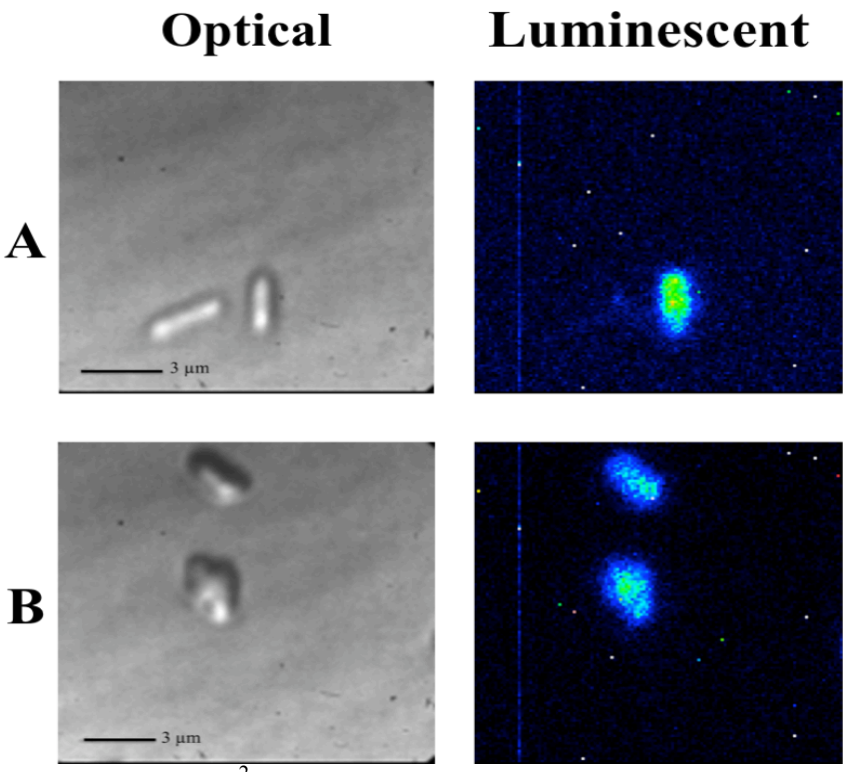

Figure 4.7 *E. coli* in 14 x 14µm^2 field of view for optical and luminescent imaging for (**A**) Probe **1**-Eu^{3+} and (**B**) Probe **4**-Tb^{3+}.

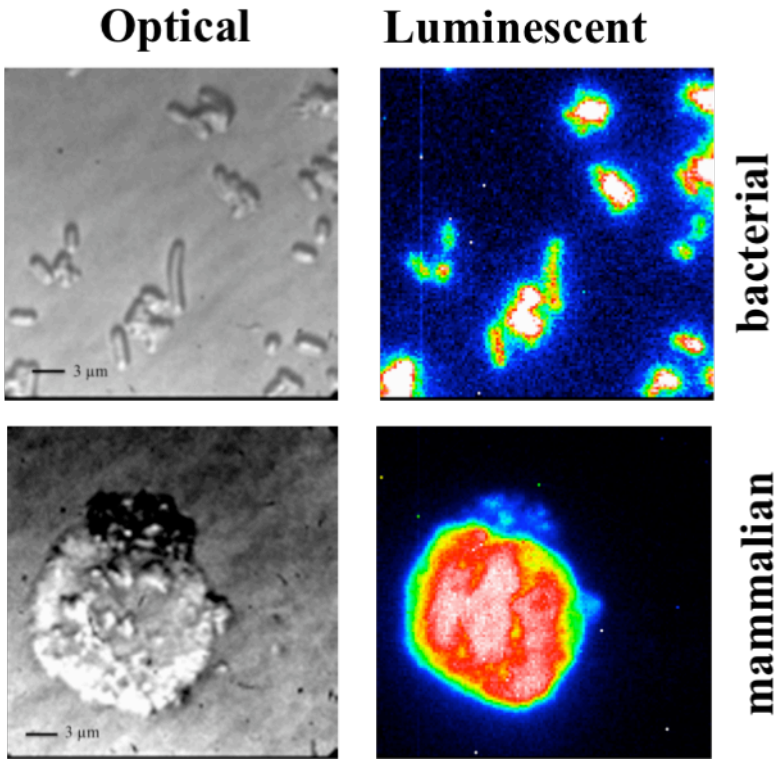

Figure 4.8 Imaging of the labeled cells using TIRF microscopy for optical and luminescent modes in 28 x 28 μm^2 field of view with Probe **1**-Eu^{3+}.

4.4 Discussion

This study demonstrates the fact that multiple luminescent chelates can be attached to avidin molecule to create hypersensitive affinity probes that can be coupled to various biomolecules of interest. Avidin is a convenient protein for design of such probes due to its relatively small size (4-5 nm) and large number of exposed Lys residues to which the lanthanide chelates can be attached. Using a high concentration of reactive lanthanide labels, we were able to attach up to 30-31 luminescent residues to a single avidin molecule producing highly bright conjugates. Eu^{3+} conjugates of probe **1** displayed fortuitous additional signal enhancement apparently caused by approximation of the labels at the protein surface, which resulted in the improvement of antenna-to-lanthanide

energy transfer. The nature of this effect is not quite clear. Enhanced energy transfer could arise due to scavenging of the fraction of the antenna light (that has not been transferred to the lanthanide) by another closely positioned antenna molecule, which then transfers the absorbed energy to the chelated lanthanide. Indeed, small overlapping of the emission and absorption spectra of the antenna fluorophore of probe **1** is consistent with the suggested mechanism. Also, the excited antenna could transfer the energy to the lanthanide ion of the neighboring probe. Finally, carboxylate amino acid residues on the protein surface can be involved in the additional coordination of the lanthanide, displacing a water molecule from its coordination sphere, thereby enhancing the quantum yield of the metal emission (Li and Selvin 1995). Terbium-based multiple label constructs displayed a significant decrease of light emission comparing to the sum of equivalent number of non-attached probes, which was most likely due to the interaction of the chelate with the protein surface. Another factor of reducing the light emission could be contact quenching resulting from the approximation of the neighboring antennae-fluorophores at high labeling density. Luminescent quenching can be suppressed by the presence of a biphenyl spacer. Generally, the rigid biphenyl group can restrict the fluorophore contacts with the protein, and also prevent the contact quenching by interfering with stacking interactions of the antennae.

Detection limit of the obtained avidin conjugates is in 1-10 fM range as estimated by the detection sensitivity of single non-attached probes used for labeling. These conjugates can find wide application in biological, biophysical and biomedical studies. They can be especially useful for imaging of single molecules, biological micro objects,

and body tissues as well as the development of highly sensitive assays in which the signal cannot be amplified (e.g. using PCR amplification technique).

CHAPTER 5

NEW QUINOLONE-BASED THIOL-REACTIVE LANTHANIDE LUMINESCENT PROBES

Luminescent lanthanide ion complexes are distinguished by unique light emitting properties that enable both highly sensitive detection of lanthanide labels when attached to biomolecules and contrast imaging of various micro objects (cells, nanoparticles, etc.). Previously discussed in Chapter 3, synthesized amine-reactive cs124-based luminescent lanthanide chelates with improved brightness and metal retention. Chapter 5 presents the synthesis of new thiol-reactive derivatives of the cs124-CH_3 and cs124-CF_3 fluorophores with bromoacetamido-, and maleimido- cross-linking groups. Maleimido-compounds displayed exceptional reactivity instantaneously coupling to thiols at physiological conditions at micromolar thiol concentrations. Surprisingly, the probes displayed strong quenching by adjacent maleimido-group, which was completely eliminated after reaction with thiols, thereby enabling their simple detection by monitoring the light emission of the reaction mixture. This reaction can be used for hypersensitive determination of biologically important sulphydryl compounds (e.g. glutathione, co-enzyme A, etc.) in time-resolved mode.

5.1 Introduction

Luminescent lanthanide ion chelates are valuable alternatives to conventional fluorophores due to unusual properties of lanthanide ion emission (Selvin 2002; Parker 2004; Hemmila and Laitala 2005; Bunzli 2006; Eliseeva and Bunzli 2010; Hagan and Zuchner 2011). These chelates possess long luminescence lifetime, which allows

suppressing short-lived background fluorescence by acquisition the signal in time-gated mode. Large spectral distance between the excitation and emission light (Stokes shift) along with sharply spiked shape of the emission spectra further contribute to detection sensitivity, which is few orders of magnitude higher than for regular fluorophores. Due to poor light absorption the lanthanide ion has to be sensitized. This is achieved by tethering the ion (typically through a chelator) to a light-absorbing molecule, which after photon capture transfers the energy to the lanthanide ion, thereby acting as an antenna. Lanthanide ion (Ln^{3+}) is attached to the antenna through the chelating group. Lanthanide probes also possess a cross-linking group used for the labeling of the objects of interest.

Carbosytril cs124-CH_3 and cs124-CF_3 (Selvin and Hearst 1994; Heyduk and Heyduk 1997; Li and Selvin 1997; Chen and Selvin 1999; Chen and Selvin 2000; Xiao and Selvin 2001; Ge and Selvin 2003; Ge and Selvin 2004; Ge and Selvin 2008) derivatives of oligoethyleneiminocarboxylate chelates represent an attractive lanthanide probes for detection of biomolecules due to high quantum yield and high solubility in water. Previously, new amine-reactive isothiocyano-derivatives of cs124-CH_3 and cs124CF_3-based lanthanide probes were described (Krasnoperov, Marras et al. 2010; Pillai, Wirpsza et al. 2012; Wirpsza, Pillai et al. 2012). The current study was aimed at the design of simple synthetic protocols for corresponding thiol-reactive derivatives. Thiol-reactive light emitting probes are widely used for labeling of proteins and nucleic acids in biochemical assays as well as for detection of biological thiols owing to their exceptional role in functioning of the living cells(Townsend, Tew et al. 2003; Demirkol, Adams et al. 2004). These thiols include: glutathione (GSH), cysteine (CYS), N-acetylcysteine (NAC), homocysteine (HCYS), γ-glutamyl cysteine (GGC) and co-

enzyme A. Several luminescent probes of this class have been previously reported (Chen and Selvin 1999; Ge and Selvin 2003) including bromoacetamide (Ge and Selvin 2004), maleimide, pyridyldithio, iodoacetamides, and methanethiosulphonates. In these studies, the reactive group has been attached to a chelating moiety of a probe, which decreases Ln^{3+}-coordination and brightness of the chelate allowing coordination of an extra water molecule. In the other study, coumarine-based chelates containing the reactive group in the fluorophore moiety were obtained (Heyduk and Heyduk 1997). These probes are free of the above shortcomings, but they possess moderate quantum yield and do not support Tb^{3+} luminescence. In this case, the reactive groups are also attached to a fluorophore moiety, which preserves their high brightness and high metal retention. A convenient synthetic protocol for bromoacetamido and maleimido lanthanide probes has been developed where all reactions occur in the same tube. Fortuitous quenching exhibited by our maleimide-based probes (which disappears upon thiol conjugation to the reactive group) allows hypersensitive determination of sulfhydryl compounds in time-resolved detection mode. The obtained compounds were used for labeling of bacterial RNA polymerase.

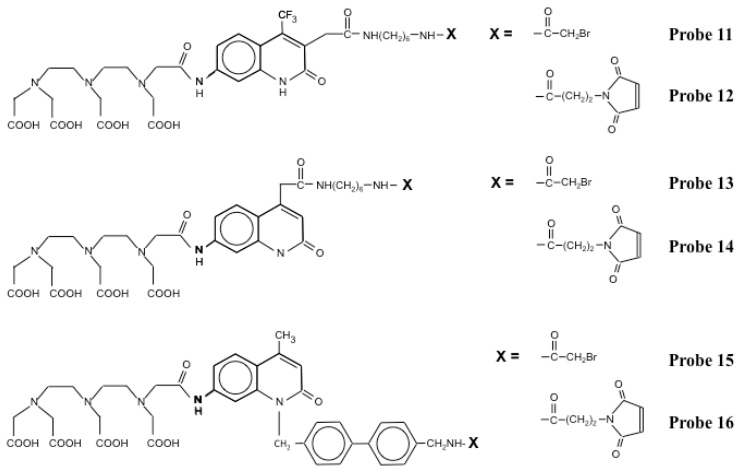

Figure 5.1 Structures of thiol reactive luminescent probes **11** to **16.**

5.2 Experimental Section

5.2.1 Synthesis

Diethylenetriaminepentaacetic acid dianhydride (DTPA); triethylamine ; butylamine; 1,3-phenylenediamine; ethyl 4,4,4-trifluoroacetoacetate; ethylacetoacetate; 1,3-dicyclohexylcarbodiimide (DCC); ethylenedianime; methylbromacetate; anhydrous dimethylformamide and dimethylsulfoxide; 1-butanol; ethylacetate; chloroform; acetonitrile; ethanol; sodium and potassium hydroxide; $TbCl_3$ and $EuCl_3$; silicagel TLC plates on aluminum foil (200 μm layer thick with a fluorescent indicator); distilled and deionized water (18 MΩ cm^{-1}) were purchased from Aldrich with a ≥99% pure and HPLC grade. All experiments including lanthanide complexes preparation and using thereof were performed either in glassware washed with mixed acid solution and rinsed with metal-free water, or in metal-free plasticware purchased from Biorad. Fluorescent intermediates used for the probes synthesis have been described in (Pillai, Kozlov et al. 2012; Wirpsza, Pillai et al. 2012).

The probe numbering is a continuation from previous work for amine and click reactive lanthanide íon probes (Krasnoperov, Marras et al. 2010; Pillai, Kozlov et al. 2012; Wirpsza, Pillai et al. 2012). In this chapter, the final product numbering begins at **11** and ends at **16**.

5.2.1.1 Probe 11. 1. 7-Amino-4-trifluoromethyl-4-carboxamido (6-aminohexyl) methyl-2-(1H) quinolone. Improved protocol (II). The solution of 94 mg of 3-carboxymethyl-cs124-CF3 (compound **I**) obtained as described (Krasnoperov, Marras et al. 2010) in 1 ml of DMSO was treated by two equivalents (84 ml) of methyliodide in the

presence of one equivalent of diisopropylethylamine at room temperature for 30 min. TLC analysis in ethyl acetate showed complete conversion to alkylation product **II**. The reaction mixture was poured into a 15 ml tube containing 10 ml of ether and 2 ml of water. After partitioning, the extraction with water was repeated two times. The organic layer was dried over anhydrous sodium sulfate and evaporated in *vacuo*. The residue was dissolved in 5 ml of acetonitrile followed by evaporation to dryness. *Yield – 110 mg*.

2. 7-Amino-4-trifluoromethyl-4-carboxamido (6-aminohexyl) methyl-2-(1H) quinolone (compound III) Solution of 100 mg of compound **II** in 10 molar excess of pre-melted 1.6-diaminohexane was heated at 100^{o} C. After 2 h TLC analysis in ethyl acetate revealed complete conversion to reaction product (R_f = 0). The product (compound **III**) was precipitated by 10 ml of ether, washed by water (3 x 10 ml), dried in *vacuo*, re-suspended in 0.5 ml of hot acetone, placed at -10 ^{o}C and centrifuged. The precipitate was finally washed with 10 ml of ether and dried in *vacuo*. *Yield – 150 mg*.

3. Probe 11 Solutions of 30 mg (0.1 mmol) of compound **III** in 0.2 ml of DMSO and 30 mg (0.1 mmol) of 4-nitrophenylbromoacetate in 0.05 ml of DMSO were mixed and incubated 5 min at 40^{o} C. TLC in chloroform – ethanol developing system revealed nearly complete conversion to the product (compound **IV**) migrated with R_f = 0.5. The reaction mixture was supplemented with the solution of 0.3 mmol of DTPA dianhydride in 0.5 ml of DMSO and incubation continued for additional 50 min at the same temperature. The mixture was poured drop-wise into 5 ml of ice-cold 0.1 M lithium citrate pH 4.0. Subsequently pH was adjusted to 5.0 by 1 M LiOH and the mixture was

extracted by 5 ml of ethyl acetate followed by centrifugation at 6000 rpm for 5 min at 4 ^{o}C. The product from supernatant was purified by preparative HPLC (20 x 250 mm) column in linear gradient (700 ml) of methanol in water (0-40% MeOH) at the elution rate 2 ml/min. Fractions corresponding to desired product (total volume 150 ml) were combined and methanol removed by evaporation in *vacuo*. Evaporated solution was applied to the same HPLC column and the product eluted in 15 ml of 80% methanol. The solution was titrated with 0.2 M aqueous europium chloride and the fluorescence of the solution was monitored at 615 nm with excitation at 350 nm. The titration was continued until fluorescence emission stopped increasing. The solution was evaporated in *vacuo* to ca. 2.5 ml affording 7.5 mM probe **1**. *Yield – 18%.* ^{1}H NMR chemical shifts (d) for compound **IV** in DMSO were as follows: 1.248 (m , 4H), 1.390 (m, 4H), 3.03 (m, 4H, J) 5.7), 3.680 (s, 2H, CH_2Br), 3.815 (s, 2H, $3CH_2$-), 6.01 (s, 2H, broad, 7 amine), 6.441 (s, 1H, 8H), 6.5 (2 d, 1 H, 6H, J) 2.9), 7.3 (d, 1H, 5H, J) 6.6), 7.796 (t, 1H), 8.243 (t, 1H), 11.8 (s, 1H, quinolone amide). UV for probe **11**: λ_{max}=347 nm (ε=14,300 $M^{-1}cm^{-1}$). MS: Eu^{3+}DTPA-cs124-CF_3-CH2C(O)-NH$(CH_2)_6$NHC(O)CH_2Br (-H^+) 1027.29 (found) 1027.62 (calc). Eu^{3+}DTPA-cs124-CF_3-CH_2C(O)-NH$(CH_2)_6$NHC(O)CH_2Br (-Eu^{3+}), (+4H^+) 880.23 (found) 880.67 (calc).

5.2.1.2 Probe 12. Solution of 39 mg (~100 μmol) of compound **III** was dissolved into 400 μl of DMSO and supplemented with 31 mg (~100 μmol) of N-succinimidyl-3-maleimidioproprionate (MIpr-OSu). After 15 min incubation at room temperature TLC analysis in chloroform- ethanol (4:1) developing system revealed nearly complete conversion of original compound (R_f=0) to reaction product with R_f=0.53. The mixture

was supplemented with ~300 μmol of DTPA dissolved in 400 μL of DMSO at 70°C and cooled to room temperature before addition. After 40 min incubation at 40°C the mixture was poured drop-wise into 5 ml of ice-cold 0.1 M lithium citrate pH 4.0. Subsequently, pH was adjusted to 5.0 by 1 M LiOH and the mixture was extracted by 5 ml of ethyl acetate followed by centrifugation at 6,000 rpm for 5 min at 4 °C. The product was purified by preparative HPLC and converted to Eu^{3+} complex as described above. *Yield - 11 μmols (11%).* Cysteine reaction product was obtained as described below. UV: λ_{max}=347 nm (ε=14,300 $M^{-1}cm^{-1}$). MS: Eu^{3+}DTPA-cs124-CF_3-$CH_2C(O)$-$NH(CH_2)_6NHC(O)$3MI-Cysteine (-H^+) 1177.411 (found) 1178.988 (calc). DTPA-cs124-CF_3-$CH_2C(O)$-$NH(CH_2)_6NHC(O)$3MI-Cysteine 1032.358 (found) 1032.028 (calc). Eu^{3+} DTPA-cs124-CF_3-$CH_2C(O)$-$NH(CH_2)_6NHC(O)$3MI 1059.838 (found) 1060.3092 (calc).

5.2.1.3 Probe 13. Solutions of 32 mg (0.1 mmol) of 7-amino-4-carboxamido (6-aminohexyl) methyl-2 (*1H*) quinolone (compound V**I**) in 0.25 ml of DMSO 30 mg of 4-nitrophenylbromoacetate in 0.1 ml in the same solvent were cooled in ice and mixed. After 10 min incubation at 0o C TLC analysis of the reaction mixture in the system chloroform-ethanol 4:1 revealed complete conversion of the reactants to acylation product **VIII** with R_f=0.4. DTPA acylation and preparation of the sample for HPLC was performed as described above for probe **12**, except that acylation was carried out at room temperature for 20 min. HPLC was performed using linear gradient (800 ml) of methanol in water (0-30%). The elution rate was 2 ml/min. The major product **III** (540 optical units at 347 nm, 30 μmol) was collected and mixed with equivalent amount of 0.1 M $TbCl_3$. The solution was concentrated without heating under reduced pressure to final volume

7.5 ml with addition of acetonitrile to facilitate evaporation. *Yield – 30 μmol (30%)*. UV: λ_{max}=332 nm (ε= 18,900 $M^{-1}cm^{-1}$). MS: Tb^{3+}DTPA-cs124-$CH_2C(O)$-$NH(CH_2)_6NHC(O)CH_2Br$ 967.2170 (found) 967.536 (calc). DTPA-cs124-$CH_2C(O)$-$NH(CH_2)_6NHC(O)CH_2Br$ 812.2607 (found) 812.668 (calc). Tb^{3+}DTPA-cs124-$CH_2C(O)$-$NH(CH_2)_6NHC(O)CH_2$ 887.1526 (found) 887.636 (calc).

5.2.1.4 Probe 14. Solution of 39 mg (0.1 mmol) of 7-amino-4-carboxamido (6-aminohexyl) methyl-2 (1H) quinolone (compound **VI**) in 0.4 ml of DMSO was supplemented with 30 mg (0.11 mmol) of MI-OSu and the mixture kept at room temperature. After 15 min incubation at room temperature TLC analysis in chloroform-ethanol (4:1) developing system revealed nearly complete conversion of original compound (R_f=0) to reaction product with R_f= 0.3). DTPA acylation step and subsequent preparation of the sample for HPLC purification was performed as described above for probe **13**. The sample was applied to HPLC column and the product eluted using linear gradient (560 ml) of methanol in water (0 – 40%) at the elution rate 2 ml/min. The fractions corresponding to desired product eluted between 140 and 210 min were combined and methanol evaporated under reduced pressure. After titration by $TbCl_3$ as described in previous section the resulting solution was freeze dried. *Yield – 20 μmol*. LC/MS samples were prepared with final product and cysteine, the reaction mixture was purified in 2.5:1 acetonitrile H_2O with R_f=0.2 of reactant and R_f=0.3 of Probe **14**. UV: λ_{max}=332 nm (ε=18,900 $M^{-1}cm^{-1}$). MS: Tb^{3+}DTPA-cs124-$CH_2C(O)$-$NH(CH_2)_6NHC(O)CH_2CH_2$-3MI-Cysteine (+H) 1120.2 (found) 1119.9 (calc). DTPA-

cs124-$CH_2C(O)$-$NH(CH_2)_6NHC(O)CH_2CH_2$-3MI-Cysteine (+4H) 964.3356 (found) 964.026 (calc).

5.2.1.5 Probe 15. 5.2 mg (14 μmol) of compound **XI** was dissolved in 200 μl of DMSO at 50°C, cooled to room temperature and mixed with the solution of 23 μmol (1.5 equivalent) of 4-nitrophenylbromoacetate. After 10 min reaction at room temperature TLC analysis in 9:1 acetonitrile-water developing system revealed complete conversion of the starting fluorophore (R_f=0.4) to the reaction product (R_f=0.7). The mixture was supplemented with the solution of 56 μmol (4 fold excess) of DTPA anhydride e in 200 μl of DMSO. After 20 min incubation the reaction mixture was supplemented with 100 μl of water and left for another 10 min at room temperature. 5 ml of BuOH and 2 ml of water were added and after the extraction the organic layer was collected. Extraction was repeated one more time, organic layers combined and the amount of the DTPA acylation product in butanol solution was determined by UV absorption. The solution was supplemented with 1.5 equivalents of 0.1 M $TbCl_3$, and evaporated *in vacuo* to 2-3 ml. The product was collected by centrifugation and purified by preparative TLC in acetonitrile-water (4:1) developing system. The product (R_f = 0.24) was recovered by elution with 50 % aqueous MeOH until complexation is complete. *Yield: 1.35 μmol (10 %).* UV: λ_{max}= 329 nm (ε = 18,900 $M^{-1}cm^{-1}$). MS: Tb^{3+}DTPA-cs124-CH_2 –BiPh-$CH_2NHC(O)CH_2Br$ ($+H^+$)1022.1 (found) 1021.7 (calc). DTPA-cs124-CH_2–BiPh-$CH_2NHC(O)CH_2Br$ ($+H^+$) 867.2 (found) 866.7 (calc).

5.2.1.6 Probe 16. Probe **16** was obtained and purified essentially as described for probe **15**. *Yield – 3%.* UV: λ_{max}=329 nm (ε=18,900 $M^{-1}cm^{-1}$). MS: Tb^{3+}DTPA-cs124-CH_2–BiPh-$CH_2NHC(O)CH_2CH_2MI$ ($+H^+$)1052.2 (found) 1051.8 (calc). DTPA-cs124-CH_2–BiPh- $CH_2NHC(O)CH_2CH_2MI$ ($+H^+$) 896.3 (found) 895.8 (calc).

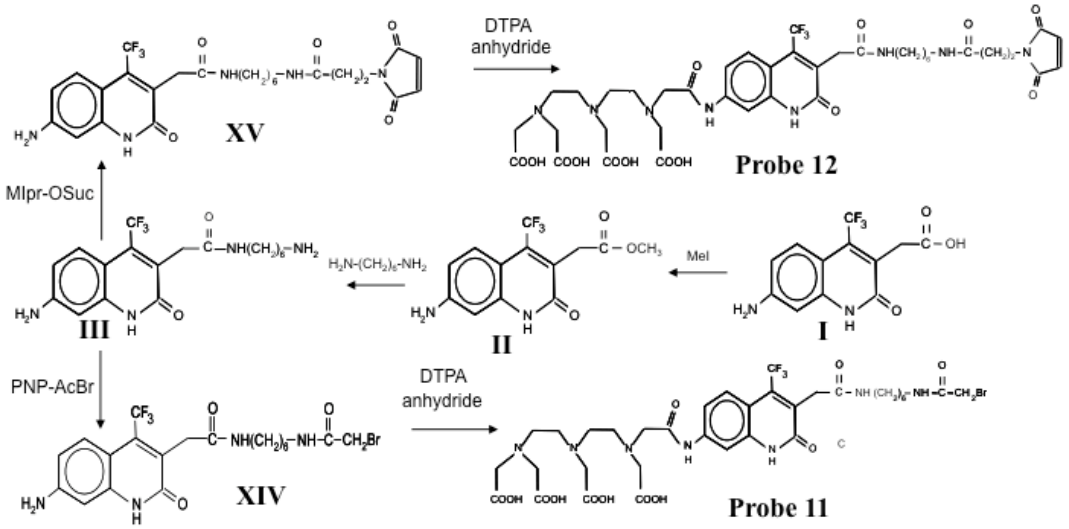

Scheme 5.1 Synthetic scheme for probes **11** and **12.**

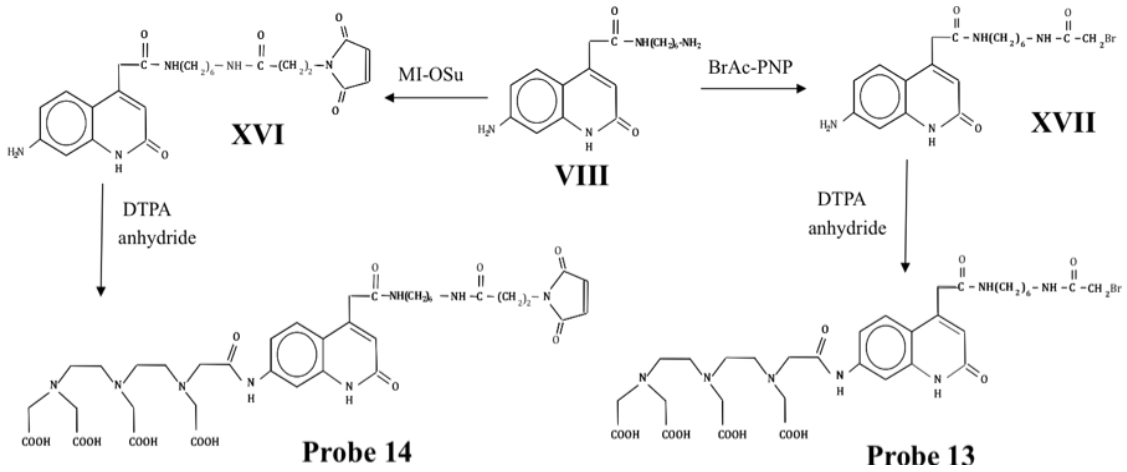

Scheme 5.2 Synthetic scheme for probes **13** and **14.**

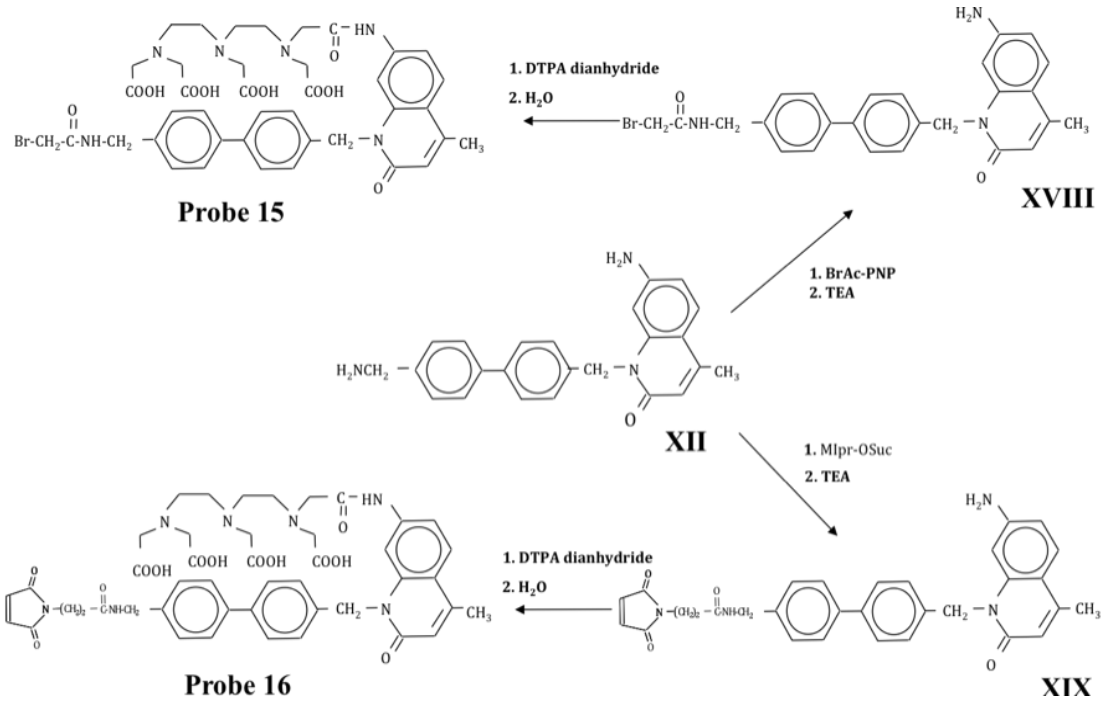

Scheme 5.3 Synthetic schemes of probes **15** and **16.**

5.2.1.7 Reaction with Cysteine. For qualitative TLC analysis the reaction mixture (10 μl) contained 50 mM sodium-borate pH 9.0, 10 mM cysteine and 0.05-1 mM reactive luminescent probe. Control mixture was the same but did not include cysteine. The mixtures were incubated at room temperature for 5 min and analyzed by TLC in acetonitrile-water 2.5:1 developing system. The reaction was monitored by appearance of the product with reduced mobility. In another version, the reactions were performed in the measuring cell at concentrations of cysteine 0.1-10 μM and the probes concentration 50 nM in 10 mM sodium borate buffer pH 9.0. The emission spectra were recorded before and after cysteine addition at time intervals indicated in Figure 5.3. Control measurements were performed in the same mixture but in the absence of cysteine. Excitation 331 nm was used for probe **14** and 328 nm for probe **16**. The emission was scanned from 350 to 650 nm.

5.2.1.8 Labeling of RNA Polymerase. RNAP sample (2 mg/ml) in 20 mM tris-HCl pH 8.0 was supplemented with 10 mM DTT and kept at 40 ^{o}C for 40 min followed by desalting on sephadex G-50 column (0.5 x 10 cm). A lanthanide probe [1 μM] was placed in the measuring cell in 50 mM sodium borate pH 9.0 (final volume 130 μl) after the light emitting spectrum was recorded the mixture was supplemented with 30 μl of 1 μM solution of RNAP. Figure 5.4 presents the time course for RNA polymerase modification was monitored by recording the emission spectrum at 545 nm in 1 min 30 s time intervals. The labeled enzyme was purified by size-exclusion chromatography on the same column.

5.2.2 Physical Methods

5.2.2.1 Continuous Excitation and Time-Resolved Fluorescence Measurements. Excitation and emission fluorescence spectra in continuous mode (displayed in Figures 5.6 and 5.7 and annotated in Table 5.2) were recorded at ambient temperature at the concentration of the compounds 0.1 μM, or 10 nM in H_2O and D_2O. The emission spectra for the compounds were recorded at maximum excitation wavelength (which coincided with the corresponding light absorption maxima for the compounds in the region 320-380 nm). Time-resolved emission measurements were executed as described in Chapter 3 (Krasnoperov, Marras et al. 2010). Lifetime measurements for thiol-reactive probes **11 - 16** and reference compounds were performed in a solution containing 1 mM Na-borate buffer at pH 9.0 and 100 nM Ln^{3+} chelate. Cysteine was added to final concentration 10 μM and the measurements resumed after 5 min incubation at room temperature.

5.3 Results

5.3.1. Synthesis of the Reactive Luminescent Probes

For the synthesis, starting amine-reactive derivatives (compounds **III** of Scheme 5.1, **VI** of Scheme 5.2, and **XI** of Scheme 5.3) obtained in previous studies (Krasnoperov, Marras et al. 2010) were used. In this chapter, an improved synthetic protocol for compound **I** was presented. This protocol took advantage of the base-catalyzed reaction leading to compound **I** previously discovered (Pillai, Kozlov et al. 2012). A quantitative methylation reaction was used to obtain compound **II**. Subsequent reaction of compound **II** with diaminohexane produced compound **III** with high yield. Amine derivatives of the fluorophores were modified with 4-nitrophenylbromoacetate, of with N-hydroxysuccinimide ester of 3-maleimidopropionic acid to obtain compounds **IV** and **V** of Scheme 5.1, **VII** and **VIII** of Scheme 5.2, and **XII** and **XIII** of Scheme 5.3. TLC analysis revealed nearly quantitative conversion of the original fluorophores to the desired products. Since these reactive products were unstable, a subsequent DTPA acylation reaction in the same mixture without purification of the reactive intermediates was performed. Acylation products were purified by preparative HPLC or TLC to yield the desired compounds (probes **11** to **16** of Figure 5.1). These probes were converted to corresponding chelates by addition of equivalent amount of $LnCl_3$. The yields of the final products were 10-30%. The yields were higher for cs124 derivatives and for bromoacetyl compounds due to shorter incubation periods with DTPA and higher stability of the thiol-reactive group. Table 5.1 indicates the mobility of reference and thiol reactive luminescent probes in a 2.5:1 acetonitrile-water TLC developing system.

Table 5.1 R_f values for Probes **11** to **16** and Reference Compounds on TLC in Acetonitrile-Water 2.5:1 Developing System

Compound	R_f of cysteine adduct	R_f of original compound
cs124DTPA-Tb^{3+}NCS (probe **2**)*	0.26	0.46
cs124-BiPh-DTPA-Tb^{3+}NCS (probe **4**)*	0.61	0.65
cs124-DTPA-Eu^{3+}*	NA	NA
cs124-DTPA-Tb^{3+}*	NA	NA
Probe **11**-Eu^{3+}	0.32	0.50
Probe **12**-Eu^{3+}	0.30	0.42
Probe **13**-Tb^{3+}	0.28	0.48
Probe **14**-Tb^{3+}	0.32	0.48
Probe **15**-Tb^{3+}	0.34	0.59
Probe **16**-Tb^{3+}	0.50	0.77

*Reference compounds described in source

Source: 1) Krasnoperov, L. N., et al. (2010). Luminescent probes for ultrasensitive detection of nucleic acids. Bioconjugate Chemistry **21**: 319-327. 2) Wirpsza, L.,et al. (2012). Highly Bright Avidin-based Affinity Probes Carrying Multiple Lanthanide Chelates. Journal of Photochemistry and Photobiology B: Biology **116**: 22-29.

5.3.2. Light Absorption Spectra of the Lanthanide Chelates

UV absorption spectra of the synthesized probes are shown n Figure 5.2. These probes all exhibit absorption in the range 300-380 nm, typical for cs124 chromophores. Probes **15** and **16** also possess strong absorption in the range 250-300 nm due to biphenyl group. The presence of the maleimide group in probes **12**, **14**, and **16** can account for the additional absorption in the range 220-240 nm. Notably, modification of the cs124 fluorophore at N1 causes a small batochromic shift (ca. 5 nm) of the spectrum in the region 280-360 nm resulting in a different excitation wavelength for probes **15** and **16**

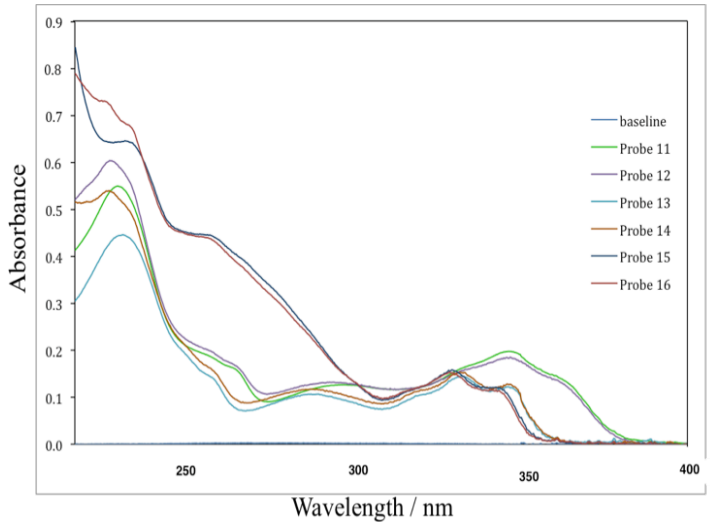

Figure 5.2 Light absorption spectra for probes **11** to **16.**

5.3.3 Light Emitting Properties of the Lanthanide Chelates

As seen from Table 5.2, bromoacetamido- compounds display nearly the same brightness compared to the corresponding isothiocyano-derivatives synthesized earlier in Chapter 3 (Krasnoperov, Marras et al. 2010). On the contrary, light emission of maleimido-compounds was significantly reduced. Nearly 10 -12 fold quenching was observed for probes **14** and **16**. This might be due to the contact quenching of the fluorophores by the maleimido group (favored by the proximation effect), since FRET quenching is unlikely, because of the absence of the spectral overlap between the fluorophores emission and the maleimido group absorption. In accord with this proposition, the reaction with cysteine (which eliminates a double bond in the maleimido group, and therefore the group's absorption) caused dramatic increase in the lanthanide light emission (see Table 6.2 and Figure 5.3). Similar, but smaller (2.4 fold) quenching effect was observed for the corresponding Eu^{3+}-DTPA-cs124CF_3 maleimide chelate. Lifetime measurements detected short- and long-lived components for maleimide cs124-based probes with the corresponding ratios 4-to-1 for probe **14** and 6-to-1 for probe **16**. It was concluded that

the long-lived components represented trace amounts of impurities, while short-lived components belonged to quenched maleimide derivatives. As seen from Table 6.2, the lifetime for probes **14** and **16** was strongly reduced compared to corresponding bromoacetamido probes, which suggests the quenching mechanism through reverse energy transfer from excited lanthanide ion to antenna fluorophore sensitized by maleimido group. The later is supported by the increase of the lanthanide emission lifetime back to that observed for reference isothiocyano, or bromacetamido compounds after reaction of probes **14** and **16** with cysteine. At the same time, the presence of maleimido group in probe **12** did not decrease the lifetime for Eu^{3+} emission, suggesting different quenching mechanism (Figure 5.3A and Table 5.2).

Table 5.2 Emission and Relative Brightness of Lanthanide Probes and Reference Compounds (at [10 nM]) in Water and Deuterium Oxide Solutions

Luminescent chelates	Emission in H_2O		Emission of cys adducts in H_2O		Quenching factor	Emission in D_2O, counts	Cysteine adducts in D_2O, counts	Relative brightness H_2O/D_2O	D_2O/H_2O cysteine adducts
	counts**	lifetime, ms	counts**	lifetime, ms					
cs124-DTPA-Eu^{3+}*	5,050*	0.6	NA	NA	NA	22,000*	NA	4.36	NA
cs124CF_3DTPA-Eu^{3+}NCS (probe **1**)*	9,450*	0.5				35,000*		3.70	
Probe **11**-Eu^{3+}	8,600	0.56	8,700	0.55	1.0	34,000	34,100	3.9	3.92
Probe **12**-Eu^{3+}	2,300	0.57	5,500	0.56	2.4	9,700	20,800	4.2	3.78
cs124-DTPA-Tb^{3+}*	169,000*	1.5	NA	NA	NA	260,000*	NA	1.54	NA
cs124DTPA-Tb^{3+}NCS (probe **2**)*	137,000*	1.2	115,000	1.12	0.84	190,000*	193,700	1.39	1.68
Probe **13**-Tb^{3+}	112,000	1.2	104,800	1.05	0.94	174,000	160,000	1.55	1.53
Probe **14**-Tb^{3+}	4,300	0.09***	50,000	1.11	11.6	7,400	66,000	1.72	1.32
Probe **15**-Tb^{3+}	90,258	1.2	88,000	1.14	0.98	119,800	119,000	1.33	1.35
Probe **16**-Tb^{3+}	3,300	0.22***	39,000	1.07	11.8	6,000	65,500	1.81	1.68

*Reference compounds described in source
**Counts are the reading for maximum wavelength emission (547 nm for Tb^{3+}, or 615 nm for Eu^{3+} chelates)
***Short-lived component

Source: 1) Krasnoperov, L. N., et al. (2010). Luminescent probes for ultrasensitive detection of nucleic acids. Bioconjugate Chemistry **21**: 319-327. 2) Wirpsza, L., et al. (2012). Highly Bright Avidin-based Affinity Probes Carrying Multiple Lanthanide Chelates. Journal of Photochemistry and Photobiology B: Biology **116**: 22-29.

As expected, the light emission of the compounds in heavy water significantly increased due to the reduction of the non-radiative dissipation of the energy of the excited state through the vibrational excitation of O-H bonds (Xiao and Selvin 2001). This

process with heavy water is less efficient due to the lower frequency of the O-D bond vibration. Interestingly, the anomalous quenching reversal has been detected in praseodymium luminescent chelates containing C-D and C-H bonds (Xiao and Selvin 2001). This process with heavy water is less efficient due to the lower frequency of the O-D bond vibration.

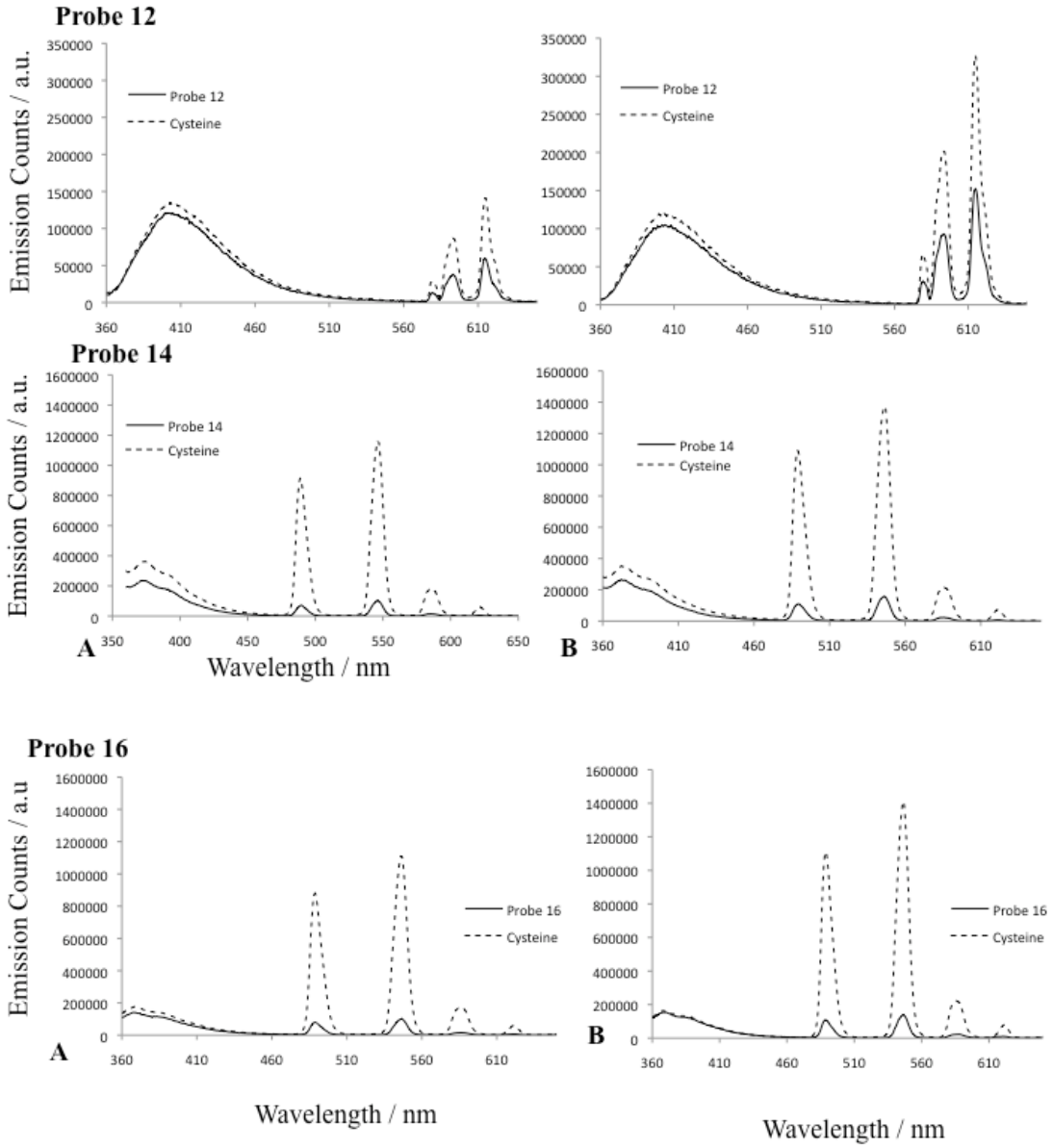

Figure 5.3 Light emission spectra for probes (**A**) **12**, **(B) 14**, and **(C) 16** and their reaction products with cysteine. The spectra were recorded in water and deuterium oxide-based solutions.

5.3.4 Reactivity of the Probes 11-16 with Cysteine

Preliminary studies showed the reactivity of the synthesized probes was tested with cysteine using TLC analysis. It turned out that incubation with cysteine in a sodium-borate buffer at pH 9.0 resulted in quantitative conversion of the probes to the products

with lower chromatographic mobility. MS analysis confirmed identification of the reaction products. Apparently, coupling to cysteine strongly increased the brightness of the maleimide compounds. In the following tests, the same reaction was monitored with various cysteine concentrations in the measuring cell by recording the light emission. The results are presented in Table 5.1 as well as in Figures 5.3 and 5.4. It appeared that the reaction with maleimido-compounds was virtually instantaneous with cysteine concentrations up to [1 μM]. At sub - micromolar concentrations the reaction proceeded slower. As a result, 30 s and 60 s half-reaction times were observed for 200 nM and 100 nM cysteine correspondingly (Figure 5.4). The results presented in Table 5.2 as well as Figures 5.3 and 5.4. It appeared that the reaction with maleimido-compounds was virtually instantaneous with cysteine concentrations up to [1 μM]. At sub-micromolar concentrations the reaction proceeded slower. Thus, 30s and 60s half-reaction times were observed for 200 nM and 100 nM [cys] correspondingly (not shown).

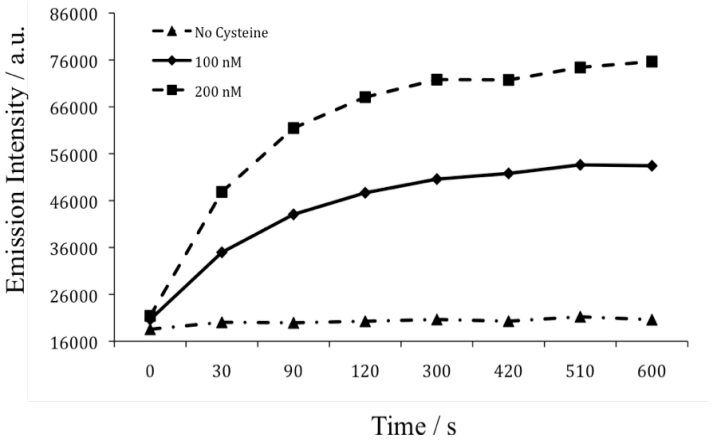

Figure 5.4 Time-course for the reaction of probe **14** with cysteine. Cysteine concentrations are indicated. Control curve represents the monitoring of the light. emission of the mixture lacking cysteine.

5.3.5 Modification of Bacterial RNA Polymerase by Maleimide-Based Probes 12, 14 and 16

The suitability of the probes for protein labeling was demonstrated with *E. coli* RNA polymerase. The reaction proceeded with high rate at sub-micromolar concentrations of the enzyme and reactive probes. As in the case of cysteine, incubation of the maleimide probes with the enzyme resulted in progressive enhancement of light emission. Subsequent size-exclusion chromatography of the samples confirmed conjugation to RNA polymerase. The highest coupling efficiency of the fluorescent material (ca. 50 %) was observed for probe **16** (Figure 5.5), while probes **12** and **14** provided 15 - 20 % efficiency. Notably after the attachment to RNA polymerase the emission of Eu^{3+} - based probe **12** was quenched, as evidenced by increased antenna-to-lanthanide emission ratio compared to the same probe reacted with cysteine. This effect was less pronounced with the Tb^{3+}-based probes **14** and **16**. The same quenching effect was observed upon attachment of corresponding isothiocyano-reactive probes to avidin(Wirpsza, Pillai et al. 2012). A normalized comparison of cysteine bound to RNA polymerase maleimide derivatives is presented in Figure 5.6. The antenna portion of the molecule decreases its emission while the lanthanide ion emission increases for both cysteine and RNA polymerase. Emission intensity for probes **12**, **14**, and **16** were compared when unbound and bound to RNA polymerase (Figure 5.7)

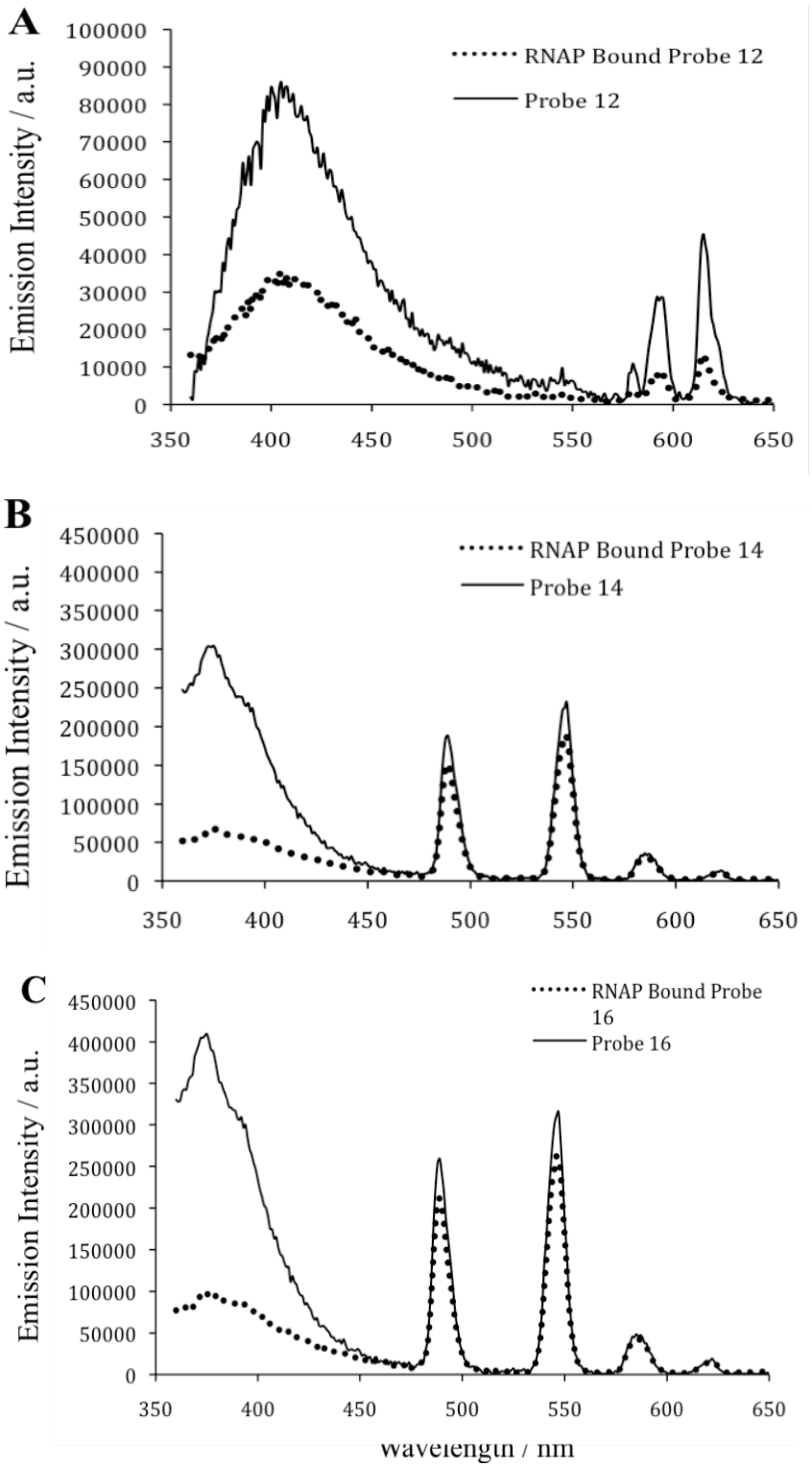

Figure 5.5 Labeling of RNA polymerase with thiol reactive probes **(A) 12**, (**B**) **14**, and (**C**) **16**. The bars show the light emission of the material covalently bound to RNA polymerase and unbound material as determined after size-exclusion chromatography of the reaction mixtures.

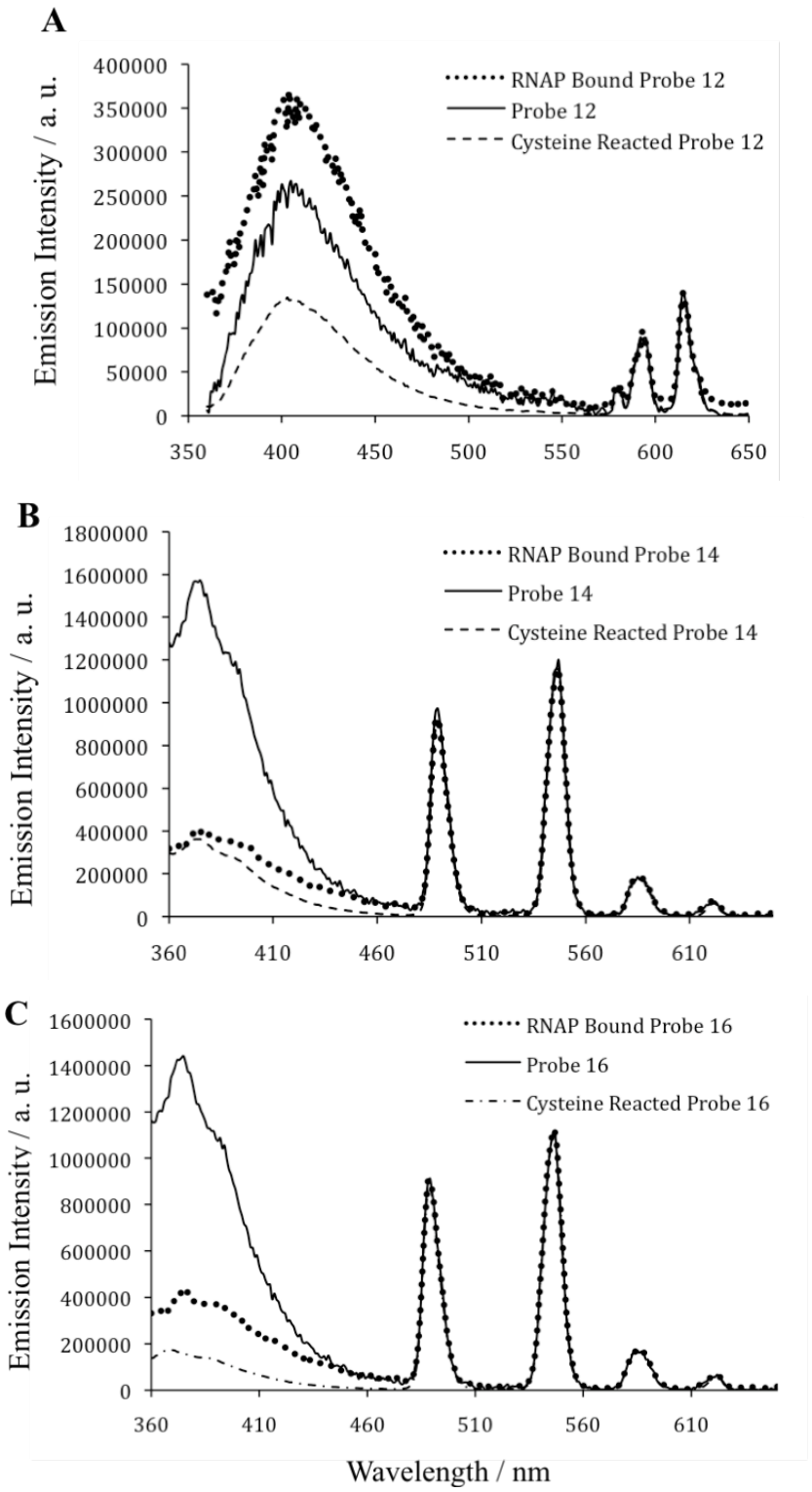

Figure 5.6 Normalized emission of Probes (**A**) **12**, (**B**) **14** and (**C**) **16** with unbound, cysteine, and RNA Polymerase.

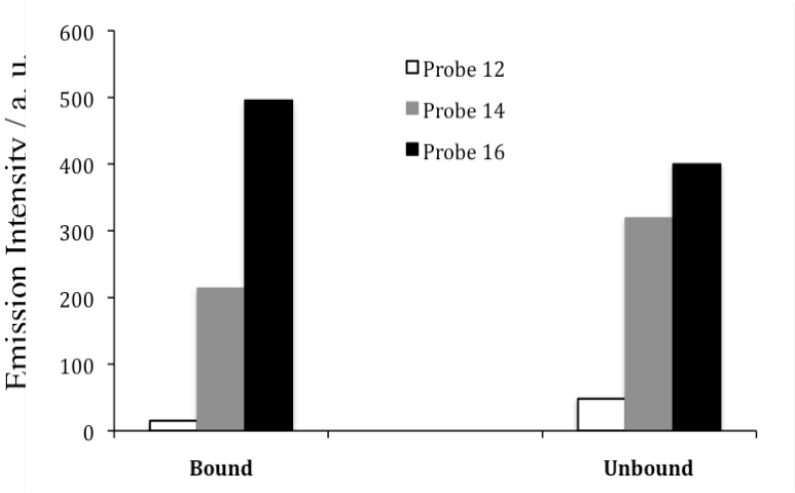

Figure 5.7 Probes **12**, **14**, and **16** bound and unbound to RNA Polymerase.

5.5 Discussion

Previous studies (Krasnoperov, Marras et al. 2010; Pillai, Kozlov et al. 2012; Pillai, Wirpsza et al. 2012; Wirpsza, Pillai et al. 2012), described the synthesis of cs124 and cs124CF_3 luminescent lanthanide ion chelates with enhanced lanthanide ion retention containing amine-reactive isothiocyano groups. The present synthetic protocols for thiol-reactive derivatives of the same chelates were obtained from amino-derivatives of the fluorophores by selective acylation. First, at the aliphatic amino group (to introduce thiol-reactive function) and then at the aromatic amino group (to introduce a chelating moiety). This was possible due to the different reactivity of the amino groups. Because the intermediate products were unstable, both reactions were performed in the same tube without purification of the intermediates. Resulting products were purified and complexed with lanthanide ions to yield the desired probes. Maleimide probes displayed exceptionally high reactivity with thiols, reacting instantaneously at micromolar thiol concentrations. Surprisngly, the maleimide group exerted strong quenching effect on the

Tb^{3+} chelates, which was due to reverse energy transfer from excited lanthanide ion to antenna. The light emission was restored after coupling to a thiol, which converted maleimido group to non-absorbing succinimido-derivative. Taking advantage of this effect, the reaction monitored the probe conjugation to cysteine and to bacterial RNA polymerase in real time mode. Enhancing of light emission of the probes upon reaction with thiols enables simple detection of sulfhydryl compounds. Therefore, these probes can detect cysteine at 100 nM concentrations. This approach can be especially valuable for ultra-sensitive determination of biologically important thiols in time-resolved mode in the cases where the amount of the material is limited.

5.5 Conclusions

Highly reactive thiol-specific luminescent lanthanide probes of enhanced brightness and metal retention were synthesized. The probes display high coupling efficiency to cysteine -containing proteins. Light emission of maleimide-based Tb^{3+} chelates strongly increases after conjugation with thiols, which can be used for ultra-sensitive determination of biologically important sulfhydryl compounds in time-resolved mode in the cases where the amount of the material is limited.

CHAPTER 6

THE SYNTHESIS AND CHARACTERIZATION OF NEW NEAR-INFRARED LIGHT-EMITTING DDAO DERIVATIVE OPTIMAL FOR BIOIMAGING

Fluorescent dyes emitting in the near-infrared region (NIR) are of a great value for bioimaging, since: i) tissue samples possess much less auto-fluorescence in this area; ii) body tissues are relatively transparent in NIR, enabling non-invasive detection. Common diagnostic platform takes advantage of labeling carrier molecules of interest with NIR dyes to obtain optical probes for imaging the corresponding targets in body tissues. While suitable for labeling of large carrier molecules, current NIR dyes suffer major deficiencies in construction of small diagnostic molecules due to large dyes size (1000-1500 Da) and stable electric charge, which drastically affect the targeting and physical properties of the resulting probe. Here the synthesis of a non-charged NIR dye, DDAO derivative with improved quantum yield is reported. The small size of the dye (ca. 300 Da) and beneficial excitation and emission red spectral shift allows the design of small NIR emitting diagnostic molecules, that are likely to retain their affinity to the target and specificity. In addition, cross-linking versions of the dye were obtained for the attachment to a carrier molecule of interest. Resulting compounds are useful in the synthesis of diagnostic targeting molecules for numerous biomedical applications.

6.1 Introduction

Although most fluorophores operate in the visible light region of the ultraviolet range of the spectrum, the near infrared (NIR) area is very promising for fluorescence detection and imaging (see reviews (Sevick-Muraca, Houston et al. 2002; Frangioni 2003; Nolting,

Gore et al. 2011; Sun 2012)). A new intensely developing approach in optical *in vivo* molecular imaging techniques uses NIR dyes for biomedical and clinical applications such as: i) tissue-specific imaging (Rasmussen, Tan et al. 2009); ii) *in vivo* cancer imaging (Kosaka, Ogawa et al. 2009); iii) tracking of specific cells (Pham, Xie et al. 2007); and iv) imaging of bacterial infections (Leevy, Gammon et al. 2008).

In the NIR region much less background is observed both *in vitro* assays and tissue samples, thereby increasing detection sensitivity. Notably, body tissues have a transparency window in the region 650-800 nm with a maximal transparency at 680 nm, which enables non-invasive imaging of NIR dyes in the living body (Figure 1.2). NIR dyes can be used as non-specific contrasting agents aiding in visualization of the body tissues (especially the lymphatic system). These dyes also can be conjugated to biological carrier molecules (‘addresses’) to yield diagnostic molecules able to detect specifically their targets. Typically, the dyes can be attached to peptides, proteins aptamers or cellular metabolites. Generally, NIR dyes are large molecules (FW 1000-1500) bearing groups with stable electric charge (to maintain solubility in water). This can affect the targeting properties of the carrier molecules and cell permeability (which is crucial for detection for intracellular targets), thereby complicating the implementation of the approach. The effect is expected to be more pronounced with smaller targeting molecules (e.g., antibiotics and cellular metabolites), justifying the search of new NIR labels with improved properties.

Recently, a new diagnostic platform for the imaging of microbial infections has been suggested (Pratt, Garcia-Effron et al. 2012). The approach takes advantage of fluorescently labeled pathogen-specific drugs, which are able to bind to their cellular

targets, thereby rendering the cells fluorescent. Previously, this approach was validated using antifungal caspofungin and posaconazole drugs labeled with green-fluorescent BODIPY label (Pratt, Garcia-Effron et al. 2012). However, for imaging the pathogens inside the body, long wavelength emitting dyes are required. Conventional NIR dyes (Figure 6.1) have a large size and possess groups with stable electric charge (introduced to enhance a solubility of the compounds), which are expected to drastically affect both interaction of with a target and cell permeability of the labeled drug derivatives. Unique properties of the DDAO fluorophore (Corey 1989; Corey, Trimmer et al. 1991) (Scheme 6.1) make it an attractive compound for labeling small molecules, since it has: i) small size (MW = 308 $gmol^{-1}$); ii) long-wavelength emission (660 nm); iii) fair brightness ($\varepsilon \times \Phi$ = 3,600). The deficiencies are: i) non-optimal light emission maximum; ii) pH-dependence of the light emission and the presence of a negative charge due to ionization of compound's hydroxyl group. The structure of the dye (compound **II** of Scheme 6.1) was modified by the substitution of the aminoalkyl group for hydroxyl group at position 7. The synthetic protocol includes a simple one-step procedure, followed by fast, non-chromatography purification. The resulting compound was converted into amine-, and thiol-reactive forms for the attachment to the object of interest. Compared to the original DDAO fluorophore, the emission of the modified DDAO was not pH-dependent. Also, this compound possesses superior light absorption and light emission properties. Thus, modification resulted in the beneficial increase in molar extinction and quantum yield as well as in shift of the emission maximum from 660 to 680 nm where the body tissues are the most transparent. This fluorophore can easily be detected in the living body as

evidenced by successful imaging of fungal infection in mice using 7-aminoDDAO attached to antifungal drugs caspofungin and posaconazole.

6.2 Materials and Methods

6.2.1 The Synthesis of DDAO fluorescent derivatives

DDAO (7-hydroxy-9H (1, 3-dichloro-9, 9-dimethyl acridin-2-one)); diaminobutane diacetate; 1,1-thiocarbonylimidazole; trifluoroacetic acid; *p*-nitrophenylbromoacetate; diisopropylamine; diisopropylethylamine; MIpr-OSu; hexane; ethyl acetate; chloroform; acetonitrile; KOH; silica gel TLC plates on aluminum foil (200 μm layer thick with a fluorescent indicator); distilled and deionized water (18 MΩ cm^{-1}) were purchased from Aldrich with a ≥99% pure and HPLC grade. Excitation and emission fluorescence spectra in the continuous excitation mode were recorded using QuantaMaster 1 (Photon Technology International) digital fluorometer at ambient temperature.

6.2.1.1 Compound II. 10 mg DDAO (7-hydroxy-9H (1, 3-dichloro-9, 9-dimethyl acridin-2-one)) (33 μmol) was dissolved in 100 μl 1M diaminobutane diacetate in 80 % aqueous DMSO. TLC analysis in acetonitrile-water (14:1) developing system detected intense-blue colored product migrating lower (R_f = 0.45) than the original product (R_f=0.9). After 10 h incubation at 95 ^oC the reaction mixture was supplemented with 2 ml of water and extracted with ethyl acetate (3 x 5 ml). The pH of the water layer was adjusted to 11-11.5 by 10 M KOH followed by extraction with ethyl acetate (2 x 5 ml). The organic layer was collected and evaporated to dryness under reduced pressure

affording 4 mg of compound **I**. UV λ_{max}=667 nm (ε=53,000 $M^{-1}cm^{-1}$). MS: DDAO-NH-$(CH_2)_4$ -NH_2 (+1) 378.0887 (found) 378.288 (calc).

6.2.1.2 Compound III. To 150 µl of 15 mM solution of compound **II** in DMSO two equivalents of 1,1-thiocarbonylimidazole dissolved in 0.2 ml of chloroform were added. After 30 min incubation at room temperature the mixture was supplemented with one µl of trifluoroacetic acid and incubation continued at 40 ^oC for another 45 min. TLC analysis in hexane-acetone (2:1) developing system showed complete conversion of the original compound (R_f = 0) to reaction product (R_f = 0.5). The reaction mixture was diluted by water and the product extracted in chloroform. The solvent was removed by evaporation in vacuo, and the residue dried by co-evaporation with acetonitrile. Preparative TLC purified the product in hexane-acetone (2:1) developing system. *Yield: 4 µmol.* UV λ_{max}=670 nm (ε = 52,000 $M^{-1}cm^{-1}$), MS: DDAO-NH- $(CH_2)_4$ -NCS (+1) 420.453 (found) 420.352 (calc).

6.2.1.3 Compound IV. To 150 µl of 15 mM solution of compound **II** in DMSO (2.25 µmol) 1 equivalent of *p*-nitrophenylbromoacetate and diisopropylamine were added, and the mixture was left at room temperature for 5 min. TLC analysis revealed a major reaction product with R_f = 0.58 in hexane-acetone developing system. Preparative TLC purified the product in the same system. *Yield 48 %.* UV λ_{max}=673 nm (ε = 53,000 $M^{-1}cm^{-1}$). MS: DDAO-NH_2 –$(CH_2)_4$ -NH-AcBr 499.045(found) 499.213 (calc). DDAO-NH_2 -$(CH_2)_4$ – NH-AcBr 9(+H) 500. 044 (found) 500.221 (calc).

6.2.1.4 Compound V. Compound **II** (0.46 μmol) in 100 ml od DMSO was mixed with equivalent amount of MIpr-OSu dissolved in 120 μl DMF and diisopropylethylamine. After 15 min incubation at 0°C TLC analysis in ethyl acetate developing system revealed one major product [R_f=0.5], which was purified by preparative TLC in the same system. *Yield: 0.14 μmol (~30%).* UV λ_{max}=673 nm (ε=53,000 $M^{-1}cm^{-1}$). MS: DDAO-NH_2-$(CH_2)_4$–NH-3MI 529.154 (found) 529.40 (calc). DDAO-NH_2-$(CH_2)_4$–NH-3MI (+H) 530.167 (found) 530.40 (calc).

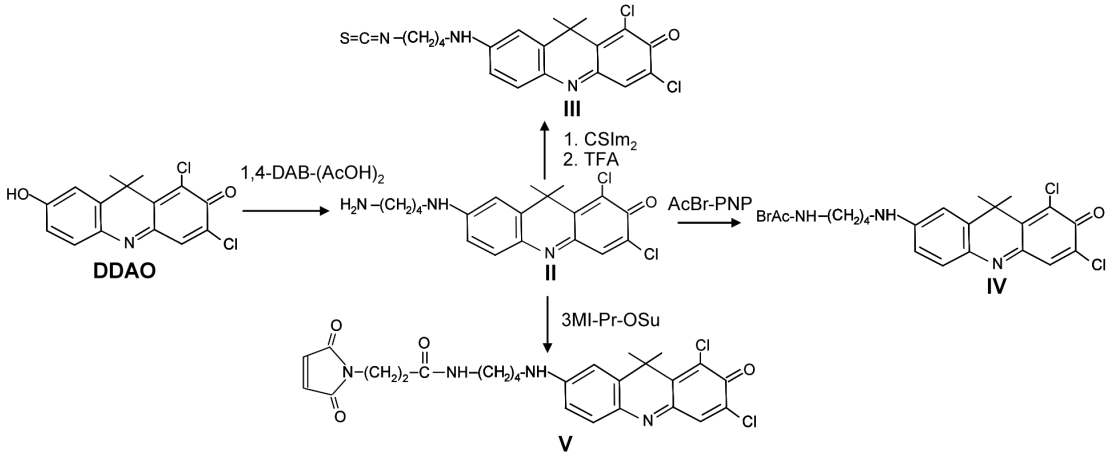

Scheme 6.1 The scheme for the synthesis of 7-aminoDDAO derivatives.

6.2.2 Synthesis of DDAO Fluorescent Probes

6.2.2.1 Caspofungin-DDAO derivative (probe 1). Caspofungin (2.6 mg, 2 μmol) was dissolved in the solution of 230 μl of 5 mM compound **III** in DMF and 0.5 μl of TEA was added followed by incubation at 60°C for 90 min. TLC in acetonitrile-water (5:1) developing system detected a blue-colored reaction product with R_f=0.65. R_fs for caspofungin and **III** were 0.48 and 1.0 respectively. The product was purified by preparative TLC in acetonitrile–water (7:1) developing system, eluted by 50 % aqueous methanol and the solution evaporated under reduced pressure to final concentration 0.33

mM. UV λ_{max} = 672 nm (ε=53,000 $M^{-1}cm^{-1}$). DDAO-NH_2-$(CH_2)_4$-NCS-Caspofungin(+H) 1515.7242 (found) 1515.673 (calculated).

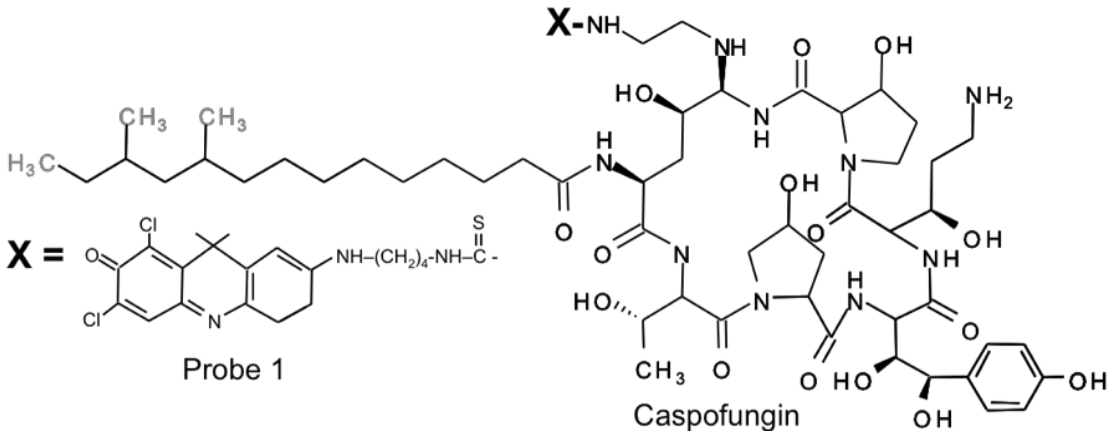

Figure 6.1 Structure of Caspofungin with 7-aminoDDAO derivative.

6.2.2.2 Posaconazole- DDAO derivative (probe 2). Two milligrams of compound **III** (Scheme 6.2) were dissolved in 0.1 ml of 20 mM solution of compound **I**. The mixture was supplemented with 2 ml of triethylamine and left for 20 min at room temperature. TLC analysis in ethylacetate-ethanol (8:1) developing mixture revealed complete conversion of compound I to reaction product. The mixture was diluted by 2 ml of water, the residue collected by centrifugation, dissolved in DMF and subjected to preparative TLC in the same system. Yield 0.5 μmol. UV λ_{max}=672 nm (ε=53,000 $M^{-1}cm^{-1}$). MS: Posaconazole-DDAO(+H) 1162.45 (found); 1162.20 (calculated).

6.2.2.3 2,4-Dinitro-1-Fluorobenzene-DDAO. Twenty two microliters of compound **II** (Scheme 6.1) and 2 μL of 20 μmol of 2,4-dinitro-1-fluorobenzene (DNFB) with 0.2 μL of concentrated triethylamine (TEA) was reacted for 10 minutes at ambient temperature. Preparative TLC purification in 3:1 ethylacetate hexane revealed a single product with R_f = 0.5. *Yield ~40μM.* UV-vis λ_{ex}= 667 nm. λ_{ex}= 360 nm.

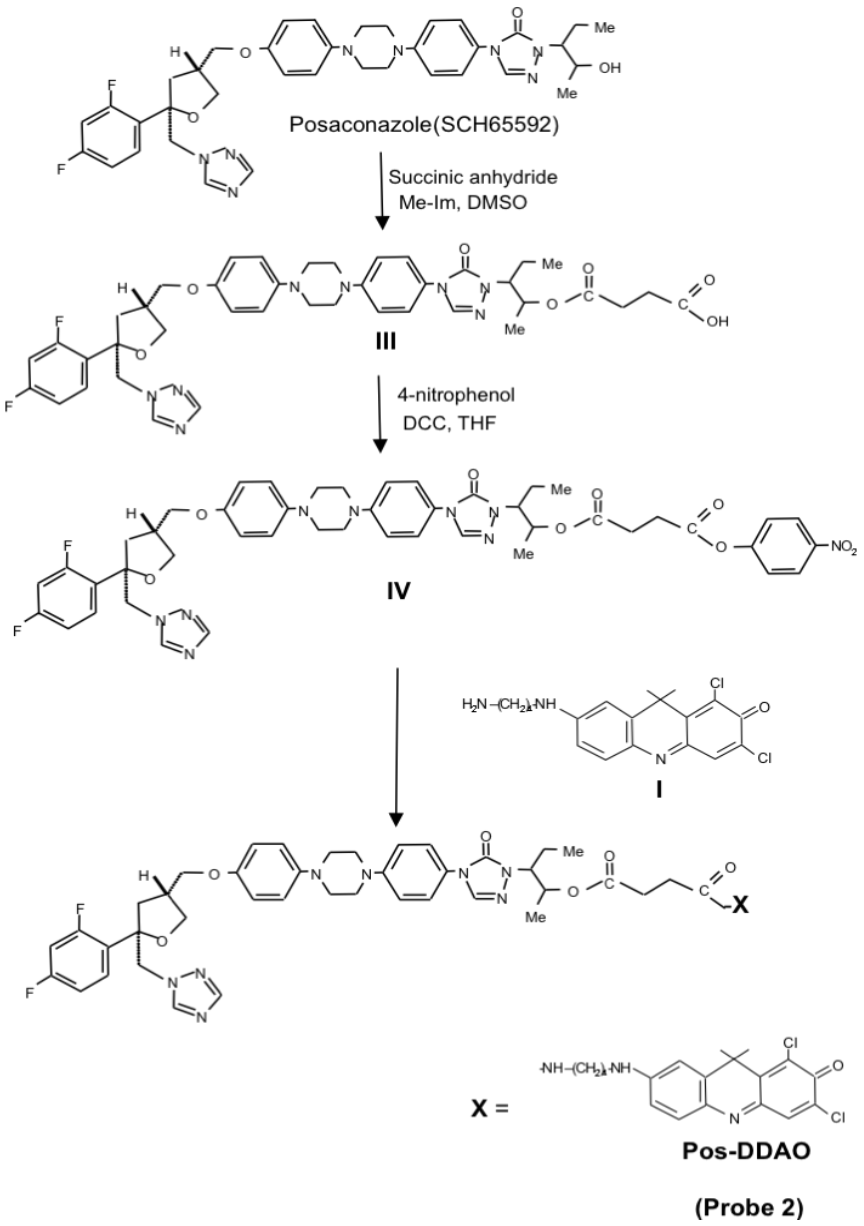

Scheme 6.2 Synthetic scheme of Posconazole-DDAO.

Source: Pratt, A., et. Al. (2012). Evaluation of fungal-specific fluorescent labeled enchinocandin probes as diagnostic adjuncts. *Journal of Medical Mycology,* (2012). ***In press***

6.2.2.4 BODIPY-DDAO. Two microliters of 20 mM BODIPY was added to 22 μL of 1 mmol compound **II** (Scheme 6.1) with 0.2 μL of concentrated triethylamine (TEA). TLC analysis in 100% ethyl acetate showed the R_f of the product=0.4 and R_f=0.8 for

BODIPY reactant. Reaction was completed within 10 minutes and purified in 100% ethyl acetate with preparative TLC. *Yield ~ 30 μM.* UV-vis λ_{ex}= 676 nm. λ_{ex}= 503 nm.

6.3 RESULTS

6.3.1 The Synthesis of DDAO Derivatives

Hamilton reaction was used to derivatize the core DDAO previously discovered with simpler phenol-, or naphtol-derivatives (Malmberg and Hamilton 1948; Willenz 1955; Corey 1989; Corey, Trimmer et al. 1991). The reaction includes acid-catalyzed attack of amino-compounds on mesomeric keto-form of the aromatic hydroxy-derivatives. The reaction product with 1,4-diaminobutane was obtained with high yield and purified by extraction. The resulting DDAO amino-derivative was converted to corresponding isothiocyanate (compound **III**) by treatment with thiocarbonyldiimidazole followed by incubation with trifluoroacetic acid (Scheme 6.1). Acylation of the compound **II** by activated esters of bromoacetic, or 3-maleimidopropionic acids yielded thiol-reactive derivatives (compounds **IV** and **V**).

6.3.2 Light Absorption and Fluorescent Spectra of 7-AminoDDAO, Caspofungin-DDAO, and Posaconazole-DDAO derivatives

Modification of DDAO (Scheme 6.1) resulted in detectable blue shift of the light absorption maximum (653 nm and 673 nm correspondingly). The molar extinction of 7-aminoDDAO (53,000 $M^{-1}cm^{-1}$) was determined by the attachment of reference chromophores (see sections **6.2.2.3** and **6.2.2.4**) with known molar absorptivity (Table 6.1). Light absorption spectra of the labeled caspofungin and posaconazole derivatives were close to superposition of those for the 7-(4-aminobutyl) amino-DDAO and the

corresponding drugs, which is illustrated in Figure 6.2 on the example of posaconazole derivative. Modification of DDAO (Figure 6.1) resulted in detectable blue shift of the light absorption maximum (653 nm and 673 nm correspondingly). The molar extinction of 7-aminoDDAO (53,000 $M^{-1}cm^{-1}$) is higher than that for the original DDAO compound (48,000 $M^{-1}cm^{-1}$) (Table 6.1).

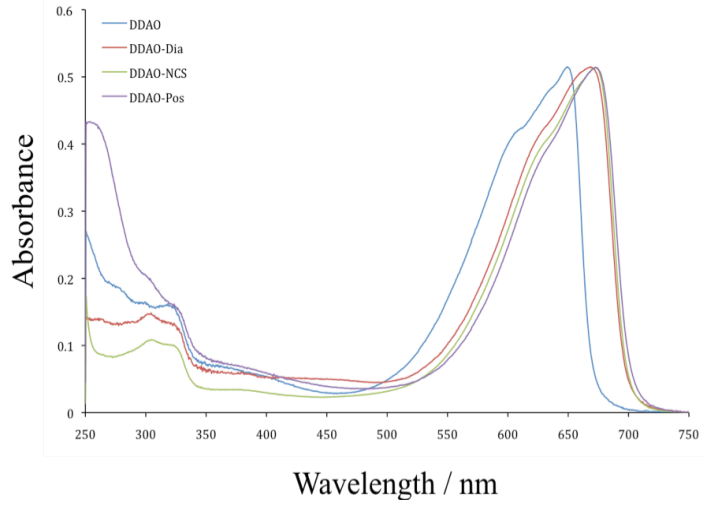

Figure 6.2 Light absorption spectra for original DDAO and 7-aminoDDAO derivatives.

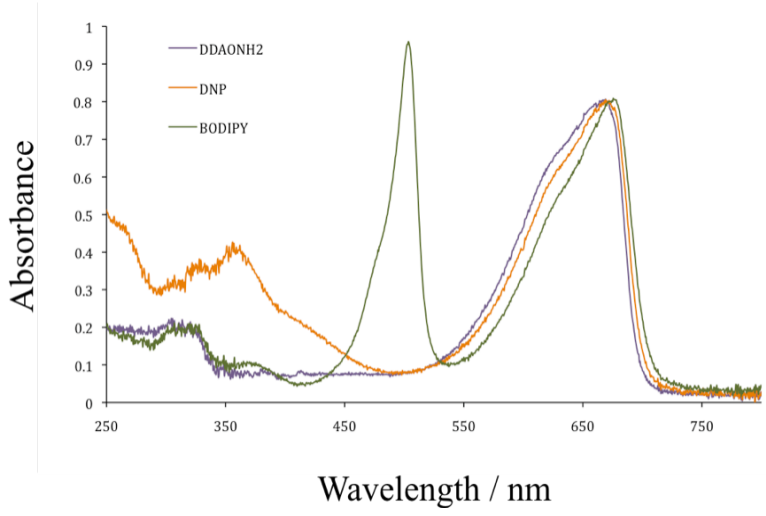

Figure 6.3 Normalized molar absorptivity of 7-aminoDDAO with BODIPY and DNP.

Table 6.1 Relative Brightness (RB) and Quantum Yield in Three Different Solvents for DDAO and its Derivatives

Bound Compound	Molar Absorptivities References (ε / $M^{-1}cm^{-1}$)	Molar Absorptivities 7-aminoDDAO (ε / $M^{-1}cm^{-1}$)
Posaconazole	34,000	59,000
DNP	17,600	32,000
BODIPY-FL	82,000	70,000
	Average	**53,000**

As expected, fluorescence spectra (Figure 6.5) of 7-(4-aminobutyl) amino-DDAO exhibited blue shift compared to ionized form of DDAO (Figure 6.4). Thus, excitation and emission maxima for DDAO were 653 nm and 660 nm correspondingly, while for 7-(4-aminobutyl) amino-DDAO shifted to 671 nm and 679 nm correspondingly. Increasing the content of the organic solvent (MeOH) resulted in the enhancement of the light emission and characteristic change in excitation. Thus substitution 50% methanol for water did not affect the shape of the excitation spectrum for 7-aminoDDAO, but increased the light emission ca. 2.5 fold. Placing the compound in 100% MeOH resulted in dramatic change of the excitation spectrum profile shifting the maximum from 670 nm to 620 nm, while only slightly shifting emission maximum from 680 to 670 nm. Notably, the light emission intensity dropped 1.7 fold. Remarkably, the shape of the excitation spectrum curve for ionized form of DDAO was the same in 50% and 100% methanol. In contrast to 7-aminoDDAO, a 1.3 fold increase in the emission was observed in 100% methanol comparing to 50% methanol.

Table 6.2 presents the data on quantum yield and brightness for 7-aminoDDAO compounds at various conditions. These parameters were determined using a reference fluorophore Cy5.5, (which has the excitation and emission maxima nearly identical to those for 7-aminoDDAO) and published data for original DDAO fluorophore. The

synthesized 7-aminoDDAO derivative possessed a higher brightness (εϕ = 10,000) compared to the ionized original DDAO compound (εϕ = 3,600). This was obviously due to higher light absorptivity and higher quantum yield of the amino-derivative. The difference in brightness further increased in 50% methanol (21,000 and 9,000 correspondingly). However, in 100% methanol the brightness became comparable (13,000 and 12,000 correspondingly).

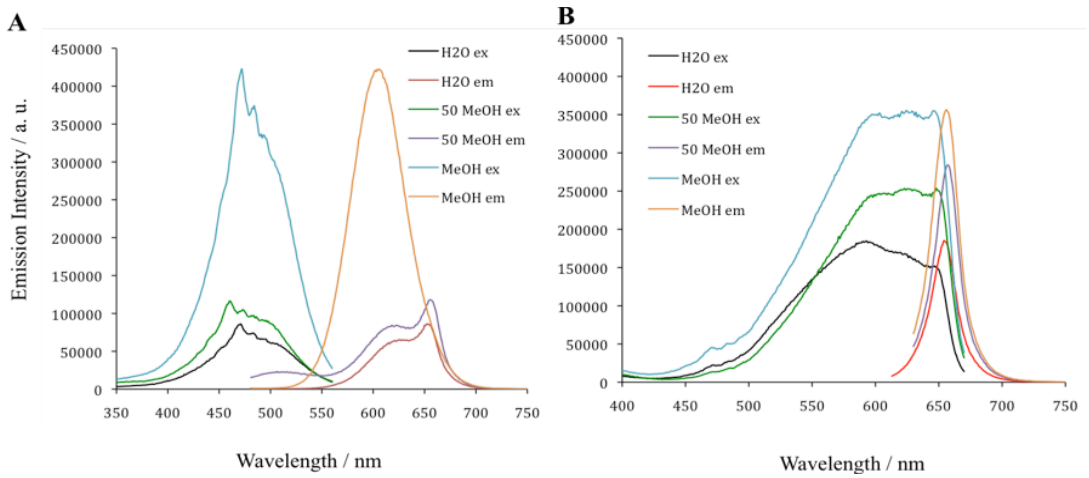

Figure 6.4 DDAO in (**A**) pH 2.0 and (**B**) pH 9.0 in three different solvents.

Table 6.2 Relative Brightness (RB) in Three Different Solvents for DDAO and Derivatives at 1 μM

Compounds	ε / $M^{-1}cm^{-1}$	RB (H_2O)	RB (50 MeOH)	RB (MeOH)	QY (H_2O)	QY (50 MeOH)	QY (MeOH)
DDAO (pH 9.0)	48,000	6,000	9,000	12,000	0.125	0.19	0.25
DDAO NH_2	53,000	10,000	21,000	13,000	0.19	0.40	0.25
DDAO Pos	53,000	0.0	3,300	13,000	0.0	0.16	0.24
DDAO Casp	53,000	6,000	13,800	22,000	0.11	0.26	0.42
Cy 5.5 (Ref)	250,000	57,500	N/A	N/A	0.23	NA	NA

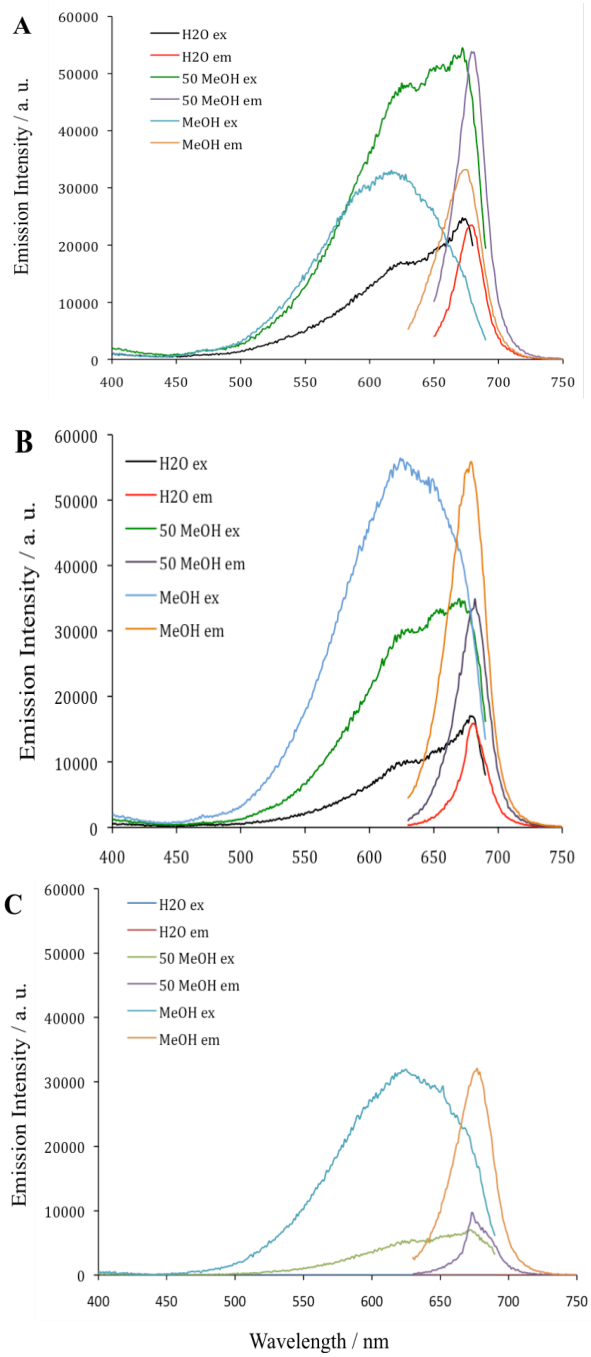

Figure 6.5 Excitation and emission spectra of (**A**)7-aminoDDAO, (**B**) DDAO-Pos and (**C**) DDAO-Caspo in three different solvents at 1 μM.

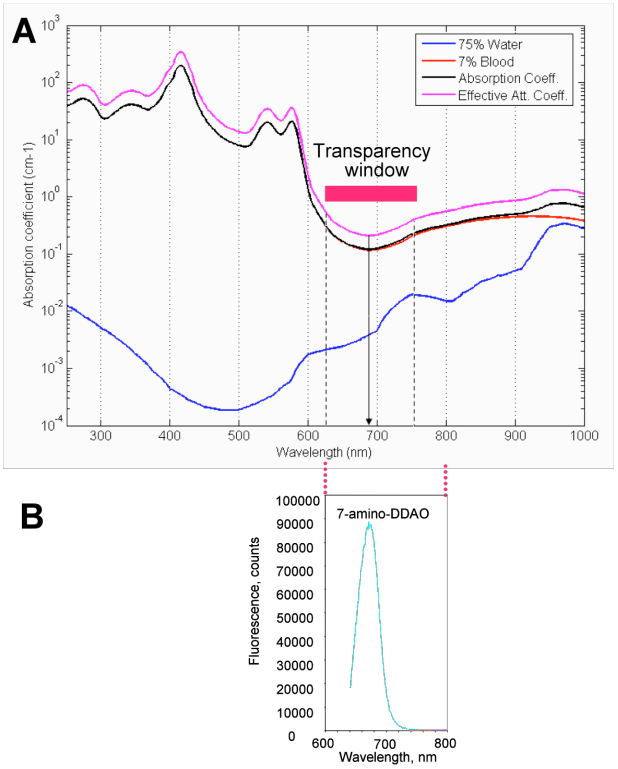

Figure 6.6 (A) Transparency window of body tissues and **(B)** the light emission spectra of 7-aminoDDAO.

Source: Biomedical Photonics Handbook. (2003) Tuan Vo-Dinh (Editor), CRC Press. New York

6.3.3 Using Caspofungin-DDAO Derivative for Imaging of Fungal Infections in Mice

Figure 6.7 shows the results on imaging of mice liver infected with a fungal pathogen along with control images. It is seen that treatment of the infected organ with caspofungin-7-aminoDDAO derivative resulted in bright fluorescent signal. At the same time no signal was detected in uninfected and/or untreated organs.

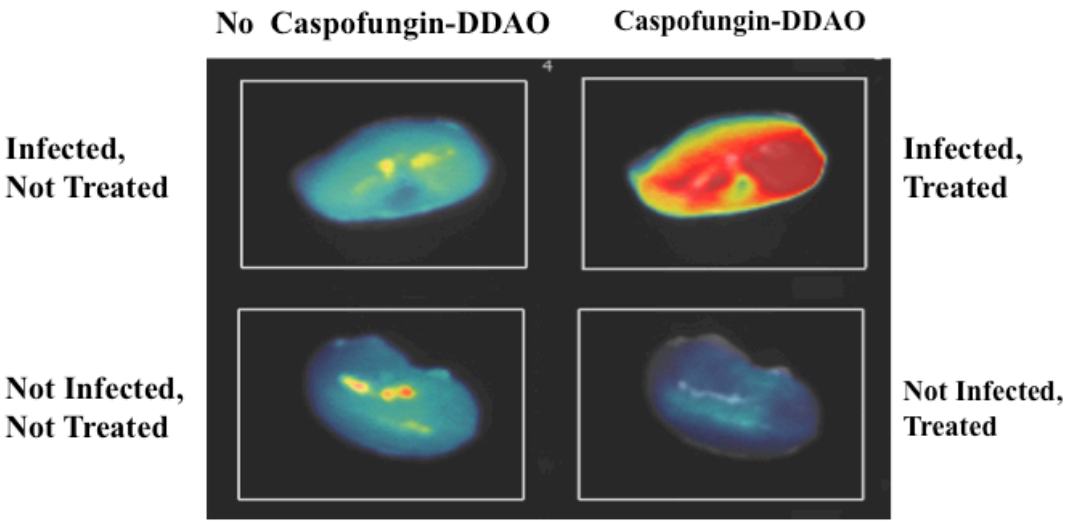

Figure 6.7 Scanning images of mice kidneys for non-treated and treated, with and without caspofungin-7amino-DDAO.

Source: Perlin, D.S. and Pratt, A. 2012. Newark, NJ

6.4 Discussion

In the present research, a modified DDAO derivative, 7-(4-aminobutyl)-aminoDDAO with improved light emission properties was synthesized. The obtained compound is 2.8 fold brighter then original DDAO. More importantly, excitation and emission maxima for the new derivative are in the spectral area in which the body tissues are the most transparent (Figures 1.2 and 6.6). This makes the new fluorophore an optimal label for numerous biomedical applications that rely on imaging in the living body. The obtained DDAO derivative was converted to amine-reactive and thiol-reactive compounds that can be used for covalent labeling of the objects of interest. Also, the obtained synthetic intermediate 7-(4-aminobutyl)-aminoDDAO can be easily modified with click-reactive groups, which are useful for bioconjugation. The unique advantage of the DDAO fluorophore compared to the other NIR dyes is its unusually small size, which is likely to

preserve targeting properties of the ‘address’ molecules (antibiotics, cellular metabolites, ‘signaling molecules’, etc.) to which the fluorophore is attached.

The observed dramatic increase of the light emission of labeled posaconazole in the media with high methanol content is of particular interest. The absence of light emission of the compound in water is obviously to stacking interaction of the fluorophore with light-absorbing moiety of the drug. This stacking interaction is destroyed in an organic solvent resulting in light emission. Remarkably, the same disruption of stacking interaction must occur in the process of the binding of the labeled drug to its cellular target (Figure 6.4). Therefore, in this process the labeled drug acts as “signaling molecule”, which activates upon contact to the target by analogy to widely known molecular beacons. This should greatly increase the detection selectivity by elimination the emission from unbound labeled drug molecules. The same effect could be expected for the other labeled ligands containing aromatic light absorbing groups able to stack to the fluorophore. In fact, many drugs and cellular metabolites contain such groups enabling to design similar “signaling molecules”. The obtained fluorophore is useful for biochemical and biophysical studies that require high detection sensitivity as well as in organ, or tissue-specific tomographic imaging and for non-invasive detection of microbial infections in clinic.

CHAPTER 7

CONCLUSIONS

This dissertation describes two unique types of luminescent probes for the sensitive detection of biopolymers, their complexes and living cells. These probes were selected based on their unique abilities to overcome autofluorescence found in biological samples. The first project (Chapters 3, 4, and 5), improved the synthetic schemes for long-lived luminescent lanthanide ion probes in three biological validation studies (e.g. molecular beacons, multiple labels to a single moiety, and sensitive detection of biologically significant thiol groups). Time-gated detection of these molecular beacons avoided short-lived background fluorescence of the media to provide high sensitivity (better than 1 pM). To further increase the sensitivity of the probes, multiple luminescent labels were attached to a single carrier molecule, avidin. It was concluded that up to 30 lanthanide chelates could be attached to avidin creating highly bright conjugates. Total Internal Reflection Fluorescence (TIRF) Microscopy of *E. coli* and Chinese Hamster Ovarian (CHO) cells exteriorly labeled with Eu^{3+} and Tb^{3+} avidin conjugates allowed highly contrast and sensitive detection, suggesting applicability of the probes for imaging material in living cells. Six thiol-reactive derivatives of cs124-CH_3 and cs124-CF_3 fluorophores with bromoacetamido- and maleimido- cross-linking groups were synthesized. Maleimido-compounds displayed exceptional reactivity instantaneously coupling to thiols at physiological conditions at micromolar thiol concentrations. In addition, the light emission of maleimide-based Tb^{3+} chelates strongly increases after conjugation with thiols, which can be used for ultra-sensitive determination of

biologically important sulfhydryl compounds in time-resolved mode in the cases where the amount of the material is limited.

The second portion of the work, described the innovation of a small NIR dye moiety, 7-aminoDDAO, for attachment to molecules of interest for in body imaging in the NIR region. Fluorescent dyes emitting in the near-infrared region (NIR) from 650 to 700 nm are of great value for bioimaging due to their capability of emitting fluorescence in the low absorbance and the light scattering region of tissues. However, the majority of current NIR dyes suffers major deficiencies due to their large size and stable electric charge which affect the target and physical properties of the resulting probe. This portion reports a synthesized non-charged small NIR derivative (7-aminoDDAO) with improved quantum yield that was characterized using UV/VIS, mass spectroscopy, and fluorescence instrumentation. 7-aminoDDAO was found to be ~2.8 fold brighter than its predecessor DDAO, with excitation and emission maxima located in the spectral area where body tissues are the most transparent (λ_{em}=680 nm). Amine and thiol reactive cross-linking groups were added to the derivative for covalent labeling of biomolecules of interest. Due to its small size, 7-aminoDDAO is able to minimize the effect of the label on the functional properties of the target (antibiotics, or cellular metabolites) and is useful in biochemical and biophysical studies that require high detection sensitivity such as the case for organ, tissue-specific tomographic imaging, and non-invasive detection of microbial infections in clinical studies.

In regards to future work for luminescent lanthanide probes, three potential directions to be taken: accurate quantum yields, energy transfer studies, and imaging within cells. Accurate quantum yields of all derivatives should be compared to model

compounds (cs124-CH_3 and cs124-CF_3). The Selvin group has provided reliable estimates; however, the procedures require an in depth experimental set up specified for quantum yields and energy transfer. Quantum yields should be compared against well known organic fluorophore standards with high molar abosorptivities at 351 nm with a high quantum yield. Evanescent microscopy is beneficial for the luminescent probes attachment to oligonucleotides for imaging within mammalian cells. In addition, classic fluorescence microscopy would be of great assistance in validation and visualization.

Upcoming developments for the newly synthesized DDAO derivative, 7-aminoDDAO, include potential attachment to larger carrier molecules (tissues, antibiotics, antibodies etc) for imaging in the body tissues. In addition, a click-reactive derivative should be synthesized and tested. Fluorescence microscopy for low concentration studies in cellular imaging would draw a direct comparison between lanthanide ion probes and NIR dyes. This compound may be also able to compare with luminescent lanthanide ion probes and their quantum yields values

REFERENCES

Alaoui, I. M. (2007). "Time-Resolved Luminescence Imaging and Applicatiosn." Imaging for Detection and Identification: 243-248.

Axelrod, D. (1981). "Cell-Substrate Contacts Illuminated by Total Internal Reflection Fluorescence." The Journal of Cell Biology **89**(April): 141-145.

Axelrod, D. (2001). "Total Internal Reflection Fluorescence Microscopy in Cell Biology." Traffic **2**: 764 - 774.

Berlier, J. E., A. Rothe, et al. (2003). "Quantitative comparison of long-wavelength Alexa Fluor dyes to Cy dyes: fluorescence of the dyes and their bioconjugates." Journal of Histochemistry & Cytochemistry **51**(12): 1699-1712.

Bunzli, J.-C. G. and C. Piguet (2005). "Taking advantage of luminescent lanthanide ions." Chemical Society Reviews **34**: 1048-1077.

Bunzli, J. C. (2006). "Benefiting from the unique properties of lanthanide ions." Accounts of Chemical Research **39**: 53-61.

Byassee, T. A., W. C. W. Chan, et al. (2000). "Probing Single Molecules in Single Living Cells." Analytical Chemistry **72**(22): 5606-5611.

Chen, J. and P. R. Selvin (1999). "Thiol-reactive luminescent chelates of terbium and europium." Bioconjugate Chemistry **10**: 311-315.

Chen, J. and P. R. Selvin (2000). "Synthesis of 7-amino-4-trifluoromethyl-2-(1H)-quinolinone and its use as an antenna molecule for luminescent europium polyaminocarboxylates chelates." Journal of Photochemistry and Photobiology A:Chemistry **135**: 27-32.

Cidalia M.G, d. S., A. J. Harte, et al. (2008). "Recent developments in the field of supramolecular lanthanide luminescent sensors and self-assemblies." Coordination Chemistry Reviews **252**: 2512-2527.

Connally, R. (2011). "A device for gated autosynchronous luminescence detection." Analytical Chemistry **82**: 4782-4787.

Connally, R. and J. Piper (2008). "Time-gated luminescence microscopy." Annuals of the New York Academy of Sciences **1130**: 106-116.

Corey, P. (1989). Chromogenic acridinone enzyme substrates. P. a. T. Office. USA. **4810636**.

Corey, P., R. Trimmer, et al. (1991). "A new chromogenic Beta-galactosidase substrates: 7-b-D-galactopyranosyloxyl-9,9-dimethyl-9H-acridin-2-one." Angewandte Chemie International Edition **30**: 1646-1648.

Delmdahl, R. F., G. Spiecker, et al. (2003). "Performance of optical fibers for transmission of high-peak-power XeCl excimer laser pulses." Applied Physics B **77**: 441-445.

Demirkol, O., C. Adams, et al. (2004). "Biologically Importat Thiols in Various Vegetables and Fruits." Journal of Agriculture and Food Chemistry **52**: 8151-8154.

Diamandis, E. (1991). "Multiple labeling and time-resolvable fluorophores." Clinical Chemistry: 1486-1491.

Dickson, E. F., A. Pollak, et al. (1995). "Time-resolved detection of lanthanide luminescence for ultrasensitive bioanalytical assasys." Journal of Photochemistry and Photobiology B: Biology **27**: 3-19.

Dickson, E. F., A. Pollak, et al. (1995). "Ultrasensitive bioanalytical assays using time resolved fluorescence detection." Pharmacology & Therapeutics **66**: 207-235.

Elia, G. (2008). "Biotinylation reagents for the study of cell surface proteins." Proteomics **8**: 4012-4024.

Eliseeva, S. and J. C. Bunzli (2010). "Lanthanide luminescence for functional materials and biosciences." Chemical Society Reviews **39**: 189-227.

Frangioni, J. V. (2003). "In vivo near-infrared fluorescence imaging." Current Opinion in Chemical Biology **7**: 626-634.

Froehilich, P. (1989). "Understanding the sensitivity specification of spectrofluorometers." International Laboratory **19**: 42-45.

Gahlaut, N. and L. W. Miller (2010). "Time-Resolved Microscopy for Imaging Lanthanide Luminescence in Living Cells." Cytometry Part A **77A**(1113-1125).

Ge, P. and P. R. Selvin (2003). "Thiol-reactive luminescent lanthanide chelates: part 2." Bioconjugate Chemistry **14**: 870-876.

Ge, P. and P. R. Selvin (2004). "Carbostyril Derivatives as Antenna Molecules for Luminescent Chelates." Bioconjugate Chemistry **15**: 1088-1094.

Ge, P. and P. R. Selvin (2008). "New 9- or 10-dentate luminescent lanthanide chelates." Bioconjugate Chemistry **19**: 1105-1111.

Giebel, K.-F., C. Bechinger, et al. (1999). "Imaging of Cell/Substrate Contacts of Living Cells with Surface Plasmon Resonance Microscopy." Biophysical Journal **76**: 509-516.

Gong, H., B. Zhang, et al. (2009). "B-galactosidase activity assay using far-red shifted fluorescent substrate DDAOG." Anaytical Biochemistry **386**: 59-64.

Hagan, A. K. and T. Zuchner (2011). "Lanthanide-based time-resolved luminescence immunoassasy." Analytical and Bioanalytical Chemistry **400**: 2847-2864.

Haralambidis, J., K. Angus, et al. (1990). "The preparation of polyamide-oligonucleotide probes containing multiple non-radiactive labels." Nucleic Acid Research **18**: 501-505.

Hemmila, I. and V. Laitala (2005). "Progress in lanthanides as luminescent probes." Journal of Fluorescence **15**: 529-542.

Heyduk, E. and T. Heyduk (1997). "Thiol-reactive, luminescent europium chelates: luminescence probes for resonance energy transfer distance measurements in biomolecules." Analytical Biochemistry **248**: 216-227.

Hohlbein, J., K. Gryte, et al. (2010). "Surfing on a new wave of single-molecule fluorescence methods." Physical Biology **7**(1-22).

Jahn, K., E. M. Olsen, et al. (2001). "Site-Specific Chemical Labeling of Long RNA Molecules." Bioconjugate Chemistry **22**: 95-100.

Johansson, M., R. M. Cook, et al. (2004). "Time gating improves sensitivity in energy transfer assays with terbium chelate/dark quencher oligionucleotide probes." Journal of American Chemical Society **126**: 16451-16455.

Kocherbitov, V. and O. Soderman (2006). "Hydration of Dimethyldodecylamine-N-oxide: Enthaply and Entropy Drive Processes." Journal of Physical Chemistry B **110**: 13649-13655.

Kosaka, N., M. Ogawa, et al. (2009). "In vivo stable tumor-specific painting in various colors using dehalogenase-based protein-tag fluorescent ligands." Bioconjugate Chemistry **20**(7): 1367-1374.

Krasnoperov, L. N., S. A. E. Marras, et al. (2010). "Luminescent probes for ultrasensitive detection of nucleic acids." Bioconjugate Chemistry **21**: 319-327.

Lakowicz, J. R. (2006). Principles of Fluorescence Spectroscopy. Balitmore, Springer.

Leevy, W., S. Gammon, et al. (2008). "Noninvasive optical imaging of staphylococcus aureus bacterial infection in living mice using a Bis-dipicolylamine-Zinc(II) affinity group conjugated to a near-infrared fluorophore." 19 **3**: 686-692.

Li, M. and P. R. Selvin (1995). "Luminescent polyaminocarboxylate chelates of Terbium and Europium: the effect of chelate structure." Journal of American Chemical Society **117**: 8132-8138.

Li, M. and P. R. Selvin (1997). "Amine-reactive forms of a luminescent diethylenetriaminepentaacetic acid chelate of terbium and europium: attachment of DNA and energy transfer measurements." Bioconjugate Chemistry **8**: 127-132.

Loboda, L. I., I. V. Sokolova, et al. (1984). "Influence of substitution and medium on spectral-luminescent properties of aminocoumarins." Zhurnal Prikladnoi Spektroskopii **40**(6): 954-957.

Malmberg, E. and C. Hamilton (1948). "The synthesis of 2- and 3-substituted napth(1,2)imidazoles." Journal of American Chemical Society **70**: 2415-2417.

Marras, S. A. E. (2003). Development of Molecular Beacons for Nucleic Acid Detection. Leiden, Leiden University. **Doctoral Dissertation**.

Nolting, D., J. Gore, et al. (2011). "Near-Infrared Dyes: Probe development and applications in optical molecular imaging." Current Organic Synthesis **8**: 521-534.

Orth, R. N., T. G. Clark, et al. (2003). "Avidin-Biotin Micropatterning Methods for Biosensor Applications." Biomedical Microdevices **5**(1): 29-34.

Parker, D. (2004). "Excitement in f block: structure, dynamics and function of a nine-coordinate chiral lanthanide complexes in aqueous media." Chemical Society Review **33**: 156-165.

Patonay, G., J. Salon, et al. (2004). "Noncovalent labeling of biomolecules with red and near-infrared dyes." Molecules **9**: 40-49.

Peck, K., L. Stryer, et al. (1989). "Single-molecule fluorescence detection: Autocorrection criterion and experimental realization with phycoerythrin." Proceedings of the National Academy of Science of the United States of America **86**: 4087-4091.

Petoud, S., G. Muller, et al. (2007). "Brilliant Sm, Eu, Tb, and Dy chiral lanthanide complexes with strong circularly polarized luminescence." Journal of American Chemical Society **129**: 77-83.

Pham, W., J. Xie, et al. (2007). "Tracking the migration of dendritic cells by in vivo optical imaging." Neoplasia **9**(12): 1130-1137.

Pillai, S., M. Kozlov, et al. (2012). New cross-linking quinoline and quinolone derivatives for sensitive fluorescent labeling. Journal of Fluoerscence.

Pillai, S., L. Wirpsza, et al. (2012). New Cross-Linking Quinolone and Quinolone based Luminescent Lanthanide Probes for Sensitive Labeling. SPIE Photonic West Proceedings Conference on Reporters, Markers, Dyes, Nanoparticles, and Molecular Probes for Biomedical Applications.

Pratt, A., G. Garcia-Effron, et al. (2012). "Evaluation of fungal-specific fluorescent labeled enchinocandin probes as diagnostic adjuncts." Journal of Medical Mycology **In Press**.

Rasmussen, J., I. Tan, et al. (2009). "Lymphatic imaging in humans with near-infrared fluorescence." Current Opinion in Biotechnology **20**(1): 74-82.

Rowley, G., T. Henriksson, et al. (1987). "Fluoroimmunoassays for Ferritin and IgE." Clinical Chemistry **33**: 1563.

Rurack, K. and M. Spieles (2011). "Fluorescence quantum yield of a series of red and near infrared dyes emitting at 600-1000 nm." Anaytical Chemistry **83**: 1232-1242.

Schmidt, T., G. J. Schutz, et al. (1995). "Characterization of Photophysics and Mobility of Single Molecules in a Fluid Liquid Membrane." Journal of Physical Chemistry **99**: 17662-17668.

Schneckenburger, H. (2005). "Total internal reflection fluorescence microscopy: technical innovations and novel applications." Current Opinion in Biotechnology **16**: 13-28.

Selvin, P. R. (2002). "Principles and biophysical applications of lanthanide-based probes." Annual Review of Biophysics & Biomolecular Structures **31**: 275-302.

Selvin, P. R. and J. E. Hearst (1994). "Luminescence energy transfer using a terbium chelate: improvements on fluorescence energy transfer." Proceedings of the National Academy of Science **91**: 10024-10028.

Selvin, P. R., T. M. Rana, et al. (1994). "Luminescence resonance energy transfer." Journal of American Chemical Society **116**: 6029-6030.

Sevick-Muraca, E. M., J. P. Houston, et al. (2002). "Fluorescence-enhanced, near infrared diagnostic imaging with contrast agents." Current Opinion in Chemical Biology **6**: 642-650.

Sueda, S., J. Yuan, et al. (2000). "Homogenous DNA hybridization assay by using europium luminescence energy transfer." Bioconjugate Chemistry **11**: 827-831.

Sun, Y. Q. L., J.Lv, X.Liu, Y.Zhao, Y.Guo, W. (2012). "Rhodamine-inspired far-red to near-infrared dyes and their applications as fluorescent probes." Angewandte Chemie International Edition **51**(31): 7634-7636.

Timtcheva, I., V. Maximova, et al. (2000). "New assymmetric monomethine cyanine dyes for nucleic-acid labeling: absorption and fluorescence spectral characteristics." Journal of Photochemistry and Photobiology A: Chemistry **130**: 7-11.

Townsend, D., K. Tew, et al. (2003). "The Importance of Glutathione in Human Disease." Biomedicine and Pharmacotherapy **57**: 145-155.

Tung, C.-H. (2004). "Fluorescent peptide probes for in vivo diagnostic imaging." Biopolymers (Peptide Science) **76**: 391-403.

Tung, C.-H., Q. Zeng, et al. (2004). "*In Vivo* Imaging of β-*Galactosidase* Activity Using Far Red Fluorescent Switch." Cancer Research **64**: 1579-1583.

Tyagi, S. and F. R. Kramer (1996). "Molecular beacons: probes that fluoresce upon hybridization." Nature Biotechnology **14**: 303-308.

Tyagi, S., S. A. E. Marras, et al. (1996). "Molecular Beacons: Hybridization Probes for Detection of Nucleic Acids in Homogenous Solutions." Nature Biotechnology **14**: 303-308.

Umezawa, K., Y. Nakamura, et al. (2008). "Bright, color-tunable fluorescent dyes in the visible-near infrared region." Journal of American Chemical Society **130**: 1550-1551.

Vargas, D. Y., A. Raj, et al. (2005). "Mechanism of mRNA transport in the nucleus." Cell Biology **102**(47): 17008-17013.

Vo-Dinh, T. (2003). Biomedical photonics handbook. New York, CRC Press.

Warther, D., F. Bolze, et al. (2010). "Live-Cell One- and Two Photon Uncaging of a Far-Red Emitting Acridinone Fluorophore." Journal of American Chemical Society **132**: 2585-2590.

Warther, D., F. Bolze, et al. (2010). "Live-cell one- and two- photo uncaging of a far-red emitting acridinone fluorophore." Journal of American Chemical Society **132**: 2585-2590.

Wazawa, T. and M. Ueda (2005). "Total internal reflection fluorescence microscopy in single molecule nanobioscience." Advances in Biochemical Engineering/Biotechnology **95**: 77-106.

Werts, M. H. (2005). "Making sense of lanthanide luminescence." **88**: 101-131.

Willenz, J. (1955). "p-nitrosoaniline." Journal of the Chemical Society: 2049.

Wirpsza, L., S. Pillai, et al. (2012). "Highly Bright Avidin-based Affinity Probes Carrying Multiple Lanthanide Chelates." Journal of Photochemistry and Photobiology B: Biology **116**: 22-29.

Xiao, M. and P. R. Selvin (2001). "Quantum yields of luminescent lanthanide chelates and far red dyes measured by resonance energy transfer." Journal of American Chemical Society **123**: 7067-7073.

Xiao, Y., F. Liu, et al. (2005). "A new class of long-wavelength fluorophores: strong red fluorescence, convenient synthesis and easy derivation." Chemical Communications(2): 239-241.

Zhang, Y., T. Hei, et al. (2012). "Affinity binding-guided fluorescent nanobiosensor for acetylcholinesterase inhibitors via distance modulation between the fluorophore and metallic nanoparticle." Anaytical Chemistry **84**: 2830-2836.